Universitat de les Illes Balears

DEPARTAMENTO DE MICROBIOLOGÍA

Sulphate-reducing bacterial diversity in a calcareous sandy sediment of Mallorca and community response to hydrocarbon contamination

TESIS DOCTORAL

Ana Belén Suárez Suárez

Palma de Mallorca, 2012

The study was supported by the ECOSIP project (200530F0182-200530F0183) funded by the CSIC, the FBBVA project BIOCON05/094, and the Spanish Ministry of Science and Innovation projects Consolider Ingenio 2010 CE-CSD2007-0005 and VEM2003-0075-C02-01 (both co-financed with FEDER funding); additional funding was provided by the Max-Planck Society and the Helmholtz Association.

Contents

Resumen

Esta tesis trata sobre el efecto de la contaminación por crudo de petróleo en el ecosistema costero mediterráneo y sobre el papel fundamental de los sedimentos marinos en la regulación y el mantenimiento de los procesos biogeoquímicos. El estudio presta especial atención a las comunidades bacterianas reductoras de sulfato y a su implicación en la degradación de contaminantes orgánicos. La diversidad, abundancia y fisiología de las bacterias reductoras de sulfato que habitan el sedimento arenoso del norte de Mallorca (Islas Baleares), fueron analizadas mediante un enfoque polifásico, basado en la combinación de experimentos *in situ* e *in vitro*, biología molecular clásica y de última generación, cultivos y determinación de actividades metabólicas. Los resultados obtenidos durante esta tesis demuestran que el sedimento mediterráneo alberga una microbiota autóctona que podría prosperar después de un derrame de crudo de petróleo y cuyo papel podría ser crucial para la transformación y la eliminación de compuestos orgánicos xenobióticos en este ambiente.

Resum

Aquesta tesi tracta sobre l'efecte de la contaminació per cru de petroli sobre l'ecosistema costaner mediterrani i sobre el paper fonamental dels sediments marins en la regulació i el manteniment dels processos biogeoquímics. L'estudi presta especial atenció a les comunitats bacterianes reductores de sulfat i la seva implicació en la degradació de contaminants orgànics. La diversitat, abundància i fisiologia dels bacteris reductors de sulfat que habiten el sediment arenós del nord de Mallorca (Illes Balears), van ser analitzades mitjançant un enfocament polifàsic, basat en la combinació d'experiments *in situ* i *in vitro*, biologia molecular clàssica i d'última generació, cultius i determinació d'activitats metabòliques. Els resultats obtinguts durant aquesta tesi demostren que el sediment mediterrani alberga una microbiota autòctona que podria prosperar després d'un vessament de cru de petroli i el paper de la qual podria ser crucial per a la transformació i l'eliminació de compostos orgànics xenobiòtics en aquest ambient.

Resume

This thesis discusses the fate and behave of crude oil contamination in the Mediterranean coastal ecosystem, and the essential role of the marine sediments in the regulation and maintenance of biogeochemical processes. The study pays particular attention to the role of sulphate reducing bacteria communities in the degradation of organic matter and pollutants entering the Mediterranean environment. A polyphasic approach based in the combination of *in situ* and *in vitro* experiments, next generation and classical molecular biology, cultivation, and the determination of metabolic activities, provided first insights into the diversity, abundance and physiology of sulphate reducing bacteria inhabiting the undisturbed sandy sediment at the north of Mallorca (Balearic Islands). The results obtained during the thesis demonstrate that the undisturbed Mediterranean sediment harbours an autochthonous microbiota that could prosper after a crude oil spill and which role might be crucial for the transformation and removal of hazardous organic compounds in this environment.

General Introduction

1. Anthropocene - Mankind as a major geological force

Humans have significantly altered nearly all Earth's systems, including its atmosphere, hydrosphere, lithosphere and biosphere. Taken together over the past 300 years, these anthropogenic changes (especially in atmospheric chemistry and global climate) provide strong evidence that humans have altered the Earth system sufficiently to indicate the emergence of a new geological epoch: the Anthropocene (Ellis, 2011; and references therein).

This term, first coined by Nobel laureate Paul Crutzen in 2002 (Crutzen, 2002), is based on a significant change in the global stratigraphic signature, distinct from that of the Holocene or the Pleistocene interglacial phases (Zalasiewicz *et al.*, 2008), and it has been recorded since the Industrial Revolution began in the late eighteenth century (Crutzen, 2002; Zalasiewicz *et al.*, 2008).

Industrial human systems have introduced at least three clearly novel biospheric processes: i) the use of fossil energy to replace human and animal labours, revolutionizing human capacity for ecosystem engineering, transport, and other activities; ii) the industrial synthesis of reactive nitrogen to impulse agroecosystem productivity; and more recently, iii) genetic engineering of species (Ellis, 2011).

Industrial human systems are globally, strongly connected and tend to evolve more rapidly than previous social systems, accelerating the rates in social change, material exchange, tool development, and human interactions with the biosphere, indeed, changing the Earth on a scale comparable to some of the major events of the ancient past. Some of these changes are now seen as permanent, even on a geological time-scale (Zalasiewicz *et al.*, 2010; Ellis, 2011).

1.1. Fossil fuel consumption

The exploitation of coal and petroleum (crude oil and gas) together with the development of an improved version of the steam engine (James Watt, 1763–1775), enabled the planet-wide industrialization, construction and transport, triggering the increase in the energy supply, world human population, and global economy (Steffen *et al.*, 2007) which had led to a continuous increase in the consumption of fossil resources (Figure 1).

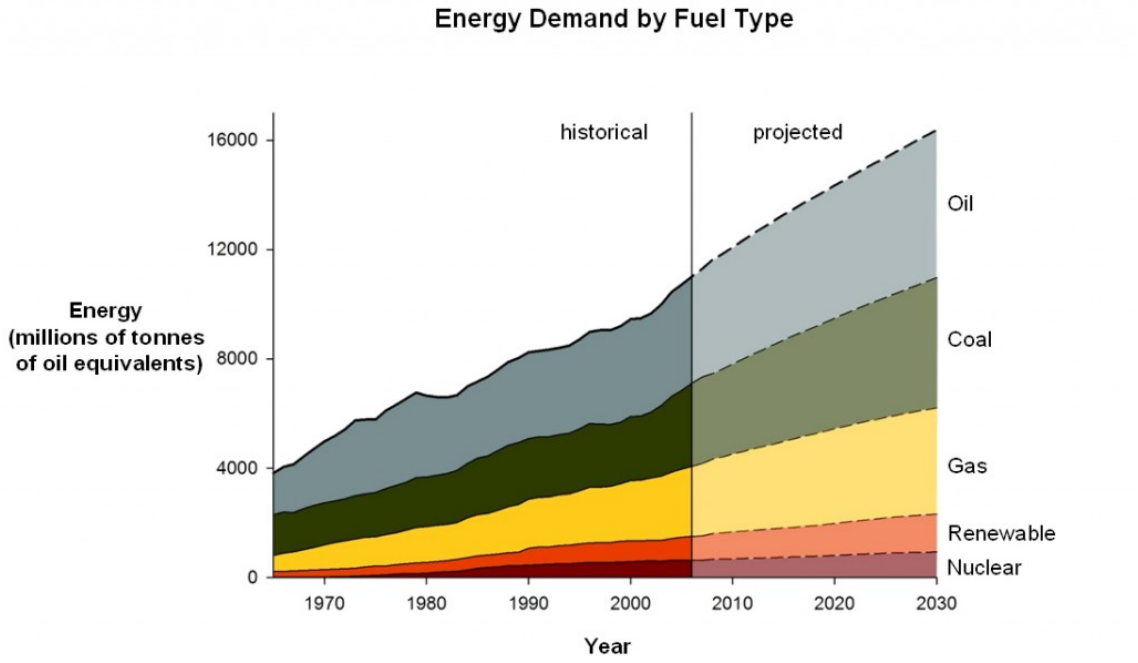

Figure 1. Historical and projected energy demand based on the fuel type from 1960 to 2030. By 2000, fossil fuel-based energy systems generated about 80% of the total energy used to power the global economy (from http://energy.sigmaxi.org/?cat=4, October 27th 2011).

Geochemically stored fossil carbon has represented the largest human energy source for more than 100 years. The worldwide production of crude oil and natural gas liquids increases steadily, with an estimated worldwide production of 89 million barrels per day in 2011 (International Energy Agency, http://omrpublic.iea.org/) from which approximately 50% is transported by sea (Ince *et al.*, 2010).

Petroleum is used to generate energy, primarily for transportation and electricity, but it is also an important feedstock for the manufacture of petrochemicals used in the creation of synthetic rubber, fibers, drugs, detergents, plastics, lubricating oils and solvents (Libes, 2009).

1.2. Petroleum composition

Petroleum is defined as any hydrocarbon mixture that can be recovered through a drill pipe and constitutes a mixture of gas, liquid, and condensate hydrocarbons. The gas phase includes low-molecular-weight hydrocarbons ($\leq C_4$) (e.g. methane, ethane, propane, and butane), while the liquid phase is commonly known as crude oil. The

condensates are gaseous or liquids hydrocarbons that, upon cooling, change into liquids or solids, respectively.

Crude oil, with over 17, 000 distinct chemical components, is considered as one of the most complex mixture of organic compounds occurring on Earth (Head *et al.*, 2006), but it is mainly constituted by two fractions of hydrocarbons that can be classified as aliphatic and aromatic.

Aliphatic hydrocarbons show their carbon atoms bonded in straight chains, branched chains, or non-aromatic rings (cyclic). They may be saturated, when all their C-C bonds are simple (alkanes) or unsaturated, with double bonds (alkenes) or triple bonds (alkynes) (Figure 2).

Aromatic hydrocarbons are very stable cyclic molecules that contain conjugated double bonds (the electrons cycle free around the circular arrangements of atoms, alternating single and double bonds and generating resonance stabilization). Aromatics may be monocyclic, such as benzene, or polycyclic (constituted for 2 or more benzene rings, e.g. naphthalene). Many important compounds in this class also contain aliphatic hydrocarbon chains bonded to aromatic rings (alkylbencenes) (Figure 2).

Other chemicals, including i) gases, such as N_2, CO_2, H_2S, and He; ii) trace metals, particularly V, Zn, Ni, and Hg; and iii) organic polar compounds containing N, S, and O, (e.g. benzothiophene, benzonaphthothiophene, indole, quinoline, benzofuran) (Figure 3) are also present in the petroleum (Libes, 2009). Geochemists have been studying these groups of compounds for years because of their importance in the origin, alteration, and properties of the petroleum.

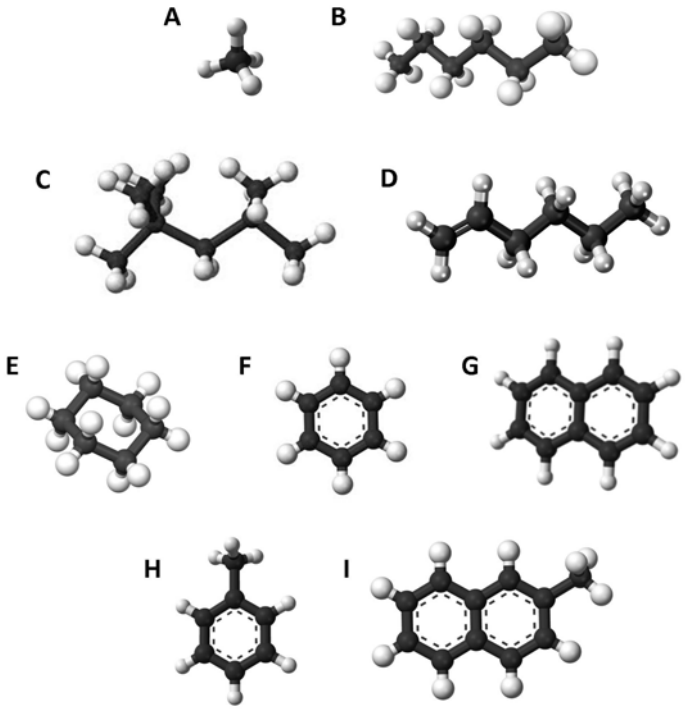

Figure 2. Molecular models of some aliphatic and aromatic hydrocarbons. Carbon atoms are represented in black and hydrogen atoms in white. **A**. Methane (gaseous aliphatic); **B**. Hexane (straight chain alkane); **C**. Methylhexane (branched chain alkane); **D**. Hexene (alkene); **E**. Cyclohexene (cyclic alkane); **F**. Benzene (single ring aromatic); **G**. Naphthalene (polycyclic aromatic); **H**. Toluene (alkylated benzene); **I**. Methylnapthalene (alkylated polycyclic aromatic); (modified from en.wikipedia.org).

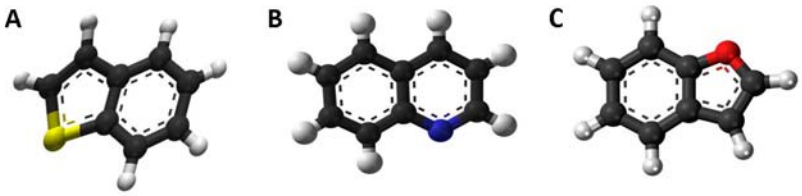

Figure 3. Molecular models of some organic polar compounds present in the crude oil. **A**. Benzothiophene (sulphur atom is represented in yellow); **B**. Quinoline (nitrogen atom in blue); **C**. Benzofuran (oxygen atom in red); (modified from en.wikipedia.org).

1.3. Petroleum formation

Petroleum is composed by hydrocarbons synthesized by organisms or generated from biogenic organic matter (OM) during a maturation process that last over millions of years (Libes, 2009). In marine environments characterized by shallow water depths, high plankton productivity and low bottom-water O_2 concentrations, large amounts of OM are accumulated and buried (Tissot and Welte, 1978). While burying, the OM is biotically transformed under temperatures not exceeding 50ºC in a process called diagenesis (Figure 4.A). Most of the diagenetic reactions take place under anoxic conditions and are mediated by nitrate-reducing, sulphate-reducing, and methanogenic microorganisms. Therefore, the oxygen, nitrogen and sulphur atoms from the sedimentary OM are removed while its hydrogen content increases (Tissot and Welte, 1978).

As the anaerobic metabolism proceeds, the degradation of the OM generates a mixture of biomonomers, biopolymers, and geopolymers commonly know as kerogen (sapropel in the case of marine habitats) (Libes, 2009).

Surface sediments become more deeply buried due to the continuous accumulation of particles on the seafloor, and to the temperature and pressure increase with depth. The OM undergoes then abiotic (catagenic) reactions that consist in i) the reduction of double bonds by incorporation of hydrogen or sulphur atoms, ii) cracking reactions, in which short-chain hydrocarbons are broken off larger parent molecules and iii) condensation reactions (Figure 4.B). The net effect of these reactions is the increase in the hydrogen content of the forming hydrocarbons which condensate to form rings (cyclic and aromatic hydrocarbons).

Finally, at temperatures over 150ºC, the metagenesis process, which is considered a very low-metamorphism, takes place.

In marine sediments, where the geothermal gradient is on the order of 15 to 50ºC km^{-1} (Figure 4.A), the formation of oil occurs at 3, 000 to 5, 000 m depth.

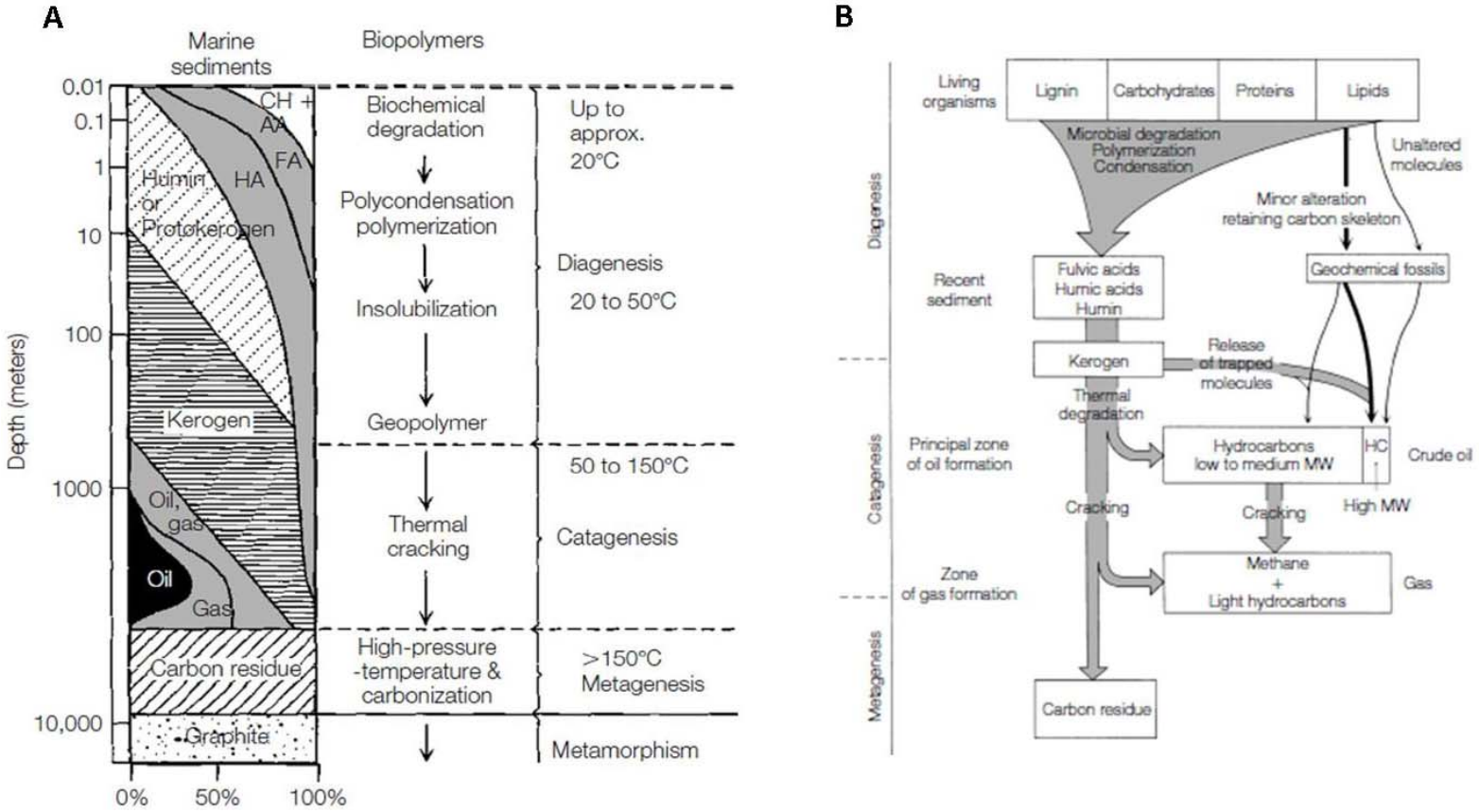

Figure 4. **A**. A general outline of the changes that occur in OM during diagenesis, catagenesis and metamorphism. The relative abundances of the various forms of OM are shown on the x-axis.**CH**. chlorophyll; **AA.** amino acids; **FA**. fulvic acids; **HA.** humic acids; **B**. The petroleum maturation process (from Libes, 2009).

1.4. Environmental consequences of fossil fuel consumption - hydrocarbon pollution in the marine environment

The anthropogenic use of fossil fuels has greatly increased the amount of sulphur and carbon in the atmosphere and ocean while depleting the sedimentary rock sink (Brimblecombe *et al.*, 1989). Without this anthropogenic intervention, sulphur and carbon mobilization would last for millions of years until they are uplifted through tectonic events and then released through erosion and weathering processes. Instead, they are being drilled, pumped and burned at a steadily increasing rate, raising the pool of oxidized sulphur (SO_4) and carbon ($C0_2$) in the global cycles at the expense of the storage of reduced forms in the Earth's crust.

In addition to the direct consequences of the increased fossil fuel consumption, those related to the global change reported during the last decades (e.g.. increased concentrations of green house gases, ocean acidification, pollution, etc), there are important consequences associated to the crude oil production, refining and distribution (e.g. uncontrolled releases, discharges during transportation or disposal by end users) (Gertler *et al.*, 2010).

Overseas oil transportation is since 1861 one of the most important ways for crude oil distribution around the world, but also represents one of the most obvious sources of hydrocarbon pollution of the seas (Gertler *et al.*, 2010). Contemporary, the Earth's largest oil fields in the Persian Gulf and Arabian countries were made available to the global markets. Because pipelines could not be constructed through the politically instable region of the Near East, the construction of oil tankers was booming, leading to the construction of larger and larger crude oil carriers (Spyrou, 2006).

Worldwide marine coasts are scattered with oil spills due to accidents or inadequate practices (Figure 5; Psarros *et al.*, 2010). The release of thousands of tons of hydrocarbons affects the marine environment and causes severe ecological and economical damage. For example, only the pollution resulting from the deliberate washing of tanks or ballast water from shipping has been estimated in about 2 million tons per year worldwide. The recent spillages of 780, 000 m^3 of oil into the Gulf of Mexico (Mitsch, 2010) (Figure 6) proves again that human activities may cause a contamination without precedents in marine environments.

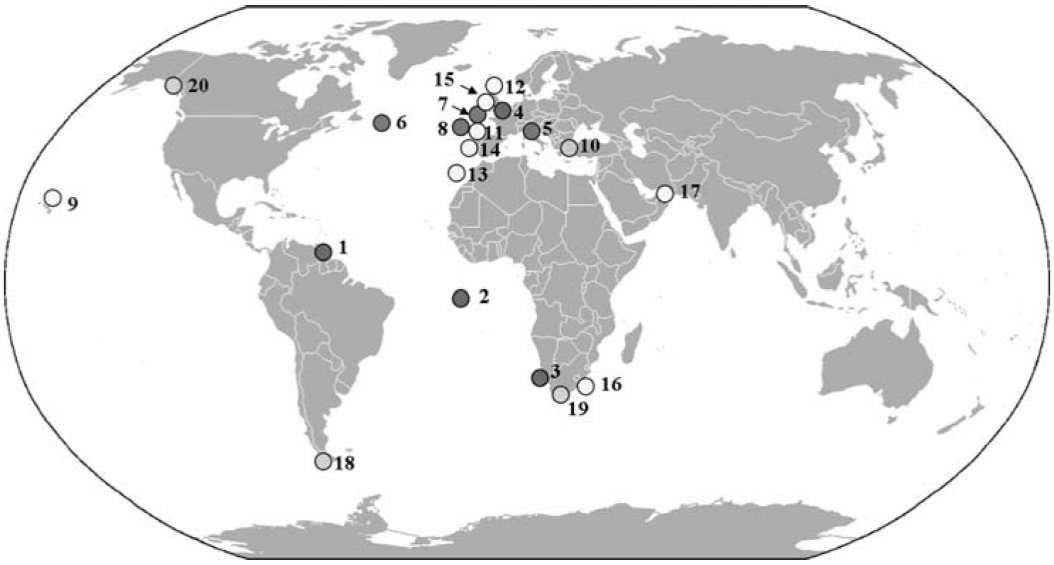

Figure 5. Positions of the 20 largest tanker-related oil spills (50,000-200,000 tons); **1** – *Atlantic Empress* (1979), **2** – *ABT Summer* (1991), **3** – *Castillo de Bellver* (1983), **4** – *Amoco Cadiz* (1978), **5** – *Haven* (1991), **6** – *Odyssey* (1988), **7** – *Torrey Canyon* (1967), **8** – *Urquiola* (1976), **9** – *Hawaiian Patriot* (1977), **10** – *Independenta* (1979), **11** – *Jakob Maersk* (1975), **12** – *Braer* (1993), **13** – *Khark* 5 (1993), **14** – *Aegan Sea* (1989), **15** – *Sea Empress* (1996), **16** – *Katina P* (1992), **17** – *Assimi* (1983), **18** – *Metula* (1974), **19** – *Wafra* (1971), **20** – *Exxon Valdez* (1991) (from Gertler *et al.*, 2010).

Figure 6. Image captured by NASA's Aqua satellite at Gulf of Mexico on July 14th, 2010.

The consequences of these events, together with the impact of the 1.7–8.8 million tons of hydrocarbons that annually enter the marine environment from both anthropogenic and natural sources, are difficult to predict (Berthe-Corti and Nachtkamp, 2010).

With an expected increase of world oil demand of 50% by 2025 (US Department of Energy, 2006), oil pollution is likely to remain a significant threat to marine ecosystems (Ince *et al.*, 2010).

1.5. Hydrocarbon pollution in the Mediterranean Sea

Due to its geographical location, the Mediterranean Sea is the main overseas rout for crude oil transport from the Middle East to the ports in Europe and North America (Ferraro *et al.*, 2007).

With an extension of 2.5 x 10^6 km^2 the Mediterranean Sea connects the European, Asiatic and African continents covering 0.8% of the world's oceans (Figure 7). It is an almost closed basin with a very slow water renewal (over one century) based in the inflow of surface water from the Atlantic Ocean through the Gibraltar Straight (300 m depth, 14 km width). It has been classified as an oligotrophic to ultraoligotrophic environment due to its low nutrient content (mainly inorganic phosphorus) and chlorophyll pools (Siokou-Frangou *et al.*, 2010). However, it hosts a 7.5% of the world's marine animal taxa and 18% of the world's marine flora which had evolved over millions of years in a unique mixture of temperate and subtropical elements. The large proportion of endemic species (28%) makes this area a hot spot of marine species diversity (Laubier, 2005).

The 46.000 km of the Mediterranean coasts, 40% represented in islands, host one third of the population of the adjacent states (Laubier, 2005), which are in constant economic expansion due to the development of a strong tourism sector. The high transit through the main Mediterranean routes (Figure 8.A) of oil and freight carriers, fishery and pleasure boats, leads to the release of about 883,000 tons of oil every year. This volume represents a 20% of the global oceanic oil pollution in a region that covers less than a 1% of the world ocean's (Gómez, 2003). This fact, coupled with the scarce water renewal in the basin, had made the Mediterranean region one of the most polluted in the world and the third most important hot spot of oil spills from vessels

worldwide (Figure 8.B) (O'Rourke and Connolly, 2003) which result in negative impacts on fragile ecosystems, on the quality of life of the resident populations and the loss of habitats and species.

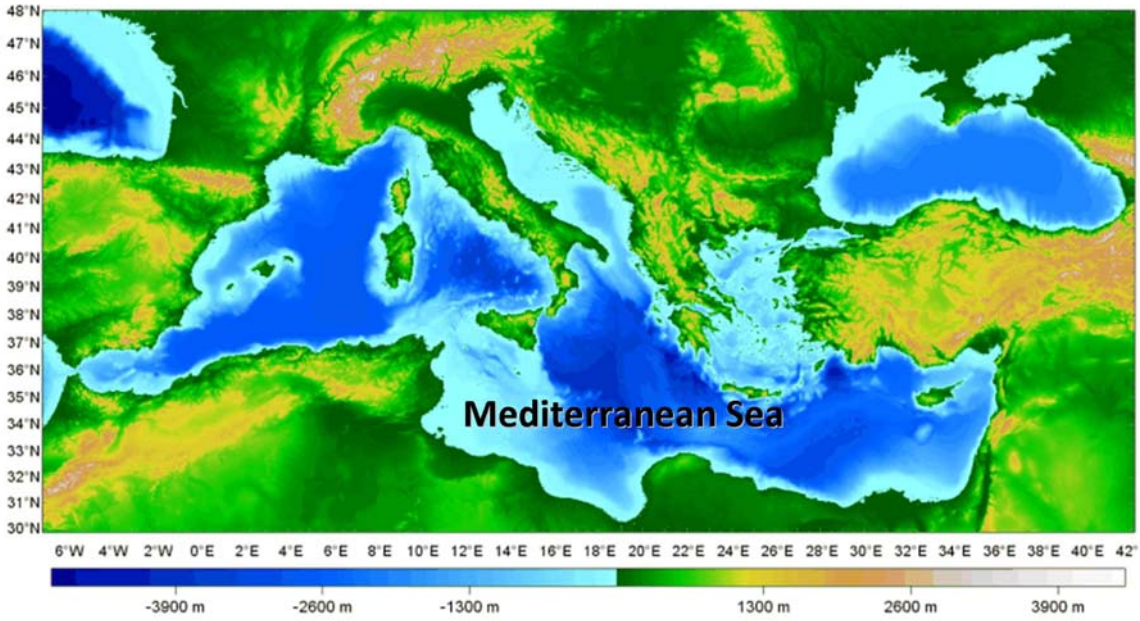

Figure 7. Topographic and bathymetric map of the Mediterranean basin (http://www-3.unipv.it/cibra/edu_Mediterraneo_uk.html).

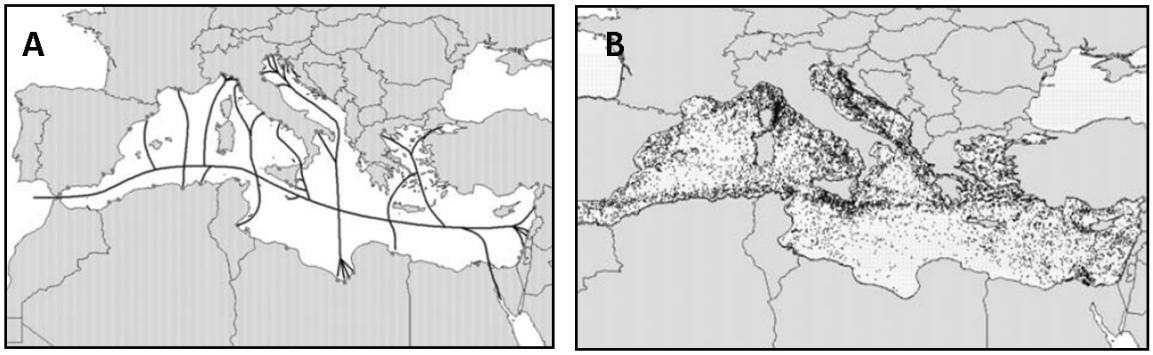

Figure 8. **A**. Main transit routes in the Mediterranean Sea and **B**. oil spills (black spots) detected from 1999 to 2004 (modified from Ferraro *et al*., 2007).

1.6. Fate and behaviour of the crude oil in the marine environment

From the first seconds since crude oil enters in contact with the seawater, a series of transformation processes start due to the interaction of physical, chemical, and biological mechanisms (Figure 9). The progression, duration, and result of these

transformations depend on the properties and composition of the crude oil itself, the parameters of the actual oil spill, and the environmental conditions (Patin, 1999).

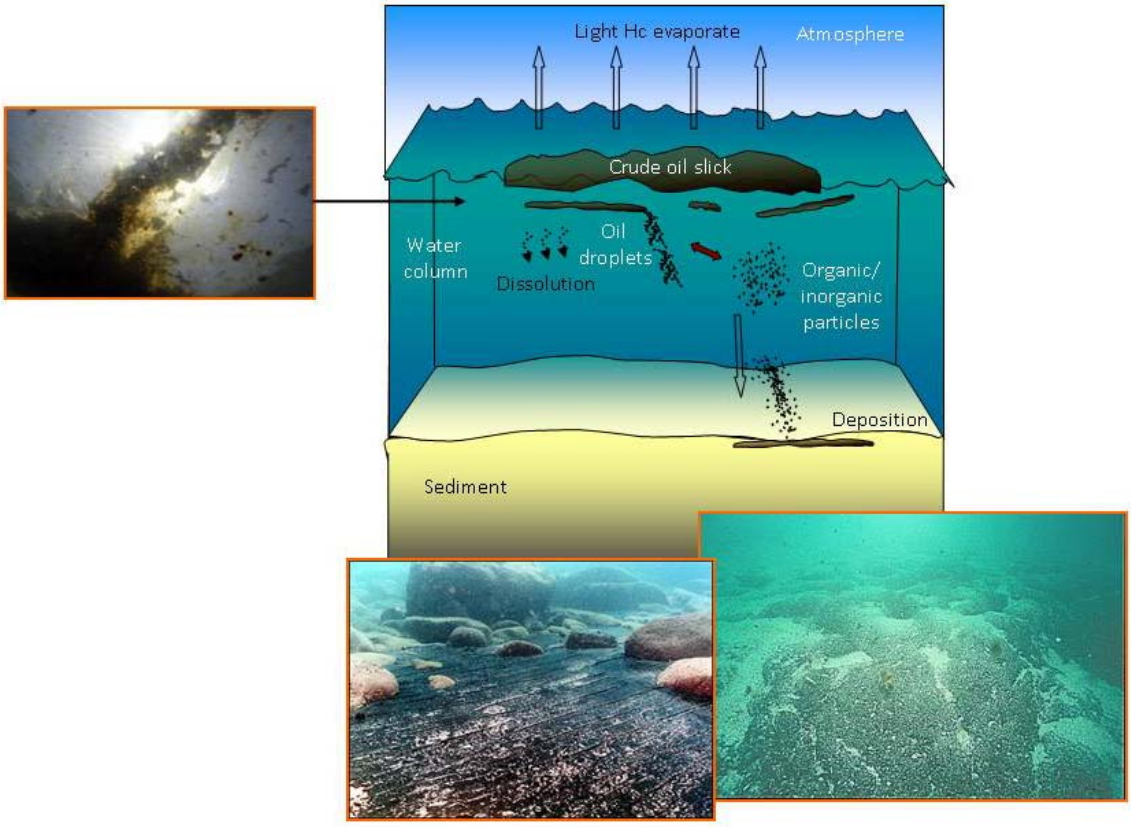

Figure 9. Distribution of crude oil in the marine environment after an oil spill event.

During the first days after an oil spill a fraction of the hydrocarbons in the slick transforms into the gaseous phase and evaporates to the atmosphere, while the water-soluble fraction dissolves in the water column (e.g. low-molecular-weight aliphatics and aromatics). Hydrodynamic and physicochemical conditions in the surface waters strongly affect the rate of these processes.

The more viscous fractions slow down the slick spreading that usually drifts in the same direction as the wind. However, when the slick gets thinner, especially after the critical thickness of about 0.1 mm, it disintegrates into emulsions or aggregates that spread over larger distances.

On the water surface, oxidative transformations occur, usually involving photochemical reactions (e.g. photolysis). As a result, there is a decomposition of the

most complex molecules into more soluble products (hydroperoxides, phenols, carboxylic acids, ketones, aldehydes, etc) that may have higher toxicity as well. The result is an increased oil viscosity and the formation of solid aggregates.

Up to 10-30% of the oil sticks to suspended organic and inorganic particles and undergoes intense chemical and microbial decomposition (Patin, 1999).

Microbiological processes of oil degradation include enzymatic reactions based on oxygenases, dehydrogenases, and hydrolases. These cause aromatic and aliphatic hydrooxidation, oxidative deamination, hydrolysis, and other biochemical transformations of the original oil substances and the intermediate products of their degradation.

The degree and rates of hydrocarbon biodegradation depend on the structure of their molecules. With increasing complexity of molecular structure (increasing number of carbon atoms, degree of chain branching or aromaticity) and molecular weight, the rate of microbial decomposition decreases. The most important environmental factors that influence hydrocarbon biodegradation include temperature, concentration of nutrients and oxygen and, of course, species composition and abundance of oil-degrading microorganisms in the environment (Patin, 1999).

But some of these particles with attached hydrocarbons are transported to bottom sediments where they may accumulate and reach higher concentrations than in the water column (Hayes and Lovley, 2002; Berthe-Corti and Nachtkamp, 2010). In the sediments, the decomposition rates of the buried hydrocarbons abruptly decreases, especially under anaerobic conditions. The heavy oil fractions accumulated inside the sediments can be preserved for many months and even years (Patin, 1999).

2. Ecological relevance of coastal ecosystems

Coastal ecosystems play an essential role in the regulation and maintenance of ecological processes and life support systems on Earth. In the near shore waters phytoplanktonic organisms, both *Bacteria* and *Eukarya*, take advantage from the high concentration of nutrients in the seawater and transform the solar energy into

biomass. In the continental shelves, covering less than 10% of the oceanic waters (Wollast, 1991) (Figure 10), this process generates about 30% of the total oceanic primary production and promotes the transfer of minerals and energy through the food chains (secondary production).

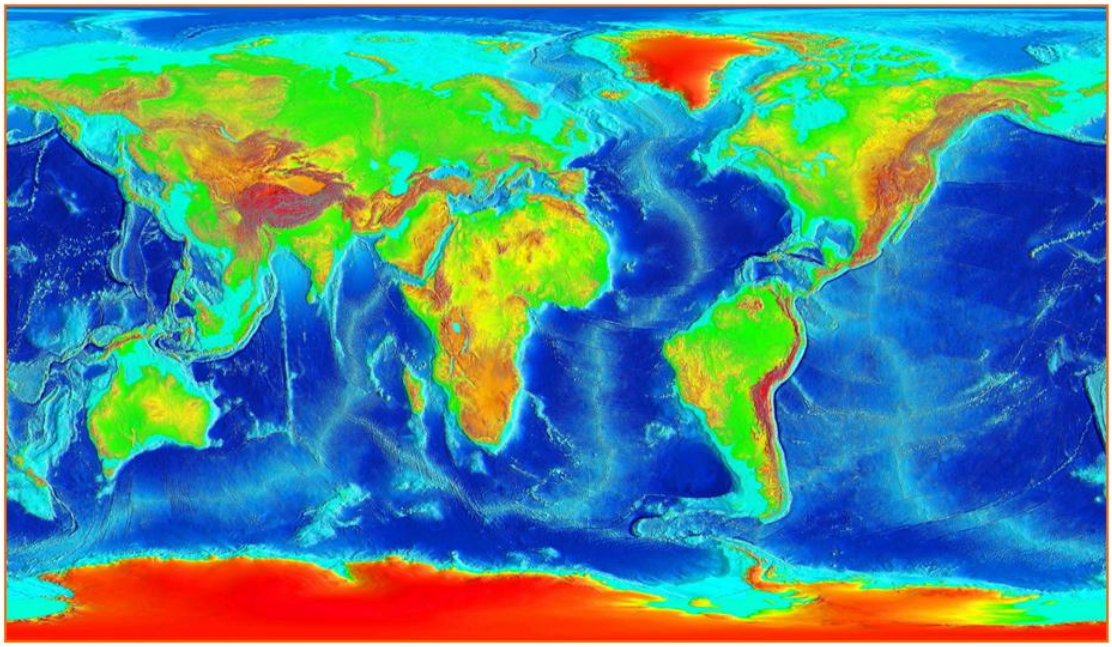

Figure. 10. The global continental shelf (highlighted in cyan) (Source: NOOA, US)

Annually, about 5 to 10 billion tons of biomass produced by marine organisms, mainly as functional, structural, carbon and energy storage components (e.g. amino acids, carbohydrates and lipids), sink and eventually accumulate in the ocean floor (Table 1). Globally, the total organic carbon (TOC) content of marine sediments ranges from 2.5 to 20 mg C g_{dw}^{-1} (Burdige, 2006) and constitutes the largest global reservoir of organic carbon in the biosphere (Parkes *et al.*, 2000).

Up to 50% of this OM is mineralized in the seafloor by the metabolic activity of microorganisms (Rowe *et al.*, 1988; Wollast, 1991; Bacon *et al.*, 1994; Huettel and Rusch, 2000). This fact points out to the importance of these areas in the regulation of the biogeochemical cycles of carbon, nitrogen, sulphur and other nutrients through the biosphere (Burdige, 2006), as well as the need to understand the wide range of metabolic processes carried out by the inhabiting microbial community.

Table 1. Percentages of the main OM constituents that annually sink in shallow water sediments.

Source		% in organisms	% in sediments	% undergoing mineralization
Amino acids	Proteins (enzymes, hormones, peptidoglycans) Nonproteint (β-alanine, γ- or α-aminobutyric acid)	30-70	10-30	10-60
Carbohydrates	Cellulose, lignin and chitin	20-40	5-20	5-15
Lipids	Hydrocarbons, wax esters, triacylglycerols, sterols, glycolipids, phospholipids, chlorophyll, carotenoids	5-25	3-5	17

2.1. Marine sediments

Marine sediments cover about 70% percent of the Earth's surface (Parkes *et al.*, 1994; Rochelle *et al.*, 1994) and are composed of two phases: i) an aqueous phase, formed by the interstitial waters, where most of the biogeochemical reactions occur, and ii) a solid phase, that greatly constrains the physical properties of the sediment.

Sediments can be classified attending to the grain size of the solid phase (from fine mud to coarse gravels) or to their origin and composition. Based in this last property we may differentiate three major types of marine sediments (Chester, 2000; Fütterer, 2006):

1. Lithogenic: formed by detrital particles of terrigenous origin deposited on coastal zones, large estuaries and shelves.

2. Biogenic: directly produced by organism's oozes or skeletal remains. Siliceous components from diatoms predominate in cold regions, while calcareous particles from foraminifera, coccolithophores and molluscs shells are mainly found in warmer sediments, as those from the Mediterranean Sea.

3. Hydrogenic: formed by direct precipitation of dissolved components or chemically modified particles from the water column.

2.2. Carbonated sediments

Carbonated sediments from biogenic origin are one of the most abundant types of marine sediment in the Earth (Figure 11) (Canals and Ballesteros, 1997).

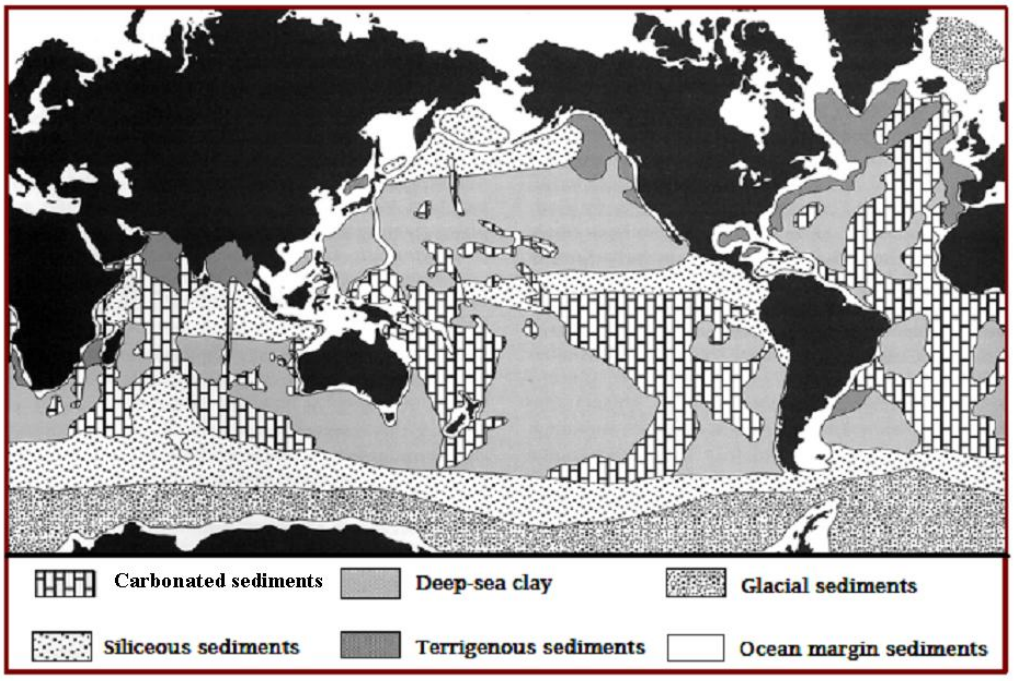

Figure 11. General distribution and type of marine sediments (from Chester, 2000).

The most important production systems of carbonates at global scale are the continental shelves (Canals and Ballesteros, 1997). Coralline, red and green algae provide the highest rates of carbonate production in shallow areas (not deeper than 90 m) of the Western Mediterranean Basin. However, the contribution of organisms associated to seagrass meadows (epiphytes, polychaetes and foraminifera) is also significant due to the extensive areas that these meadows occupied (Canals and Ballesteros, 1997). This is especially true in the coast of the Balearic Islands where the lithogenic (terrigenous origin) fraction is small due to the lack of rivers and land runoffs. Carbonate contents ranging from 77 to 84% had been reported in the

Mallorca-Menorca shelf with an average production of 100 g m^{-2} $year^{-1}$ (Alonso *et al.*, 1988).

2.3. Coastal sandy sediments as biocatalytical filters

Permeable sands are the most common sediments in coastal environments (Riggs *et al.*, 1996), as they cover approximately 70% of the continental shelves (Emery, 1968). In contrast to fine-grained cohesive sediments, where the main transport mechanism is molecular diffusion, in permeable sediments the pore water can flow through the interstices. Pressure gradients are developed at the sediment water interface when bottom currents interact with small surface topography (e.g. ripples, mounds, funnels generated by benthos fauna). The water and its suspended particulate matter is force into the sediment, while the pore water goes out of the bed causing advection transport of solutes and particles (Figure 12) (Huettel and Rusch, 2000).

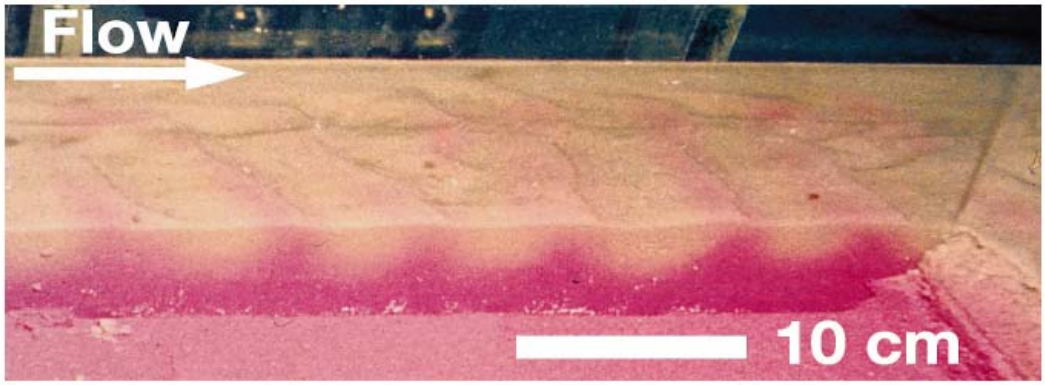

Figure 12. Advective pore water transport in permeable sediment in a laboratory experiment. Red tracer dye shows the flushing of pore water from the sediment due to the advective pore water flows caused by unidirectional bottom flow (Photo by: M. Huettel, COSA Project, 2003).

The velocity of this advection transport can exceed that of molecular diffusion by orders of magnitude (Huettel, 2003) providing a fast carrier for the exchange of substances (substrates and electron acceptors) between the water column and the upper sediment layers (Huettel and Rusch, 2000). More than 90% of the bacteria that live in the surface layers of permeable marine sands are attached to the sand grains, and these organisms process and degrade the substances that are filtered through the bed converting the sands into biocatalytical filters (Huettel, 2003).

2.4. Dynamic ecology of sandy sediments

Sandy sediments had been considered geochemical deserts that harbour no life due to their usually low concentration of OM and other reactive substances. But another reason had been the reported negative correlation between organic carbon content and median grain size. Maximum organic carbon contents (1-5%) are at about 10-20 µm median grain size from which they rapidly decrease to <0.05% at grain sizes >200 µm (Boudreau *et al.*, 2001). However, observations of OM degradability at shelf and coastal sediments, from different locations and different temperature regimes, had shown a positive relationship between degradability and grain size (Figure 13).

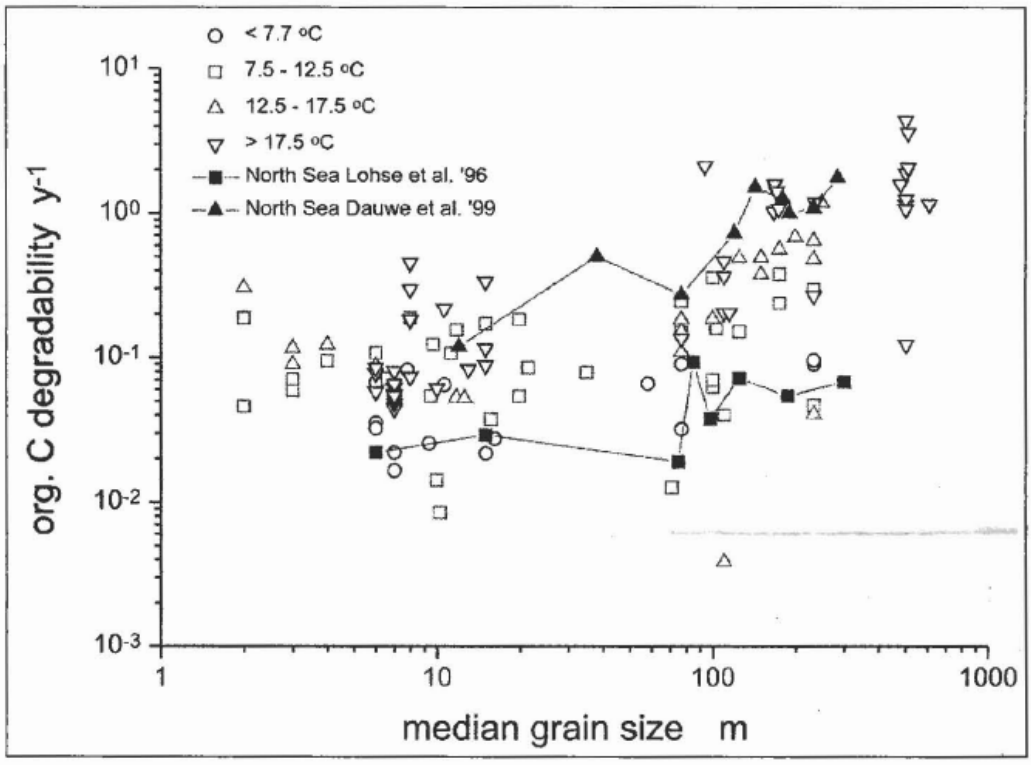

Figure 13. Estimated degradability of OM in shelf and coastal sediments from Australia, Europe and North America, at different temperatures, plotted *versus* the median grain size (from Boudreau *et al.*, 2001).

Several pioneering (Riedl and Macmahan, 1969; Riedl and Machan, 1972; Mclachlan *et al.*, 1985; McLachlan and Turner, 1994) and also more recent studies (Anschutz *et al.*, 2009) in sands of exposed beaches, suggest that filtration through the sands represents a mechanism that enhance the decomposition of OM in the coastal zone.

Altogether, those results point out to permeable sediment as a fundamental component to understand the biogeochemical cycles of the biogenic components (Middelburg and Soetaert, 2004).

2.5. Biogeochemical gradients in marine sediments - Diversity of ecological niches

Both physical and chemical properties of the sediments (e.g., size, quality of particulate OM, variations in sedimentation rates, etc) are influenced by environmental parameters (e.g. seasonal variation in the temperature, oxygen content, nutrient fluxes, primary production, salt concentration, freshwater or organic inputs, the existence of plant roots or burrow macrofauna) which make them highly variable habitats. This variability is reflected by the wide range of suitable ecological niches for highly diverse microbial communities (Fenchel *et al.*, 1998; Llobet-Brossa *et al.*, 1998; Rosselló-Móra *et al.*, 1999; Holmer *et al.*, 2004), and a high diversity of biogeochemical processes (Danovaro *et al.*, 2001; Tankéré *et al.*, 2002).

In shallow-water sediments, especially in those with high rates of primary production, OM production and deposition usually overcome the oxygen availability for mineralization processes, and it is already depleted within the first millimetres beneath the surface (Llobet-Brossa *et al.*, 1998). The further decomposition of OM at the suboxic and anoxic layers is generally mediated by chemoorganotrophic mutualistic microbial consortia (Kristensen *et al.*, 1995) which respiration processes are based on different inorganic electron acceptors.

The occurrence of specific respiratory processes appears to be controlled by the free energy yield (ΔG^o) per mol of organic carbon oxidized by each kind of electron acceptor (Froelich *et al.*, 1979; Burdige, 2006, 2007). The sequence of electron acceptors shows that oxidants are consumed in a predictable order with preferential use of electron acceptors yielding higher ΔG^o (Figure 14).

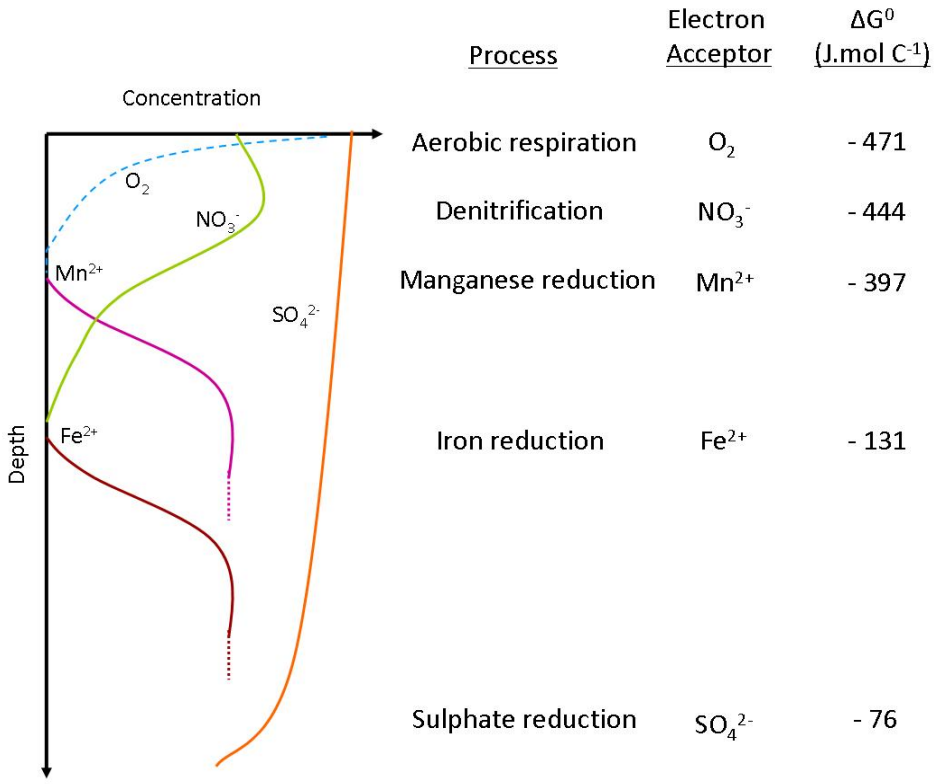

Figure 14. Pore-water profiles predicted by successive utilization of inorganic terminal electron acceptors during the remineralisation of OM in marine sediments (modified from Burdige, 2006).

As a general trend it is observed a vertical stratification in decreasing redox potential (O_2 > NO_3^- > Mn (IV) > Fe (III) > SO_4^{2-}), OM quality, and overall metabolic activity across depth (Fenchel *et al.*, 1998; Kristensen and Holmer, 2001; Llobet-Brossa *et al.*, 2002). Marine sediments also harbour a wide range of chemolithotrophic prokaryotes which metabolisms are not based on organic compounds, but inorganic chemicals, to obtain energy. Most of them have an autotrophic way of life as they obtain all their carbon from CO_2. Although they do not contribute directly to the mineralization of the OM, the end products of their metabolism are substrates that may play as electron acceptor in the metabolism of anaerobic chemoorganotrophs (Figure 15).

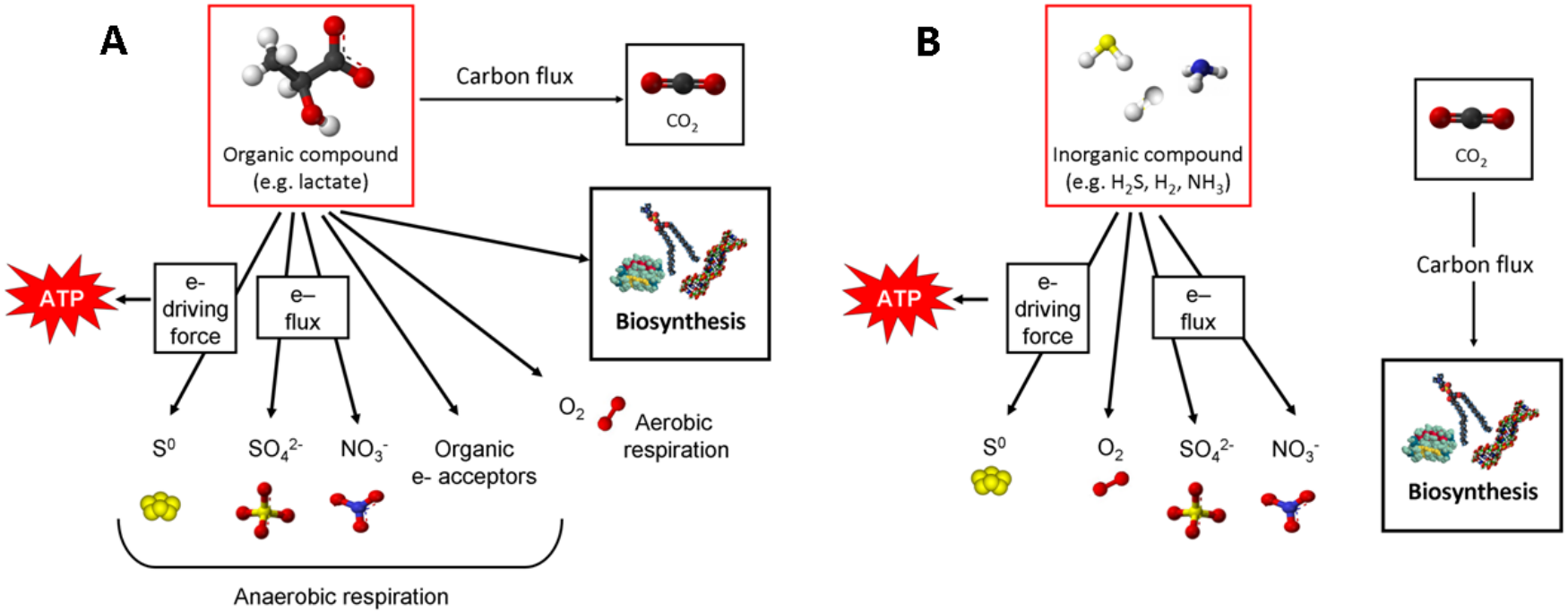

Figure 15. Energy and carbon fluxes in **A**. chemoorganotrophic and **B**. chemolithotrophic metabolisms. In the molecular structures, the colours make reference to the carbon (black), hydrogen (white), sulphur (yellow), oxygen (red) and nitrogen (blue) atoms.

2.5.1. Relevant microbial chemoorganotrophic metabolisms in marine sediments

2.5.1.1. Aerobic respiration

The aerobic respiration is the most efficient process in terms of energy acquired per mol of carbon oxidized (Figure 16). Oxygen serves as terminal electron acceptor but also as a reactant in the oxygenase-catalyzed primary attack of substrate molecules. The first function may be transferred to other oxidized compounds as sulphate or nitrate (in the absence of O_2) but there is no equivalent to O_2 that can fulfil its function as a reactant (Wakeham and Canue, 2006). Aerobic metabolism is generally more direct than the anaerobic due to the involvement of diverse enzymes, many of which are specific to individual types of organic functional groups, and therefore each substrate is often rapidly and completely metabolized to CO_2 and biomass by a single microorganism (Canfield, 1994). As a result, the concentration of O_2 usually decreases with the sediment depth.

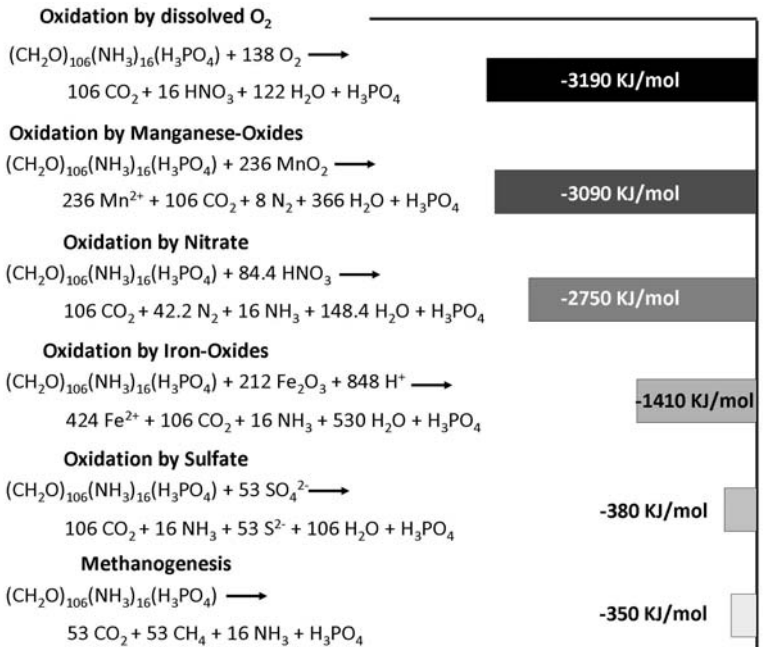

Figure 16. Schematic representation of the redox reactions in the biogeochemical decomposition of organic substances in marine sediments. The reactions are shown in the order of decreasing energy yields for the microorganisms involved (modified from Schulz, 1999).

The aerobic metabolism is mainly carried out by heterotrophs (e.g. *Pseudomonas* spp., *Flavobacterium* spp., *Bacillus* spp., etc). Some of them are facultative aerobes,

therefore when O_2 is depleted they have the possibility to switch to alternative pathways as fermentation, the reduction of nitrate or other metals for their survival (Nealson and Stahl, 1997). In this fermentative metabolism, through disproportionation of organic carbon, volatile fatty acids (acetate, lactate, pyruvate, etc) and H_2 are produced as end products that constitute the main substrates for different anaerobic bacteria (e.g. sulphate-, manganese- and iron-reducers). Members of *Bacteroidetes-Chlorobi* phylogenetic cluster had been proposed as one of the major fermenting groups in marine sediments (Rosselló-Móra *et al.*, 1999).

2.5.1.2. Denitrification

Due to the aerobic metabolism, the concentration of O_2 decreases with depth, while the nitrate concentration increases as a result of nitrification coupled to aerobic respiration. When the O_2 concentration falls bellow 2-8 µM, nitrate becomes the preferred electron acceptor as the denitrification provides a greater amount of ΔG^o per mol of carbon oxidized than the aerobic oxidation (Burdige, 2006).

However, in most marine environments, denitrification accounts for less than 4 % of the total carbon oxidation (Jørgensen, 1982). This fact may be related to its relatively low concentration in the seawater (30 µM), to processes in which nitrate is reduced to ammonium (nitrate fermentation or nitrate ammonification) (Sørensen, 1987; Koike and Sørensen, 1988; Fenchel *et al.*, 1998; Burdige, 2006), or to an inhibition of the denitrification process by high sulphide concentrations (An and Gardner, 2002; Burdige, 2006).

The phylogenetic distribution of denitrification among the prokaryotes does not follow a distinct pattern. The reaction is carried out by a diversity of bacteria belonging to various subclasses of the *Proteobacteria* (e.g. *Alpha*- and *Betaproteobacteria*), but it also extends to the *Archaea*, where it has been found among the halophilic and hyperthermophilic branches (Zumft, 1997).

2.5.1.3. Manganese and iron reduction

In the sequence of redox processes, Mn (IV) and Fe (III) reduction begins after depletion of O_2 and nitrate, and they can be chemically or microbiologically mediated (Thamdrup *et al.*, 2000). Unlike the other respiratory processes discussed here,

reduction of Mn and Fe oxides uses solid rather than dissolved electron acceptors (reduced forms are usually soluble while oxidized forms are highly insoluble) (Burdige, 2006). Thus, if metal oxide reduction is used for respiration, the responsible organism needs a way to couple electron transport to metal oxide reduction. In many cases this is accomplished by direct contact with the solid oxides (Nealson and Saffarini, 1994), electron shuttling compounds or Fe (III) chelators (Nevin and Lovley, 2002).

These metabolic pathways are believed to be of secondary importance in the overall oxidation of sedimentary organic carbon (Canfield *et al.*, 1993b). Nevertheless, in environments where Mn oxides are abundant, dissimilatory Mn reduction can be the dominant pathway for organic carbon oxidation (Aller, 1990; Canfield *et al.*, 1993a; Canfield *et al.*, 1993b; Vandieken *et al.*, 2006). Dissimilatory Fe reduction has been shown to be the first or second most important pathway of organic carbon oxidation in many shelf sediments (Canfield *et al.*, 1993b; Thamdrup and Canfield, 1996; Jensen *et al.*, 2003; Magen *et al.*, 2011).

Manganese and Fe oxides reducers belong to diverse phylogenetic bacterial groups (e.g. *Geobacter*, *Desulfuromonas*, *Pelobacter, Shewanella*, *Geovibrio* and several Gram-positive microorganisms). Also fermenters, methanogens and sulphate-reducing bacteria had been observed to use them as electron acceptors (Lovley, 1991; Lovley *et al.*, 1993; Bond and Lovley, 2002).

2.5.1.4. Sulphate reduction

Sulphate is one of the most abundant electron acceptor in marine sediments (in seawater up to 28 mM) (Thauer *et al.*, 2007). Due to the low ΔG^{o} of sulphate reduction, this metabolism is relegated to a much later point in the sequence of stratification, when most of the other electron acceptors have been exhausted (Figure 14 and 16) (Lam and Kuypers, 2011). However, sulphate reduction had been estimated to produce energy enough to carry out the mineralization of about 50% of the deposited material in continental shelves (Jørgensen, 1982). In organic rich sediments, sulphate respiration accounts for up to 70–100% of the microbial metabolism (Kristensen, 2000; Holmer *et al.*, 2003) which indicates the importance of sulphate-reducing bacteria (SRB) for the sulphur and carbon cycles.

Most of the SRB described to date belong to four main lineages: i) mesophilic *Deltaproteobacteria* (e.g. *Desulfovibrio*, *Desulfobacterium*, *Desulfobacter*, *Desulfobulbus*); ii) thermophilic Gram-negative bacteria (e.g. *Thermodesulfovibrio*); iii) Gram-positive bacteria (e.g. *Desulfotomaculum*) and iv) *Euryarchaeota* (e.g. *Archaeoglobus*) (Thauer *et al.*, 2007).

Many SRB may use electron acceptors other than sulphate for anaerobic respiration (S^0, fumarate, nitrate, dimethylsulfoxide, Mn (IV) and Fe (III)). Sulphate reduction is inhibited by the presence of O_2 but some SRB are capable of aerobic respiration. Although this process is not sustaining growth it may provide with energy for maintenance (Thauer *et al.*, 2007).

Common electron donors and carbon sources for SRB are the low molecular mass products produced in the primary anaerobic (mainly fermentative) breakdown of carbohydrates, proteins and lipids, such as low molecular weight fatty acids (lactate, acetate, propionate and butyrate), aromatic compounds, alcohols, amino acids, and H_2. Some groups of SRB oxidize these carbon compounds only to acetate (incomplete oxidizers, e.g. *Desulfovibrio*), while others can completely oxidize them to CO_2 (complete oxidizers, e.g. *Desulfobacter*).

2.5.1.5. Methanogenesis

Methane production only occurs by the hand of *Archaea* when the sediment becomes highly reducing and the sulphate is almost completely exhausted (< 1 Mm). This zonation appears to occur because sulphate reducers outcompete for acetate and H_2, substrates that are used by both groups of organisms. There are two major types of methanogenesis: i) the acetate disproportionation that yields CH_4 y CO_2 as products (e.g. *Methanosarcina*) and the CO_2 reduction yielding CH_4 and H_2O, *Methanobacterium*, *Methanococcus*) using only CO and formate as carbon substrates. Some organisms may produce methane using methanol and certain methyl amines. This type of methanogenesis appears to be the most important source of the small amounts of methane that are produced in anoxic sediments (Burdige, 2006).

2.5.1.6. Chemolithotrophic metabolisms in marine sediments - Linkages with the organic matter mineralization

As mentioned above, in addition to the redox reactions involving organic carbon oxidation, the oxidation of inorganic substances also take place in the marine sediments. The reduced end-products from the aerobic and anaerobic respiration (e.g. ammonium, Fe (II) and Mn (II), sulphide, methane) are substrates for chemolithotrophic organisms (e.g. methanotrophs, nitrifying, sulphur-oxidizing and metal oxidizing bacteria) and to abiotic oxidation processes, which leads to an internal redox cycling of these elements in the sediment (Burdige, 2006), and therefore couple chemolithotrophy to the anoxic OM mineralization.

These processes can be imagine as an electron "shuttle" that brings O_2 oxidation equivalents into the anoxic layers by the coupling with anoxic metabolisms that may occur by pore water diffusive processes. In this way, redox sensitive elements as Mn or S^0 undergo repetitive oxidation-reduction cycles before being buried in the sediment (Figure 17). The occurrence of such as interactions suggests the closed interplay of the biogeochemical cycles of Mn, Fe, N, S, C and O_2 in the marine sediments.

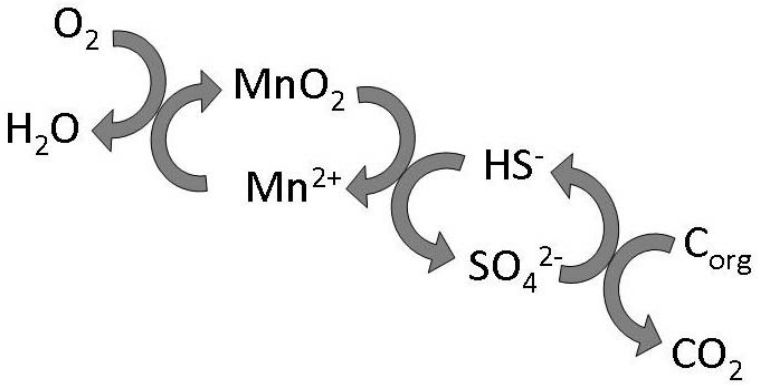

Figure 17. Schematic representation of the coupling of O2, Mn, S^0 and C redox cycling that may occur in some marine sediments (modified from Burdige, 2006).

3. Approaches in the study of microbial ecology in marine environments.

Since 1894, when Professor Bernhard Fischer (Kiel University, Germany) first observed the existence of indigenous bacteria inhabiting the marine environment, several fundamental questions had been open to debate:

- What and how many microbes inhabit the variety of marine environments?
- What are their adaptive strategies for performance and persistence in their environments?
- How does the playing out of their adaptive strategies in the ocean integrate into the structure and behaviour of marine ecosystems?
- How do they respond to anthropogenic disturbances?

The ability of researchers to answer those issues had been subjected to chronic method-limitations (Azam, 2001). However, during the last decades, revolutionary discoveries in marine microbiology had changed our concepts about the structure and functioning of marine ecosystems.

From the pioneering effort of Dr. Claude E. ZoBell (1946), cultivation, microscopy, genetic, genomic, metagenomic, and radiotracer approaches had been developed to provide quantitative information about the abundance, taxonomy and activity of microorganisms, as well as the cycling of the elements within ecosystems (Atlas and Bartha, 1997).

3.1. Culture-dependent techniques for the characterization of microbial communities

Until the 1980's, the studies of marine microbiology were mainly carried out using cultured based techniques. A sufficient biomass required for the analyses, isolation, and purification of microorganisms was obtained by multiplication of cells. This was conveniently achieved using dispersal and dilution techniques, most commonly in an aqueous medium, followed by enrichment on semisolid media that allowed to separated cells proliferate and form visible colony forming units (CFUs) that could be finally enumerated (ZoBell, 1946).

Although the culture-dependent techniques have shown to be selective and do not reflect accurately the overall properties of a microbial community (Amann *et al.*, 1995; Glöckner *et al.*, 1999; Eilers *et al.*, 2000; Ritz, 2007), they had provided isolated microorganisms for biochemical, physiological, or developmental studies. Thus, they have given a context to corroborate the findings of the later developed genetic and genomic approaches (Nichols, 2007).

3.2. Direct enumeration of microorganisms in their environment

The application of DNA intercalating agents, such as acridine orange and 4',6-diamidino-2-phenylindole (DAPI), combined with epifluorescence microscopy (Francisco *et al.*, 1973; Hobbie *et al.*, 1977), to directly enumerate the microorganisms in an environmental sample, had demonstrated that the bacterial biomass is actually higher than determined on the basis of viable counts (Amann *et al.*, 1995; Glöckner *et al.*, 1999; Eilers *et al.*, 2000). The cultivable fraction of organisms present in an environmental sample had been estimated to represent less than 1% of the total number of cells in most of the environments (Table 2) (Amann *et al.*, 1995). The remaining majority of cells visualized by microscopy were shown to be viable, although were not able to form visible colonies on plates (Staley and Konopka, 1985; Roszac and Colwell, 1987). This fact may be related to unsuitable cultivation conditions, for both known and unknown species, or to a change in the physiology of the cells that enter in a viable but uncultivable state (Amann *et al.*, 1995).

Table 2. Culturability determined as a percentage of culturable bacteria in comparison with total cell counts estimated in different environments (from Amann *et al.*, 1995).

Habitat	Culturability (%)[a]
Seawater	0.001–0.1
Freshwater	0.25
Mesotrophic lake	0.1–1
Unpolluted estuarine waters	0.1–3
Activated sludge	1–15
Sediments	0.25
Soil	0.3

[a] Culturable bacteria are measured as CFU.

3.3. Culture-independent techniques for the characterization of microbial communities

3.3.1. 16S rRNA analysis

In the late 1980's, the recognition that phylogenetic relationships between microorganisms can be inferred from molecular sequences (Woese, 1987), and the possibility to selectively amplify genes form small amounts of nucleic acids extracted from environmental samples by the polymerase chain reaction (PCR) (Saiki *et al.*, 1988), permitted the development of culture-independent techniques for the characterization of microbial communities.

After more than 20 years of nucleic acid based analysis of natural microbial communities, the 16S rRNA gene phylogenies have largely stood the test of time in describing the evolutionary relationships between organisms (Ludwig and Klenk, 2001; Rosselló-Móra, 2005).

This gene is present in all the prokaryotes and its product shows functional constancy, as it is part of the ribosomes that are required by all organisms to produce proteins. The gene is sufficiently long (1.5 kb) to be used as a document of evolutionary history and the evidence for horizontal gene transfer of rRNA genes is limited (Woese, 1987). Due to its functional role, its primary and secondary structure is constrained. 16S rRNA consists of several sequence domains that have evolved at different rates. Some domains have remained almost universally conserved while other interspersed regions are more variable and specific for phylum up to the subspecies level. This permits unambiguous alignment of homologous positions in a sequence and the identification of near universally conserved and taxon-specific signature motifs (Röling and Head, 2005). Those highly conserved domains serve as templates for designing amplification primers that are used to retrieve 16S rDNA sequences from microorganisms, even from those not amenable to cultivation, from environmental samples.

Several approaches, from the construction of 16S rRNA gene clone libraries to the fingerprinting techniques (those based on the generation of characteristic band patterns for a given community such us: denaturing and temperature gradient gel electrophoresis (DGGE and TGGE), single-strand conformation polymorphism (SSCP) and terminal-restriction fragment length polymorphism (tRFLP)) (Marzorati *et al.*,

2008), had been successfully applied to study temporal and spatial changes in bacterial genetic diversity and to discover new rDNA species (Muyzer *et al.*, 1995; Muyzer and Smalla, 1998).

As a consequence, the number of sequences deposited in public databases has increased exponentially by about three orders of magnitude in approximately 15 years (Figure 18). Most of the sequences deposited correspond to uncultured organisms and only the minority of sequences corresponds to cultured prokaryotes.

However, PCR-based techniques still have shortcomings (e.g. PCR bias due to preferential amplification of certain templates, production of chimerical sequences and the limitation of the amount of sequences that can be gathered by 16S rRNA clone libraries), and that must be taken into account when describing environmental communities (Amann *et al.*, 1995; Eilers *et al.*, 2000; Stach and Bull, 2005).

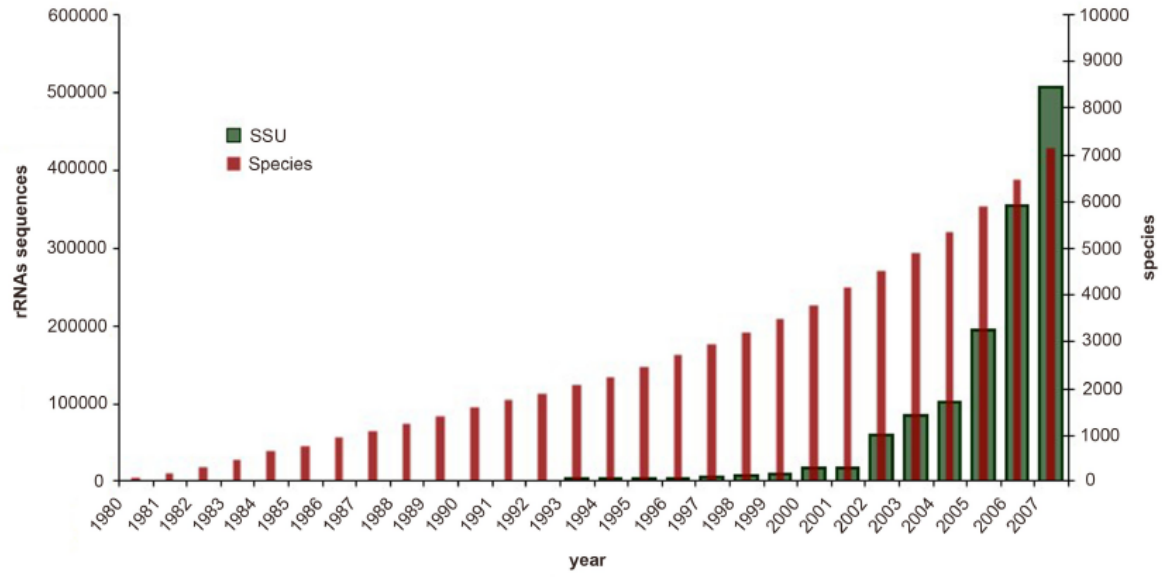

Figure 18. Increase in the number of validated species from 1980 to 2007, and the 16S rRNA sequence (SSU) submissions to public databases until SILVA release 93 (updated to 566.047 sequences) (Yarza, 2011).

3.3.2. In situ *quantification and phylogenetic affiliation*

The development of fluorescence *in situ* hybridization techniques (FISH) provided microbiologists with quantitative means to assess microbial diversity and abundance in the nature, without cultivation or DNA amplification (DeLong *et al.*, 1989; Amann *et al.*, 1995). Hence, the *in situ* hybridization reported about unknown diversity not retrieved before and that hided novel metabolisms (such as the photoheterotrophy in the sea) that forced a re-evaluation of carbon and energy fluxes in the oceans (Pedros-Alió, 2006).

The FISH techniques are based on the utilization of fluorescent labelled oligonucleotide probes that are complementary to signature motifs of the 16S rRNA, universally conserved or taxon-specific (Röling and Head, 2005). Therefore, each probe, under optimized conditions, specifically binds to one ribosome of the target organism. The signal can be detected by epifluorescence microscopy (DeLong *et al.*, 1989; Amann *et al.*, 1995), but the success of the visualization greatly depends on the size and ribosomal content of the target cell.

Thus, FISH must deal with the great challenge to measure specific organism that occurs admixed with diverse assemblages of non-target organisms, particles and detritus. Moreover, the majority of bacteria in aquatic habitats are small, slowly growing or starving, and the signal intensities of hybridized cells are frequently under the detection limits, due to low ribosomal content, or because they are lost in high levels of background fluorescence (Pernthaler *et al.*, 2002).

Those facts had led to the development of brighter fluorochromes to label the probes, image-intensified video microscopy, and protocols for the amplification of the signal by enzymatic reactions. The last approach, also known as catalyzed reporter deposition (CARD), has been successfully used in the hybridization of marine samples (Pernthaler *et al.*, 2002). It is based on the utilization of horseradish peroxidase (HRP) labelled probes and tyramide signal amplification (TSA). After the hybridization with the 16S ribosomal RNA, the HRP catalyzes the deposition of a large number of tyramide-labelled molecules within the target cells, amplifying the signal, with the resulting increase of detection rates in comparison with the original method (Pernthaler *et al.*, 2002). The critical step of this approach is the diffusion of large molecules, such as HRP, into the cells. Therefore, prior to the hybridization it is necessary to include an

optimized permeabilization step in which the permeability and the cellular integrity are balanced.

It is important to remark that in CARD-FISH detection the signal intensity of individual cells can not be linked with potential cellular metabolic activity as is not directly dependent on the number of ribosomes.

3.3.3. Environmental genomics

Our awareness about the unculturable majority of microorganisms in the environment comes from the hand of a great uncertainty about their role on ecosystem functioning and nutrient cycling. Based solely on rRNA gene phylogeny it is difficult, and definitely risky, to predict the physiology of uncultivated microorganisms and therefore their putative role in the environment.

During the last years, microbial ecology research has taken advantage of the technological advances developed on the field of genomics (e.g. mapping, sequencing, and analysing functional aspects of entire genomes), in order to get insights about "adaptive" pool of metabolic, resistance, and defence genes that ensure survival in the environment (Meyerdierks and Glöckner, 2010). In order to assess the genetic information of communities without prior cultivation, the collective genomes from an environmental sample (or in an enrichment of target cells) are extracted and analyzed by a combination of molecular and bioinformatic tools. This approach is commonly known as metagenomics or environmental genomics.

The field of metagenomics is evolving very rapidly, especially due to newly developed high-throughput sequencing technologies and increased computational power. The most extensive metagenomic study hitherto undertaken is the SORCERER II Global Ocean Sampling Expedition (Venter *et al.*, 2004; Rusch *et al.*, 2007), which generated almost around 7.7-30 million of reads.

The addition of metagenomic techniques to the toolbox of microbial ecologists has certainly opened a new window to the study of the metabolic equipment of uncultured microorganisms. Nowadays, the efforts focus in providing functional information of the vast majority of genes retrieved in order to support current and future sequence annotation. In this regard, metatranscriptomics (Poretsky *et al.*, 2005;

Bailly *et al.*, 2007), metaproteomics (Ram *et al.*, 2005; Wilmes and Bond, 2006), and the improvement of cultivation methodologies, are promising.

3.3.4. Integrated approaches in marine microbiology - attempts to close the loop

In the light of the findings achieved in the field of marine microbiology during the last decades, it seems unquestionable that the current understanding of marine ecological systems may only be enriched by the use of polyphasic approaches.

The integration of multidisciplinary approaches, despite of the intrinsic deficiencies of each methodology, fills the gaps existing between genomics, population genetics, biochemistry, physiology, biogeochemistry and ecology (DeLong, 2009).

An accurate deduction of phenotypes, metabolisms and physiologies of the "unknown majority" of microorganisms from marine environments, can only be inferred from laboratory culture-based experiments. However, the lack of knowledge about their nutritional requirements makes very difficult the designing of media and incubation conditions (Alain and Querellou, 2009). In this regard, environmental genetic and genomic information should greatly support the decisions of microbiologists when decide to undertake that challenge. Moreover, the analysis of isolated microorganisms and consortia together with the emerging metatranscriptomics and metaproteomics, are the main information source for the correct functional annotation of the vast majority of genes retrieved from environmental DNA (Meyerdierks and Glöckner, 2010).

On the other hand, the recording of relevant physicochemical characteristics from the environment, as well as the *in situ* monitoring of microbial activities and dynamics, are essential in order to correlate genomic features with habitat properties (Figure 19) (DeLong, 2009).

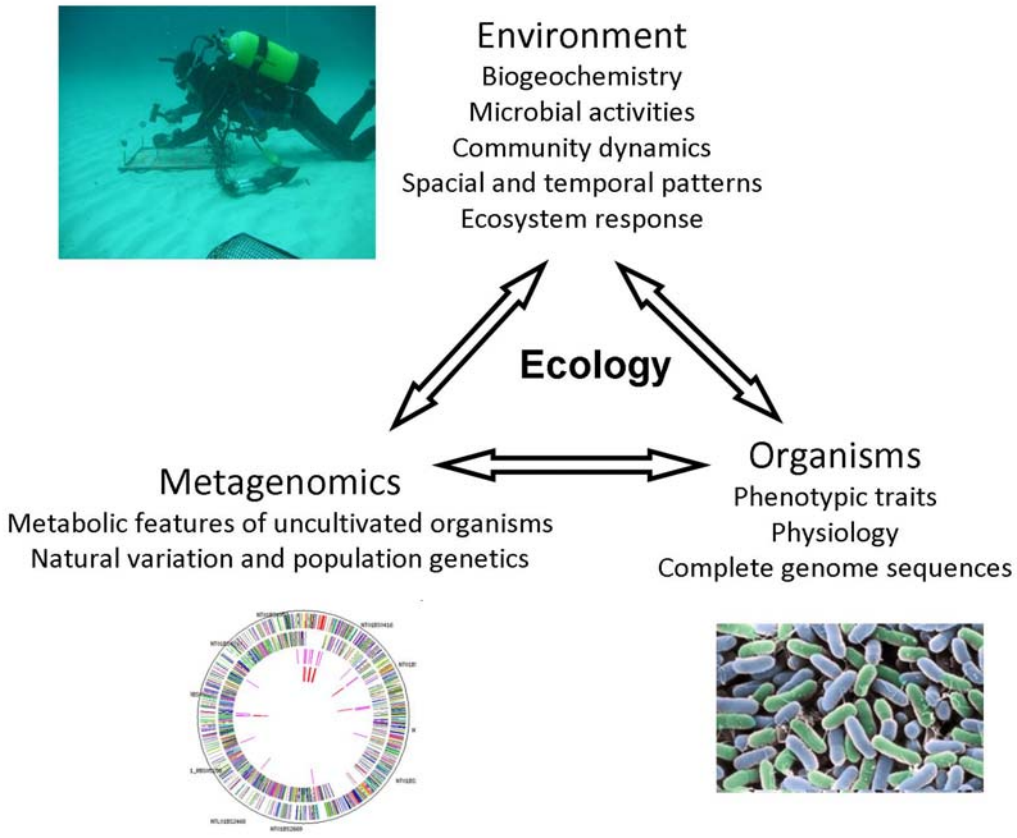

Figure 19. Ideal integrated workflow in the study of ecological marine systems (modified from DeLong, 2009).

Currently, the rate of data accumulation is exponentially growing due to the development of sophisticated and cheaper methodologies for environmental data retrieval. However, the pressure on individual researchers facing ecological issues increments as fast as the databases growth (Peplies *et al.*, 2008; Galperin and Koonin, 2010).

The standardization in the generation, storage and accurate environmental data contextualization, seems the best and unique way to overcome the actual imbalance between the rates of data accumulation and knowledge generation (Meyerdierks and Glöckner, 2010). Therefore, a close collaboration and feedback between disciplines, such as biogeochemistry, geology, geophysics, microbiology, molecular biology and chemistry, taxonomy and bioinformatics, has become essential.

Remarkable are the efforts of projects as for instance:

- Genomic Standards Consortium (GSC), intending to provide richer descriptions of complete collection of genomes and metagenomes (Field *et al.*, 2007; Field *et al.*, 2008).

- Minimum Information about a Metagenome Sequence (MIMS), focusing on the standardization of contextual data acquisition (e.g. GPS coordinates, depth/altitude, sampling time, etc) (http://gensc.org).

- SILVA (http://www.arb-silva.de/) and LTP ("The All-Species Living Tree Project", http://www.arb-silva.de/projects/living-tree/, (Yarza *et al.*, 2008)), generating and updating high quality and non-redundant rRNA databases.

- The ARB and JCoast packages, bioinformatic tools for DNA sequences management (e.g. alignment, comparison and identification) (Ludwig *et al.*, 2004; Richter *et al.*, 2008).

All these projects, together with other not mentioned here but not less helpful, facilitate the workflow to microbial ecologists and are the trigger for a new era in the science of ecosystems biology (Meyerdierks and Glöckner, 2010).

4. Background and aim of the thesis

During the last decades several studies pointed out to microbial communities as the key players in the degradation of the majority of hydrocarbons entering the marine environment (Leahy and Colwell, 1990; Atlas, 1991; Lindstrom *et al.*, 1991; Bragg *et al.*, 1994; Rosenberg *et al.*, 1996; Kostka *et al.*, 2011).

In marine sediments, the degradation of hydrocarbons is limited by similar factors than the organic matter oxidation, such as availability of nutrients (e.g. nitrogen and phosphorous) and oxygen. However, while the aerobic biodegradation of hydrocarbons has been extensively studied for many years, the documentation on anaerobic degradation is relatively recent and mainly related to *in vitro* experiments using isolated strains (Foght, 2008; Widdel *et al.*, 2010).

During the last two decades, hydrocarbon degradation under sulphate-reducing conditions gained interest due to several *in vitro* and *in situ* studies suggesting the

potential of this process for the removal of hydrocarbon in the marine environment (Coates *et al.*, 1997; Hayes *et al.*, 1999; Widdel *et al.*, 2010). Most of the *in situ* studies were carried out on chronically contaminated sediments and showed that oil impact depended on the contamination history of the environment. Thus, the response of bacterial communities previously adapted to the presence of oil would occur faster than in pristine environments as they contained a higher abundance of organisms able to utilize and/or survive toxic hydrocarbons (Coates *et al.*, 1997; Paissé *et al.*, 2008).

Unfortunately, oil spills affect natural environments indistinctly and research concerning their effects on pristine marine sediments is still scarce (Miralles *et al.*, 2007). This assertion is especially true for the Mediterranean environment and the sulphate-reducing communities inhabiting its sediments. Therefore, **the aim of this thesis has been to evaluate the effect of an artificial oil spill over the microbial community inhabiting the sandy sediment of an undisturbed area in the north of Mallorca (Balearic Islands, Spain)**.

Chapter 1 describes the most relevant ecological features of the studied Mediterranean carbonated sediment. Physico-chemical parameters, microbial diversity, abundance and culturability are discussed in order to provide an accurate environmental data contextualization for the following *in situ* and metagenomic experiments.

Chapter 2 focuses in the *in situ* monitorization of the response of sulphate-reducing bacteria (SRB) to the hydrocarbon contamination by a polyphasic approach combining in field mesocosm experiments, molecular biology, cultivation approaches, and metabolic activity rates.

Chapter 3 presents the first insights into the phylogeny and physiology of a Mediterranean SRB hydrocarbon degrading consortium derived from metagenomic and metabolomic studies.

5. References

Alain, K., and Querellou, J. (2009) Cultivating the uncultured: limits, advances and future challenges. *Extremophiles* **13**: 583-594.

Alonso, B., Guillen, J., Canals, M., Serra, J., Acosta, J., Herranz, P., Sanz, J.L., Calafat, A., and Catafau, E. (1988) Los sedimentos de la plataforma continental balear. *Acta Geol. Hisp.* **23**: 185-196.

Aller, R.C. (1990) Bioturbation and manganese cycling in hemipelagic sediments. *Philos. Trans. R. Soc. A.* **331**: 51-68.

Amann, R.I., Ludwig, W., and Schleifer, K.H. (1995) Phylogenetic identification and *in situ* detection of individual microbial cells without cultivation. *Microbiol. Rev.* **59**: 143-169.

An, A., and Gardner, W.S. (2002) Dissimilatory nitrate reduction to ammonium (DNRA) as a nitrogen link, versus denitrification as a sink in a shalow estuary (Laguna madre/Baffin Bay, Texas). *Mar. Ecol. Prog. Ser.* **237**: 41-50.

Anschutz, P., Smith, T., Mouret, A., Deborde, J., Bujan, S., Poirier, D., and Lecroart, P. (2009) Tidal sands as biogeochemical reactors. *Estuar. Coast. Shelf S.* **84**: 84-90.

Atlas, R.M. (1991) Microbial hydrocarbon degradation-bioremediation of oil spills. *J. Chem. Tech. Biotechnol.* **52**: 149-156.

Atlas, R.M., and Bartha, R. (1997) Microbial ecology-fundamentals and applications. Benjamin-Cummings Science Publishing, Menlo Park, California, US.

Azam, F. (2001) Introduction, history, and overview: the 'methods' to our madness. *In* Methods in Microbiology, Marine Microbiology (vol 30). Paul, J.H. (ed.), Academic Press, London, UK, pp.1-12.

Bacon, M.P., Belastock, R.A., and Bothner, M.H. (1994) ^{210}Pb balance and implications for particle transport on the continental shelf, U.S. Middle Atlantic Bight. *Deep-Sea Res.* **41**: 511-535.

Bailly, J., Fraissinet-Tachet, L., Verner, M.C., Debaud, J.C., Lemaire, M., Wesolowski-Louvel, M., and Marmeisse, R. (2007) Soil eukaryotic functional diversity, a metatranscriptomic approach. *ISME J.* **1**: 632-642.

Berthe-Corti, L., and Nachtkamp, M. (2010) Bacterial communities in hydrocarbon-contaminated marine coastal environments. *In* Handbook of hydrocarbon and lipid microbiology. Timmis, K.N. (ed.), Springer-Verlag, Berlin Heidelberg, DE, pp. 2350-2359.

Bond, D.R., and Lovley, D.R. (2002) Reduction of Fe(III) oxide by methanogens in the presence and absence of extracellular quinones. *Environ. Microbiol.* **4**: 115-124.

Boudreau, B.P., Huettel, M., Froster, S., Jahnke, R.A., McLachlan, A., Middelburg, J.J., Nielsen, P., Sansone, F., Taghon, G., Van Raaphorst, W., Webster, I., Marcin Weslawski, J., Wiberg, P., and Sundby, B. (2001) Permeable marine sediments: overturning an old paradigm. *EOS.* **82**: 133-136.

Bragg, J.R., Prince, R.G., Harner, E.J., and Atlas, R.M. (1994) Effectiveness of bioremediation for the Exxon-Valdez oil-spill. *Nature* **368**: 413–418.

Brimblecombe, P., Hammer, C., Rodhe, H., Ryaboshapko, A., and Boutron, C.F. (1989) Human influences on the sulphur cycle. *In* Evolution of the global biogeochemical sulphur cycle. Brimblecombe, P. and A.Y. Lein (eds.), Wiley, NY, pp. 77–121.

Burdige, D.J. (2006) Geochemistry of Marine Sediments. Princeton University Press, US.

Burdige, D.J. (2007) Preservation of organic matter in marine sediments: controls, mechanisms, and an imbalance in sediment organic carbon budgets? *Chem. Rev.* **107**: 467-485.

Canals, M., and Ballesteros, E. (1997) Production of carbonate particles by phytobenthic communities on the Mallorca-Menorca shelf, northwestern Mediterranean Sea. *Deep-Sea. Res. Pt II.* **44**: 611-629.

Canfield, D.E. (1994) Factors influencing organic carbon preservation in marine sediments. *Chem. Geol.* **114**: 315-329.

Canfield, D.E., Thamdrup, B., and Hansen, J.W. (1993a) The anaerobic degradation of organic matter in Danish coastal sediments: iron reduction, manganese reduction, and sulfate reduction. *Geochim. Cosmochim. Ac.* **57**: 3867-3883.

Canfield, D.E., Jorgensen, B.B., Fossing, H., Glud, R., Gundersen, J., Ramsing, N.B., Thamdrup, B., Hansen, J.W., Nielsen, L.P., and Hall, P.O. (1993b) Pathways of organic carbon oxidation in three continental margin sediments. *Mar. Geol.* **113**: 27-40.

Coates, J.D., Woodward, J., Allen, J., Philp, P., and Lovley, D.R. (1997) Anaerobic degradation of polycyclic aromatic hydrocarbons and alkanes in petroleum-contaminated marine harbor sediments. *Appl. Environ. Microbiol.* **63**: 3589-3593.

Crutzen, P.J. (2002) Geology of mankind. *Nature.* **415**: 23.

Chester, R. (2000) Marine Geochemistry. Blackwell Science Ltd, London, UK.

Danovaro, R., Armeni, M., Dell'Anno, A., Fabiano, M., Manini, E., Marrale, D., Pusceddu, A., and Vanucci, S. (2001) Small-scale distribution of bacteria, enzymatic activities, and organic matter in coastal sediments. *Microb. Ecol.* **42**: 177-185.

DeLong, E.F. (2009) The microbial ocean from genomes to biomes. *Nature* **459**: 200-206.

DeLong, E.F., Wickham, G.S., and Pace, N.R. (1989) Phylogenetic stains: ribosomal RNA-based probes for the identification of single cells. *Science.* **243**: 1360-1363.

Eilers, H., Pernthaler, J., Glöckner, F.O., and Amann, R. (2000) Culturability and *in situ* abundance of pelagic bacteria from the North Sea. *Appl. Environ. Microbiol.* **66**: 3044-3051.

Ellis, E.C. (2011) Anthropogenic transformation of the terrestrial biosphere. *Philos. Transact. A. Math. Phys. Eng. Sci.* **369**: 1010-1035.

Emery, K.O. (1968) Relict sediments on continental shelves of the world. *Am. Assoc. Pet. Geol. Bull.* **52**: 445-464.

Fenchel, T., King, G.M., and Blackburn, T.H. (1998) Bacterial Biogeochemistry: The ecolphysiology of mineral cycling. Elsevier Academic Press, San Diego, US.

Ferraro, G., Bernardini, A., David, M., Meyer-Roux, S., Muellenhoff, O., Perkovic, M., Tarchi, D., and Topouzelis, K. (2007) Towards an operational use of space imagery for oil pollution monitoring in the Mediterranean basin: a demonstration in the Adriatic Sea. *Mar. Pollut. Bull.* **54**: 403-422.

Field, D., Garrity, G., Gray, T., Morrison, N., Selengut, J., Sterk, P., Tatusova, T., Thomson, N., and Allen, M.J. (2008) The minimum information about a genome sequence (MIGS) specification. *Nat. Biotechnol.* **26**: 541–547.

Field, D., Garrity, G., Gray, T., Selengut, J., Sterk, P., Thomson, N., Tatusova, T., Cochrane, G., Glöckner, F.O., Kottmann, R., Lister, A.L., Tateno, Y., and Vaughan, R. (2007) eGenomics: cataloguing our complete genome collection II. *Comp. Funct. Genom.* 1-7.

Foght, J. (2008) Anaerobic biodegradation of aromatic hydrocarbons: pathways and prospects. *J. Mol. Microbiol. Biotechnol.* **15**: 93-120.

Francisco, D.E., Mah, R.A., and Rabin, A.C. (1973) Acridine oange-epifluorescence technique for counting bacteria in natural waters. *T. Am. Microsc. Soc.* **92**: 416-421.

Froelich, P.N., Klinkhammer, G.P., Bender, M.L., Luedtke, N.A., Heath, G.R., Cullen, D., Dauphin, P., Hammond, D., Hartman, B., and Maynard, V. (1979) Early oxidation of organic matter in pelagic sediments of the eastern equatorial Atlantic: suboxic diagenesis. *Geochim. Cosmochim. Ac.* **43**: 1075-1090.

Fütterer, D.K. (2006) The solid phase of marine sediments. *In* Marine Geochemistry. Schulz H.D. and M. Zabel (eds.), Springer-Verlag, Berlin Heidelberg, DE, pp.1-25.

Galperin, M.Y., and Koonin, E.V. (2010) From complete genome sequence to 'complete' understanding? *Trends Biotechnol.* **28**: 398-406.

Gertler, C., Yakimov, M.M., Malpass, M.C., and Golyshin, P.N. (2010) Shipping-related accidental and deliberated release into the environment. *In* Handbook of hydrocarbon and lipid microbiology (Vol 1). Timmis, K.N. (ed.), Springer-Verlag, Berlin Heidelberg, DE, pp. 244-256.

Glöckner, F.O., Fuchs, B.M., and Amann, R. (1999) Bacterioplankton compositions of lakes and oceans: a first comparison based on fluorescence *in situ* hybridization. *Appl. Environ. Microbiol.* **65**: 3721-3726.

Gómez, F. (2003) The role of the exchanges through the Strait of Gibraltar on the budget of elements in the Western Mediterranean Sea: consequences of human-induced modifications. *Mar. Pollut. Bull.* **46**: 685-694.

Hayes, L.A., and Lovley, D.R. (2002) Specific 16S rDNA sequences associated with naphthalene degradation under sulfate-reducing conditions in harbor sediments. *Microb. Ecol.* **43**: 134-145.

Hayes, L.A., Nevin, K.P., and Lovley, D.R. (1999) Role of prior exposure on anaerobic degradation of naphthalene and phenanthrene in marine harbor sediments. *Or. Geochem.* **30**: 937-945.

Head, I.M., Jones, D.M., and Roling, W.F. (2006) Marine microorganisms make a meal of oil. *Nat. Rev. Microbiol.* **4**: 173-182.

Hobbie, J.E., Daley, R.J., and Jasper, S. (1977) Use of nuclepore filters for counting bacteria by fluorescence microscopy. *Appl. Environ. Microbiol.* **33**: 1225-1228.

Holmer, M., Duarte, C.M., and Marbà, N. (2003) Sulfur cycling and seagrass (*Posidonia oceanica*) status in carbonate sediments. *Biogeochemistry.* **66**: 223-239.

Holmer, M., Duarte, C.M., Boschker, H.T.S., and Barrón, C. (2004) Carbon cycling and bacterial carbon sources in pristine and impacted Mediterranean seagrass sediments. *Aquat. Microb. Ecol.* **36**: 227-237.

Huettel, M. (2003) Coastal sands as biocatalytical filters (COSA). *http://www.coastalguide.org/projects/index.html*.

Huettel, M., and Rusch, A. (2000) Transport and degradation of phytoplankton in permeable sediment. *Limnol. Oceanogr.* **45**: 534–549.

Ince, O., Kolukirik, M., and Ince, B.K. (2010) Molecular Microbial Ecology of Marmara Sea Sediments. *In* Current research, technology and education topics in applied Microbiology and Microbial Biotechnology. Mendez-Vilas, A. (ed.), Formatex, SP, pp. 53-63.

Jensen, M.M., Thamdrup, B., Rysgaard, S., Holmer, M., and Fossing, H. (2003) Rates and regulation of microbial iron reduction in sediments of the Baltic-North Sea transition. *Biogeochemistry* **65**: 295–317.

Jørgensen, B.B. (1982) Mineralization of organic matter in the sea bed – role of sulfate reduction. *Nature* **296**: 643-645.

Koike, I., and Sørensen, J. (1988) Nitrate reduction and denitrification in marine sediments. *In* Nitrogen cycling in coastal marine sediments. Balckburn, T.H. and J. Sørensen (eds.), John Wiley and Sons, US, pp. 251-274.

Kostka, J.E., Prakash, O., Overholt, W.A., Green, S.J., Freyer, G., Canion, A., Delgardio, J., Norton, N., Hazen, T.C., and Huettel, M. (2011) Hydrocarbon-degrading bacteria and the bacterial community response in Gulf of Mexico beach sands Impacted by the Deepwater Horizon oil spill. *Appl. Environ. Microbiol.* **77**: 7962–7974.

Kristensen, E. (2000) Organic matter diagenesis at the oxic/anoxic interface in coastal marine sediments, with emphasis on the role of burrowing animals. *Hydrobiologia* **426**: 1–24.

Kristensen, E., and Holmer, M. (2001) Decomposition of plant materials in marine sediment exposed to different electron acceptors (O^{2-}, NO^{3-}, and SO_4^{2-}), with emphasis on substrate origin, degradation kinetics, and the role of bioturbation. *Geochim. Cosmochim. Ac.* **65**: 419-433.

Kristensen, E., Ahmed, S., and Devol, A. (1995) Aerobic and anaerobic decomposition of organic matter in marine sediment: Which is fastest? *Limnol. Oceanogr.* **40**: 1430-1437.

Lam, P., and Kuypers, M.M. (2011) Microbial nitrogen cycling processes in oxygen minimum zones. *Ann. Rev. Mar. Sci.* **3**: 317-345.

Laubier, L. (2005) Mediterranean Sea and humans. Inproving a conflictual partnership. *In* The Mediterranean Sea. Saliot, A. (ed.). *In* Handbook of Environmental Chemistry (Vol 5). Springer-Verlag Berlin Heidelberg. p.p. 3-27.

Leahy, J.G., and Colwell, R.R. (1990) Microbial degradation of hydrocarbons in the environment. *Microbiol. Rev.* **54**: 305-315.

Libes, S.M. (2009) The origin of petroleum in the marine environment. *In* Introduction to Marine Biogeochemistry (Vol 2). Academic Press, Elsevier Inc., London, UK, pp. 759−782.

Lindstrom, J.E., Prince, R.C., Clark, J.C., Grossman, M.J., Yeager, T.R., Braddock, J.F., and Brown, E.J. (1991) Microbial populations and hydrocarbon biodegradation potentials in fertilized shoreline sediments affected by the T/V Exxon Valdez oil spill. *Appl. Environ. Microbiol.* **57**: 2514-2522.

Lovley, D.R. (1991) Dissimilatory Fe(III) and Mn(IV) reduction. *Microbiol. Rev.* **55**: 259-287.

Lovley, D.R., Roden, E.E., Phillips, E.J.P., and Woodward, J.C. (1993) Enzymatic iron and uranium reduction by sulfate reducing bacteria. *Mar. Geol.* **113**: 41-53.

Ludwig, W., and Klenk, H.P. (2001) Overview: a phylogenetic backbone and taxonomic framework for prokaryotic systematics. *In* Bergey's Manual of Systematic Bacteriology, 2º ed. Boone, D.R., Castenholz, R.W. and G.M. Garrity (eds.), Springer, N Y, pp. 49-65.

Ludwig, W., Strunk, O., Westram, R., Richter, L., Meier, H., Yadhukumar, Buchner, A., Lai, T., Steppi, S., Jobb, G., Forster, W., Brettske, I., Gerber, S., Ginhart, A.W., Gross, O., Grumann, S., Hermann, S., Jost, R.,

Konig, A., Liss, T., Lussmann, R., May, M., Nonhoff, B., Reichel, B., Strehlow, R., Stamatakis, A., Stuckmann, N., Vilbig, A., Lenke, M., Ludwig, T., Bode, A., and Schleifer, K.H. (2004) ARB: a software environment for sequence data. *Nucleic. Acids. Res.* **32**: 1363-1371.

Llobet-Brossa, E., Rossello-Mora, R., and Amann, R. (1998) Microbial community composition of Wadden Sea sediments as revealed by fluorescence *in situ* hybridization. *Appl. Environ. Microbiol.* **64**: 2691-2696.

Llobet-Brossa, E., Rabus, R., Böttcher, M.E., Könneke, M., Finke, N., Schramm, A., Meyer, R.L., Grötzschel, S., Rosselló-Móra, R., and Amann, R. (2002) Community structure and activity of sulfate-reducing bacteria in an intertidal surface sediment: a multi-method approach. *Aquat. Microb. Ecol.* **29**: 211-226.

Magen, C., Mucci, A., and Sundby, B. (2011) Reduction rates of sedimentary Mn and Fe oxides: an incubation experiment with arctic ocean sediments. *Aquat. Geochem* . **17**: 629-643.

Marzorati, M., Wittebolle, L., Boon, N., Daffonchio, D., and Verstraete, W. (2008) How to get more out of molecular fingerprints: practical tools for microbial ecology. *Environ. Microbiol.* **10**: 1571-1581.

McLachlan, A., and Turner, I. (1994) The interstitial environment of sandy beaches. *Mar. Ecol.* **15**: 177–211.

Mclachlan, A., Eliot, I.G., and Clarke, D.J. (1985) Water filtration through reflective microtidal beaches and shallow sublittoral sands and its implications for an inshore ecosystem in Western Australia. *Estuar. Coast. Shelf S.* **21**: 91–104.

Meyerdierks, A., and Glöckner, F.O. (2010) Metagenome analyses. *In* Introduction to Marine Genomics, Advances in Marine Genomics. Cock,J.M., Tessmar-Raibler, K., Boyen, C., and F. Viard, (eds.). Springer-Verlag, Berlin Heidelberg, DE, pp. 33-71.

Middelburg, J.J., and Soetaert, K. (2004) The role of sediments in shelf ecosystem dynamics. *Geochim. Cosmochim. Ac.* **68**: A343.

Miralles, G., Nerini, D., Mante, C., Acquaviva, M., Doumenq, P., Michotey, V., Nazaret, S., Bertrand, J.C., and Cuny, P. (2007) Effects of spilled oil on bacterial communities of mediterranean coastal anoxic sediments chronically subjected to oil hydrocarbon contamination. *Microb. Ecol.* **54**: 646-661.

Mitsch, W.J. (2010) The 2010 oil spill in the Gulf of Mexico: What would mother Nature do? *Ecol. Eng.* **36**: 1607-1610.

Muyzer, G., and Smalla, K. (1998) Application of denaturing gradient gel electrophoresis (DGGE) and temperature gradient gel electrophoresis (TGGE) in microbial ecology. *Antonie Van Leeuwenhoek* **73**: 127-141.

Muyzer, G., Teske, A., Wirsen, C.O., and Jannasch, H.W. (1995) Phylogenetic relationships of *Thiomicrospira* species and their identification in deep-sea hydrothermal vent samples by denaturing gradient gel electrophoresis of 16S rDNA fragments. *Arch. Microbiol.* **164**: 165-172.

Nealson, K.H., and Saffarini, D. (1994) Iron and manganese in anaerobic respiration: environmental significance, physiology, and regulation. *Ann. Rev. Microbiol.* **48**: 311-343.

Nealson, K.H., and Stahl, D.A. (1997) Microorganisms and biogeochemical cycles: what we can learn from layered microbial communities? *Rev. Mineral. Geochem.* **35**: 5-34.

Nevin, K.P., and Lovley, D.R. (2002) Mechanisms foe Fe(III) oxide reduction in sedimentary environments. *Geomicrobiol. J.* **19**: 141-159.

Nichols, D. (2007) Cultivation gives context to the microbial ecologist. *FEMS Microbiol. Ecol.* **60**: 351-357.

O'Rourke, D., and Connolly, S. (2003) Just oil? The distribution of environmental and social impacts of oil production and consumption. *Annu. Rev. Environ. Resour.* **28**: 587–617.

Paissé, S., Coulon, F., Goñi-Urriza, M., Peperzak, L., McGenity, T.J., and Duran, R. (2008) Structure of bacterial communities along a hydrocarbon contamination gradient in a coastal sediment. *FEMS Microbiol. Ecol.* **66**: 295-305.

Parkes, R.J., Cragg, B.A., and Wellsbury, P. (2000) Recent studies on bacterial population and processes in subseafloor sediments: a review. *Hydrogeol. J.* **8**: 11-28.

Parkes, R.J., Cragg, B.A., Bale, S.J., Getlifff, J.M., Goodman, K., Rochelle, P.A., Fry, J.C., Weightman, A.J., and Harvey, S.M. (1994) Deep bacterial biosphere in Pacific Ocean sediments. *Nature* **371**: 410-413.

Patin, S.A. (1999) Biogeochemical and ecotoxicological characteristics of crude oil and oil hydrocarbons in the marine environment. *In* Environmental impact of the offshore oil and gas industry. EcoMonitor Pub, East Northport, NY.

Pedros-Alió, C. (2006) Marine microbial diversity: can it be determined? *Trends. Microbiol.* **14**: 257-263.

Peplies, J., Kottmann, R., Ludwig, W., and Glockner, F.O. (2008) A standard operating procedure for phylogenetic inference (SOPPI) using (rRNA) marker genes. *Syst. Appl. Microbiol.* **31**: 251-257.

Pernthaler, A., Pernthaler, J., and Amann, R. (2002) Fluorescence *in situ* hybridization and catalyzed reporter deposition for the identification of marine bacteria. *Appl. Environ. Microbiol.* **68**: 3094-3101.

Poretsky, R.S., Bano, N., Buchan, A., LeCleir, G., Kleikemper, J., Pickering, M., Pate, W.M., Moran, M.A., and Hollibaugh, J.T. (2005) Analysis of microbial gene transcripts in environmental samples. *Appl. Environ. Microbiol.* **71**: 4121-4126.

Psarros, G., Skjong, R., and Vanem, E. (2010) Risk acceptance criterion for tanker oil spill risk reduction measures. *Mar. Pollut. Bull.* **62**: 116-127.

Ram, R.J., Verberkmoes, N.C., Thelen, M.P., Tyson, G.W., Baker, B.J., Blake, R.C., 2nd, Shah, M., Hettich, R.L., and Banfield, J.F. (2005) Community proteomics of a natural microbial biofilm. *Science* **308**: 1915-1920.

Richter, M., Lombardot, T., Kostadinov, I., Kottmann, R., Duhaime, M.B., Peplies, J., and Glockner, F.O. (2008) JCoast - a biologist-centric software tool for data mining and comparison of prokaryotic (meta)genomes. *BMC Bioinformatics* **9**: 177.

Riedl, R.J., and Macmahan, E.A. (1969) High energy beaches. *In* Coastal ecological systems of the United States. Odum, H.T., Copeland, B.J., and E.A. Mcmahan (eds.), Federal Water Pollution Control Administration, US, pp. 197–269.

Riedl, R.J., and Machan, R. (1972) Hydrodynamic patterns in lotic intertidal sands and their bioclimatological implications. *Mar. Biol.* **13**: 179–209.

Riggs, S.R., Synder, S.W., Hine, A.C., and Mearns, D.L. (1996) Hardbottom morphology and relationship to the geologic framework—Mid-Atlantic continental shelf. *J. Sediment. Res.* **66**: 830–846.

Ritz, K. (2007) The plate debate: cultivable communities have no utility in contemporary environmental microbial ecology. *FEMS Microbiol. Ecol.* **60**: 358-362.

Rochelle, P.A., Cragg, B.A., Fry, C.J., Parkes, R.J., and Weightman, A.J. (1994) Effect of sample handling on estimation of bacterial diversity in marine sediments by 16S rRNA gene sequence analysis. *FEMS Microbiol. Ecol.* **15**: 215-226.

Röling, W.F.M., and Head, I.M. (2005) Prokaryotic systematics: PCR and sequence analysis of amplified 16S rRNA genes. In Molecular Microbial Ecology. Osborn A.M. and C.J. Smith (eds.). Taylor and Francis group, UK, pp. 25-63.

Rosenberg, E., Legman, R., Kushmaro, A., Adler, E., Abir, H., and Ron, E.Z. (1996) Oil bioremediation using insoluble nitrogen source. *J. Biotechnol.* **51**: 273-278.

Rosselló-Móra, R. (2005) Updating prokaryotic taxonomy. *J.. Bacteriol.* **187**: 6255-6257.

Rosselló-Móra, R., Thamdrup, B., Schafer, H., Weller, R., and Amann, R. (1999) The response of the microbial community of marine sediments to organic carbon input under anaerobic conditions. *Syst. Appl. Microbiol.* **22**: 237-248.

Roszac, D.B., and Colwell, R.R. (1987) Survival strategies of bacteria in the natural environment. *Microbiol. Rev.* **51**: 365-379.

Rowe, G.T., Theroux, R., Phoel, W., Quinby, H., Wilke, R., Koschoreck, D., Whitledge, T.E., Falkowski, P.G., and Fray, C. (1988) Benthic carbon budgets for the continental shelf south of New England. *Cont. Shelf. Res.* **8**: 511-527.

Rusch, D.B., Halpern, A.L., Sutton, G., Heidelberg, K.B., Williamson, S., Yooseph, S., Wu, D., Eisen, J.A., Hoffman, J.M., Remington, K., Beeson, K., Tran, B., Smith, H., Baden-Tillson, H., Stewart, C., Thorpe, J., Freeman, J., Andrews-Pfannkoch, C., Venter, J.E., Li, K., Kravitz, S., Heidelberg, J.F., Utterback, T., Rogers, Y.H., Falcon, L.I., Souza, V., Bonilla-Rosso, G., Eguiarte, L.E., Karl, D.M., Sathyendranath, S., Platt, T., Bermingham, E., Gallardo, V., Tamayo-Castillo, G., Ferrari, M.R., Strausberg, R.L., Nealson, K., Friedman, R., Frazier, M., and Venter, J.C. (2007) The Sorcerer II Global Ocean Sampling expedition: northwest Atlantic through eastern tropical Pacific. *PLoS Biol.* **5**: e77.

Saiki, R.K., Gelfand, D.H., Stoffel, S., Scharf, S.J., Higuchi, R., Horn, G.T., Mullis, K.B., and Erlich, H.A. (1988) Primer-directed enzymatic amplification of DNA with a thermostable DNA polymerase. *Science.* **239**: 487-491.

Schulz, H.D. (1999) Redox measurements in marine sediments. *In* Redox: Fundamentals, processes and applications. Schüring, J. and Schulz, H.D. and Fischer, W.R. and Böttcher, J. and W.H. Dijnisveld, (eds.), Springer-Verlag, Berlin Heidelberg, DE, pp. 235-246.

Siokou-Frangou, I., Christaki, U., Mazzocchi, M.G., Montresor, M., Ribera d'Alcalá, M., Vaqué, D., and Zingone, A. (2010) Plankton in the open Mediterranean Sea: a review. *Biogeosciences* **7**: 1543–1586.

Sørensen, J. (1987) Nitrate reduction in marine sediments: pathways and interactions with iron and sulfur cycling. *Geomicrobiol. J.* **5**: 401-421.

Spyrou, A.G. (2006) From T-2 to Supertanker: development of the oil tanker. Lin-coln, NE: iUniverse, Inc. pp. 1940–2000.

Stach, J.E., and Bull, A.T. (2005) Estimating and comparing the diversity of marine actinobacteria. *Antonie Van Leeuwenhoek.* **87**: 3-9.

Staley, J.T., and Konopka, A. (1985) Measurement of *in situ* activities of nonphotosynthetic microorganisms in aquatic and terrestrial habitats. *Annu. Rev. Microbiol.* **39**: 321-346.

Steffen, W., Crutzen, J., and McNeill, J.R. (2007) The Anthropocene: are humans now overwhelming the great forces of Nature? *Ambio.* **36**: 614-621.

Tankéré, S.C.P., Bourne, D.G., Muller, F.L.L., and Torsvik, V. (2002) Microenvironments and microbial conmunity structure in sediments. *Environ. Microbiol.* **4**: 97-105.

Thamdrup, B., and Canfield, D.E. (1996) Pathways of carbon oxidation in continental margin sediments off central Chile. *Limnol. Oceanogr.* **41**: 1629-1650.

Thamdrup, B., Rossello-Mora, R., and Amann, R. (2000) Microbial manganese and sulfate reduction in Black Sea shelf sediments. *Appl. Environ. Microbiol.* **66**: 2888-2897.

Thauer, R.K., Stackebrandt, E., and Hamilton, W.A. (2007) Energy metabolism and phylogenetic diversity of sulphate-reducing bacteria. *In* Sulphate-reducing bacteria: environmental and enfineered systems. L.L. Barton and W.A. Hamilton (eds.), Cambridge University Press, UK, pp. 1-37.

Tissot, B.P., and Welte, D.H. (1978) Petroleum Formation and Occurrence: A New Approach to Oil and Gas Exploration. Tissot, B.P. and D.H. Welte (eds.), Springer-Verlag, Berlin-Heidelberg, DE.

Vandieken, V., Finke, N., and Jørgensen, B.B. (2006) Pathways of carbon oxidation in an Arctic fjord sediment (Svalbard) and isolation of psychrophilic and psychrotolerant Fe(III)-reducing bacteria. *Mar. Ecol. Prog. Ser.* **322**: 29-41.

Venter, J.C., Remington, K., Heidelberg, J.F., Halpern, A.L., Rusch, D., Eisen, J.A., Wu, D., Paulsen, I., Nelson, K.E., Nelson, W., Fouts, D.E., Levy, S., Knap, A.H., Lomas, M.W., Nealson, K., White, O., Peterson, J., Hoffman, J., Parsons, R., Baden-Tillson, H., Pfannkoch, C., Rogers, Y.H., and Smith, H.O. (2004) Environmental genome shotgun sequencing of the Sargasso Sea. *Science.* **304**: 66-74.

Wakeham, S.G., and Canue, E.A. (2006) Degradation and preservation of organic matter in marine sediments. *Hdb. Env. Chem.* **2**: 295–321.

Widdel, F., Knittel, K., and Galushko, A. (2010) Anaerobic hydrocarbon-degrading microorganisms: an overview. *In* Handbook of hydrocarbon and lipid microbiology. Timmis, K. N. (ed). Berlin Heidelberg, DE: Springer-Verlag, pp. 1998-2021.

Wilmes, P., and Bond, P.L. (2006) Metaproteomics: studying functional gene expression in microbial ecosystems. *Trends Microbiol*. **14**: 92-97.

Woese, C.R. (1987) Bacterial evolution. *Microbiol. Rev.* **51**: 221-271.

Wollast, R. (1991) The coastal organic carbon cycle: fluxes, sources and sinks. *In* Ocean margin processes in global change. Mantoura, R.F.C., Martin, J.-M. and R. Wollast (eds.), Wiley-Interscience, NY, pp. 365-381.

Yarza, P. (2011) The All-Species Living Tree Project. PhD dissertation, University of Balearic Islands.

Yarza, P., Richter, M., Peplies, J., Euzeby, J., Amann, R., Schleifer, K.H., Ludwig, W., Glöckner, F.O., and Rosselló-Móra, R. (2008) The All-Species Living Tree project: A 16S rRNA-based phylogenetic tree of all sequenced type strains. *Syst. Appl. Microbiol.* **31**: 241-250.

Zalasiewicz, J., Williams, M., Steffen, W., and Crutzen, P. (2010) The new world of the Anthropocene. *Environ. Sci. Technol.* **44**: 2228-2231.

Zalasiewicz, J., Williams, M., Smith, A., Barry, T.L., Coe, A.L., Bown, P.R., Brenchley, P., Cantrill, D., Gale, A., Gibbard, P., Gregory, F.J., Hounslow, M.W., Kerr, A.C., Pearson, P., Knox, R., Powell, J., Waters, C., Marshall, J., Oates, M., Rawson, P., and Stone, P. (2008) Are we now living in the Anthropocene? *GSA Today* **18**: 4-8.

ZoBell, C. (1946) Marine microbiology, a monograph on hydrobacteriology. Chronica Botanica Company, US.

Zumft, W.G. (1997) Cell biology and molecular basis of denitrification. *Microbiol. Mol. Biol. Rev.* **61**: 533-616.

Experimental procedures

1. Sampling site

During the summer of 2006, an experimental site was established at the north of Mallorca Island (39º 52,1' N; 3º 08,7' E) in a semi-confined bay (Alcúdia Bay) of low maritime transit (Figure 1.A). Relevant industrial activities and terrestrial water flows are minimal in and nearby the Balearic Islands. A water circulation model for the sampling site was generated as previously described (Orfila et al., 2005). The experiment was set up on carbonated sandy sediments placed 1.5 miles away from the seashore and 12 m deep, in order to facilitate the scuba diving activities and to reduce the effects of sediment transport and/or re-suspension due to storms and local coastal currents. The sediments were bare (Figure 1.B) but surrounded by *P. oceanica* meadows with the closest meadow edge about 20 m from the experimental spot.

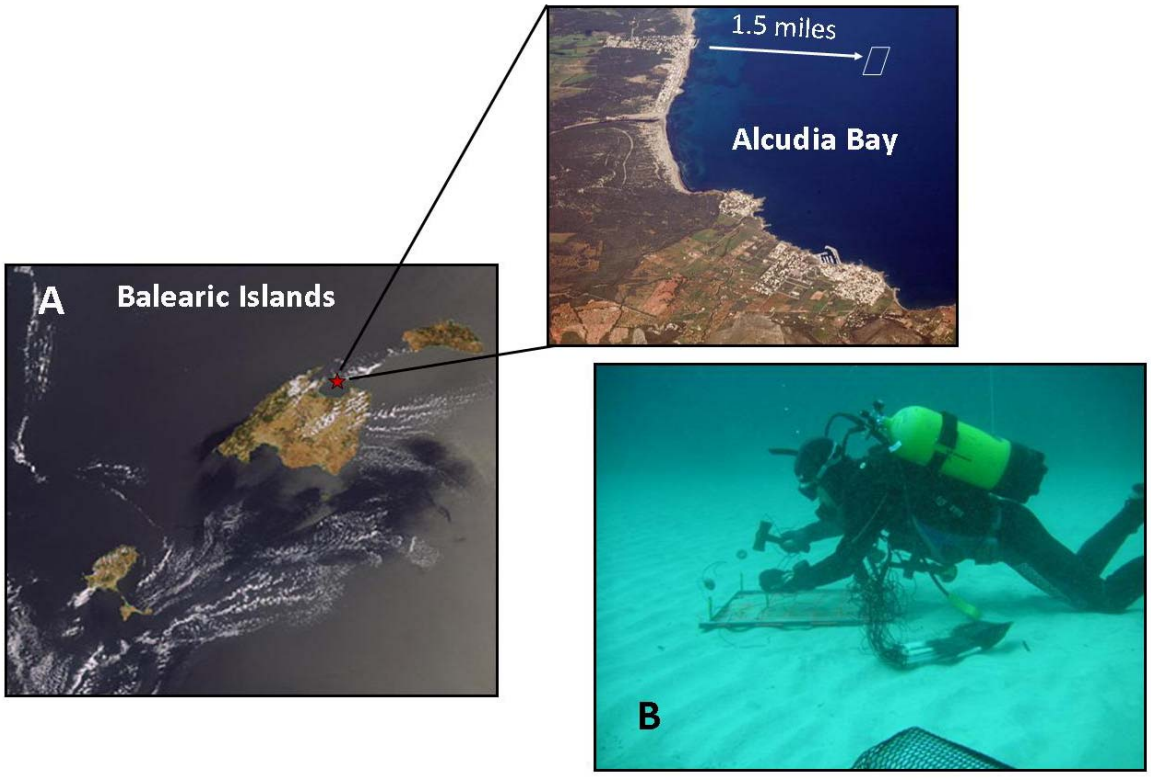

Figure 1. A. Sampling site at Alcúdia Bay on the north of Mallorca island (39º 52,1' N; 3º 08,7' E)**; B. S**et up on bare carbonated sandy sediments.

2. Mesocosms set up and sampling

The experiment consisted in three mesocosms (70 x 70 x 30 cm) enclosing 150 dm^3 of sediment each one. Two of them were artificially contaminated with naphthalene and crude oil respectively, while a third mesocosm of untreated sediment served as a control. The distance between plots was 4 m.

Naphthalene and crude oil plots were prepared by introducing contaminated inserts every 10 cm following a square grid pattern of 6 x 6 inserts (Figure 2.A.). Naphthalene inserts were prepared by using 10 ml polypropylene sterile pipettes filled with naphthalene crystals (Figure 2.B. left). About 350 g of naphthalene were inserted into the plot. In order to let the contaminant diffuse, the pipette had four equidistant lanes of 1 mm holes distributed along it. Heavy crude oil original from the Prestige oil tanker (Franco et al., 2006) was impregnated onto nylon threads (7 mm i.d. x 30 cm length) (Figure 2.B. right). In this way, a total of 50 g of crude oil (approximately 1.5 g per stick) were distributed homogeneously between the sticks and directly exposed to the sediment.

Sediment mesocosm installation and sampling were carried out by scuba diving on the following dates: June 24th, July 19th and September 25th (2006), representing 0, 23 and 92 days after contamination. The sediment samples were manually collected in the internal area of 10 x 10 cm between inserts using cylindrical methacrylate cores (3.6 cm i.d. x 30 cm height) (Figure 2.C., D. and E.) and transported to the laboratory within 1–2 h. For each analytic approach carried out in this study triplicate samples were collected at each sampling event from every mesocosm.

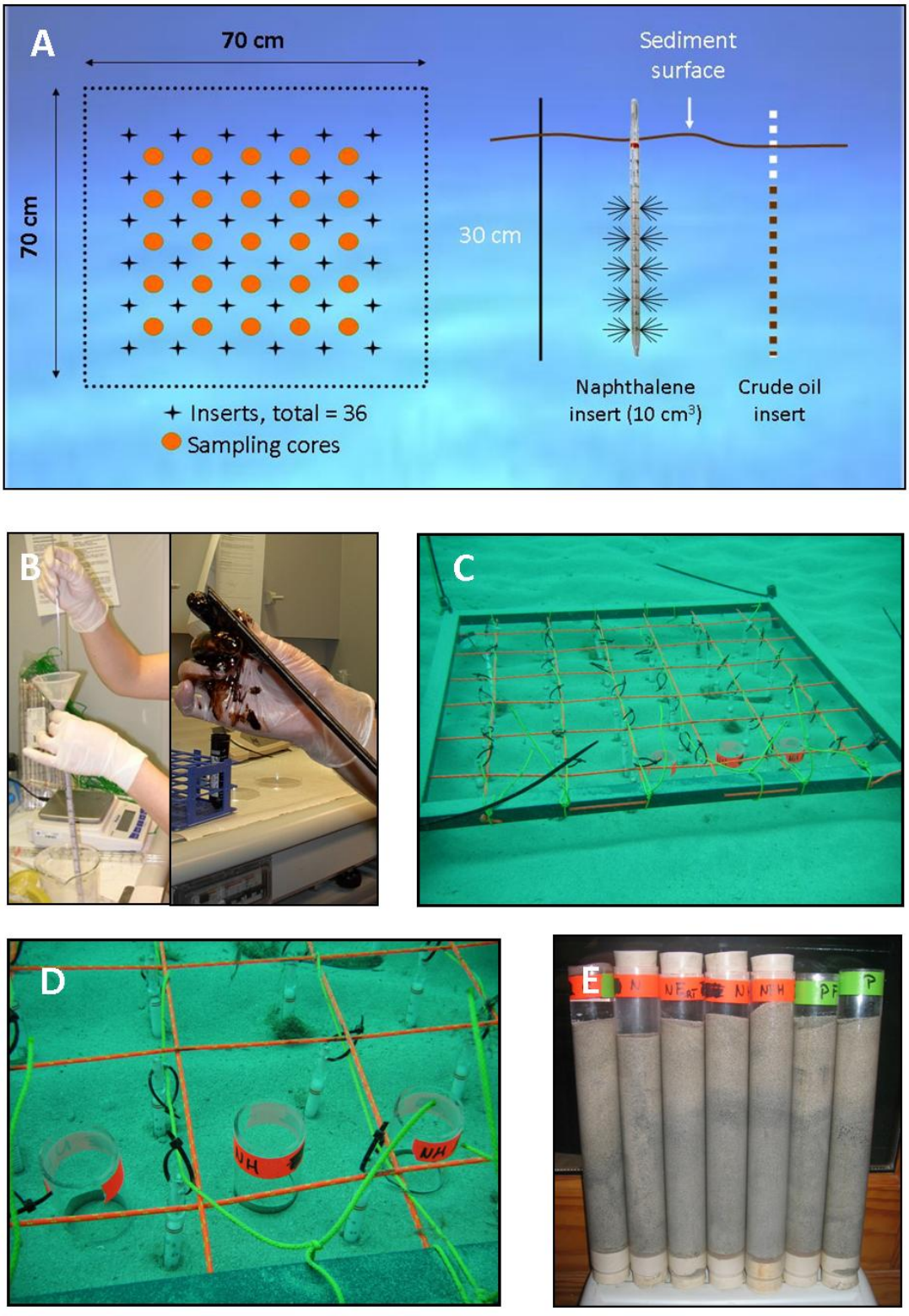

Figure 2. Mesocosms set up and sampling. **A**. Mesocosm schematic representation; **B**. Naphthalene (left) and crude oil (right) inserts preparation; **C**. Appearance of a mesocosm after installation; **D**. Closed view of sample collection using cylindrical methacrylate cores; **E.** Core samples after collection.

3. Additional sampling

Samples of undisturbed and vegetated sediment were collected during the sampling events of September 25th (2006).

Two samples of vegetated sediment were collected from the closest meadow to the experimental spot using methacrylate cores (3.6 cm i.d. x 30 cm height). These sediment samples were used as inocula for the most probable number (MPNs) cultures presented in Chapters 1, in order to complement a previous research focused in the microbial diversity and abundance on calcareous sandy sediment associated to the rizosphere of *P. oceanica* at the Balearic Islands (García-Martinez et al., 2008).

One sample of undisturbed sediment was collected using a methacrylate core (5 cm i.d. x 32 cm height) and carefully transported to the laboratory. The sample, consisting in 295 cm^3 of sediment overlaid by 295 cm^3 the same volume of seawater, was contaminated with naphthalene by placing an insert into the centre of the core and then kept in darkness at 20°C during 3 years. This sediment was used as inoculum for the crude oil enrichment cultures described in Chapter 3.

4. Physico-chemical features

4.1. Sediment density, porosity and organic matter content

Sediment density was obtained by weighing a known volume of sample, and the water content was obtained after drying it at 60ºC during 48 hours. Porosity was calculated from sediment density and water content.

Organic matter content was obtained by ignition of the dried sediment at 450ºC during 5 hours as described by Erftemeijer and Koch (2001).

Sediment grain size was determined by sieving dried sediments (30-40 g) over a graded set of sieves (63, 125, 250, 500, 1,000 and 2,000 µm) and measuring the weight of each fraction, including the <63 µm fraction. The geometric mean for each sample was determined using Gradistat 4.0 (Blott and Pye, 2001).

4.2. Pore water sulphate concentration

Sulphate concentration was determined from triplicate sediment cores (30 cm long and 3.6 cm i.d.). Each core was sliced each 2 cm intervals and sulphate reduction stopped by adding 20% zinc acetate. Pore water was separated by centrifugation (5 min at 4,000 rpm) and filtration through a 0.40-Am syringe filter. After appropriate dilution, the samples were analyzed by unsuppressed anion chromatography using a Waters 510 high-performance liquid chromatography pump, Waters WISP 712 autosampler (100 µl injection volume), Waters IC-Pak anion exchange column (50 x 4.6 mm), and a Waters 430 conductivity detector. Buffer isophthalate 1 mM was used as eluent (in 10% methanol pH 4.5). The flow rate was 1 ml min^{-1} (Ferdelman et al., 1998).

4.3. Sulphate reduction rates

Sulphate reduction rates (SRRs) were measured by the core injection technique (Jørgensen, 1978) in 20 cm long sediment cores that were retrieved from the three experimental plots after 3 months of incubation with the contaminants. Twenty-five cm long and 2.6 cm i.d. core tubes with silicone-filled injection ports where used for the sampling. Ten microliters of carrier-free $^{35}SO_4$ tracer (50 Kbq) were injected at 1 cm intervals and the cores were incubated in darkness at *in situ* temperature (24ºC) during 24 h. Subsequently, each core was sliced each 2 cm intervals and the reaction was stopped by adding 20% zinc acetate. The zinc precipitated the dissolved compounds of H_2S and Sn^{2-} and exchanged with FeS to form ZnS. In this way all ^{35}S reduced was preserved as solid compounds (ZnS, S°, and FeS_2). The samples were stored at room temperature (RT) until the single step cold Cr-II distillation for radiotracer determination (Kallmeyer et al., 2004). Figure 3 represents a schematic view of the cold distillation system.

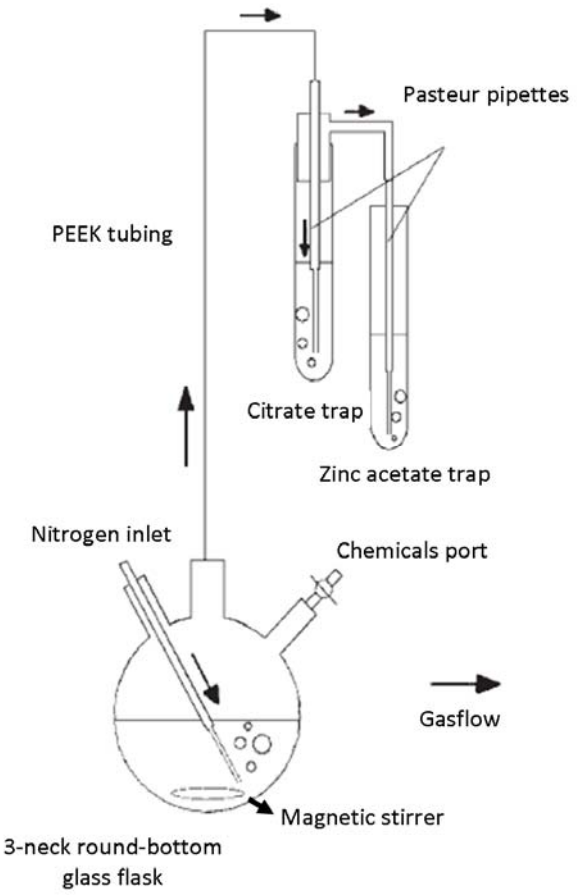

Figure 3. Schematic view of the cold distillation system (from Kallmeyer et al., 2004).

The $^{35}SO_4^{2-}$ was separated from its radioactive products by centrifugation (5 min at 4,500 rpm). Each sample was transferred to a 3-neck round-bottom glass flask and 20 ml of N, N-dimethylformamide (DMF) were added together with a magnetic stir bar to ensure an efficient mechanical breakup of the sample. DMF enhances the reactivity of reduced sulfur species, but also allows oxidation to take place at an enhanced rate. To prevent oxidation prior to distillation, extended contact of the sediment-DMF slurry with air was avoided. As soon as the sample was mixed with DMF, the reaction flask was connected to the gas line and flushed with N_2 for 10 min. Subsequently, 8 ml of 6N HCl were injected through the chemical port followed by 16 ml 1 M $CrCl_2$ solution in order to dissolve or reduced the gaseous $H_2{}^{35}S$ to solid phase of ^{35}Sred. As the samples were highly carbonated, the acid was added slowly (by dropping) to avoid heavy foaming during the liberation of CO_2. The sample was then bubbled at a rate of 2 to 5 bubbles per second with N_2 for 2 h and continuously stirred. Over the last 15 min, the

gas flow rate was increased to remove the last vestiges of sulphide from the system. The liberated sulphide was trapped as zinc sulphide in 7 ml of 5% (w/v) zinc acetate solution with a drop of antifoam.

The radioactivity was determined by liquid scintillation counting (Packard 2500 TR) using Lumasafe Plus® (Lumac BV, Holland) mixed with the trapped ZnS 2:1 (v:v). Sulphate reduction rate blanks were determined by slicing not injected cores into zinc acetate as described above and then adding 5 µl of tracer 30 min just before the distillation. Further processing proceeded as explained before. By comparing the activity of the radiolabeled total reduced inorganic sulfur (TRIS) to the total sulphate radiotracer injected, the SRR can be calculated from the following equation:

$$SRR = [SO_4] \times P_{SED} \frac{a_{TRIS}}{a_{TOT}} \times \frac{1}{t} \times 1.06 \times 1000$$

where *SRR* is the sulphate reduction rate (nmol cm^{-3} d^{-1}); $[SO_4]$ is the sulphate concentration in the porewater of the sediment sample (mmol L^{-1}); P_{SED} is the porosity of the sediment (ml porewater cm^{-3} sediment); a_{TRIS} is the radioactivity of the TRIS (counts per minute [cpm]); a_{TOT} is the total radioactivity used (cpm); *t* is the incubation time in days; 1.06 is the correction factor for the expected isotopic fractionation (Jørgensen and Fenchel, 1974) and 1,000 is the factor for the change of units from mmol L^{-1} to nmol cm^{-3}.

5. Molecular biology approaches

5.1. Sample manipulation

Sediment layers between 13 cm and 19 cm below the surface (300 g of sediment approximately) were homogenized in sterile 500 ml glass bottles (Figure 4). For total cell counts (by DAPI-staining), an aliquot of 5 g was fixed in 4% formaldehyde-PBS 4X (PBS: 0.13 M NaCl, 7 mM Na_2HPO_4 and 3 mM NaH_2PO_4 [pH 7.2 in water]).

In order to increase the DNA extraction efficiency and simplify the *in situ* fluorescence hybridization (FISH) procedure, the microbial fraction was separated from the sand sediments by washing with 80 ml of PBS buffer followed by 5 min incubation in an

ultrasonic bath (AP Selectra Ultrasonic, 40 KHz, 200W). Supernatant was collected after sand grains sedimentation, the remained sediment washed four more times and the supernatants pooled together. Five milliliters of the 320 ml extract were fixed in 4% formaldehyde-PBS 4X for the FISH procedure. The rest of the extract was centrifuged at 15,000 rpm and the pellets were stored at -80 ºC for nucleic acid extraction. The cell extraction efficiency was 75% (± 5.8% SD, n = 3), as shown by the comparison with the total DAPI counts on crude sediment.

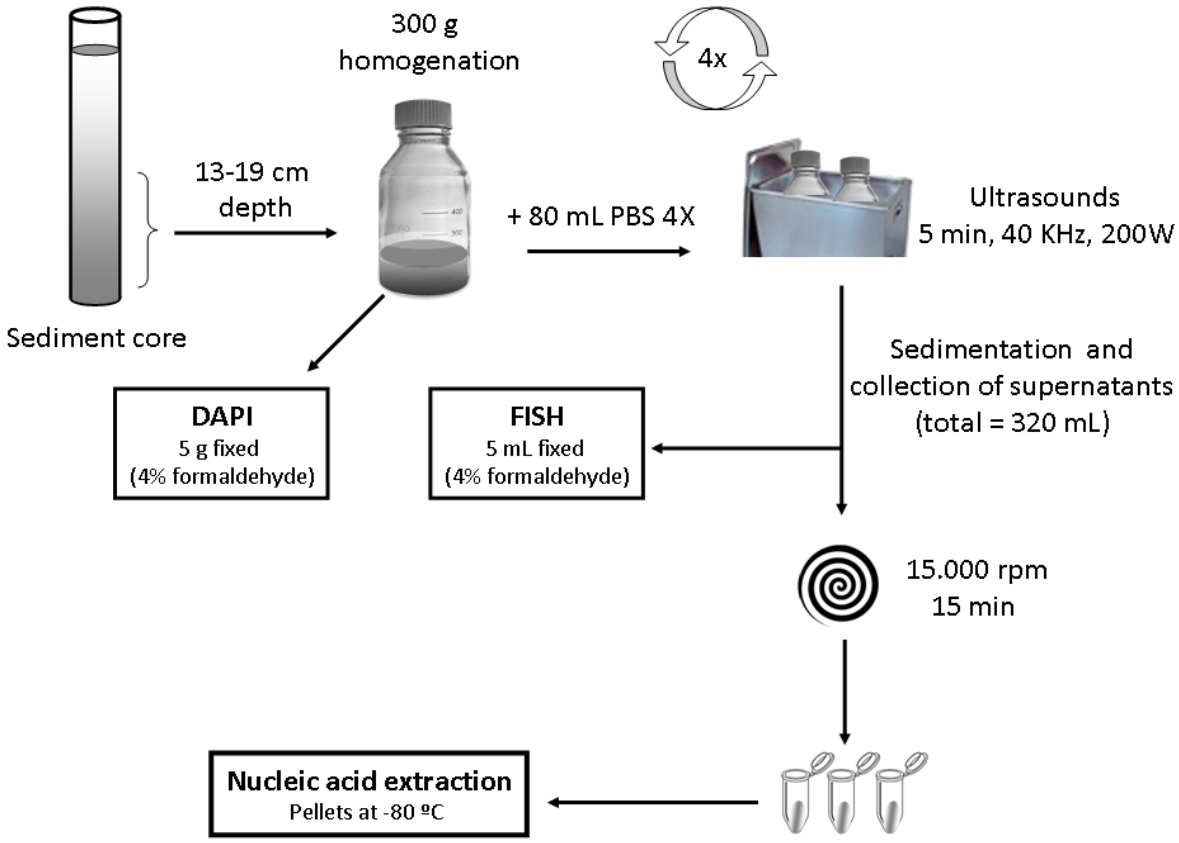

Figure 4. Procedure for the separation of the microbial biomass from sand particles

5.2. DNA extraction from marine sandy sediment

Total DNA was extracted from the cell pellets following the protocol described previously (Zhou et al., 1996; Nogales et al., 1999). The pellets were resuspended in extraction buffer (100 mM Tris-HCl, pH 8.0, 20 mM sodium EDTA, pH 8.0, 100 mM sodium phosphate buffer, pH 8.0) with proteinase K and lisozime (0.08 mg ml^{-1} and 3 mg ml^{-1}, respectively) and then incubated at 37°C for 30 min in a horizontal shaker at

900 rpm (Shaker ST3). After this treatment, 2% SDS was added, the sample was then gently mixed and incubated at 37°C and 900 rpm for 30 min. NaCl 1.2 M was added, the sample was gently mixed and after the addition of hexadecylmethylammonium bromide (CTAB)/ NaCl (10% w/v and 0.7 M, respectively) the sample was subsequently incubated at 65°C for 15 min (reactive concentrations are given as final concentrations). The samples were frozen in liquid nitrogen and thawed immediately in a water bath at 65°C for 10 min. This freeze–thawing step was repeated three times. The nucleic acids were extracted twice with one volume of phenol–chloroform–isoamyl alcohol (25:24:1, v/v). The mixture was shaken and centrifuged at 13,000 rpm for 4 min (Eppendorf 5415R). The aqueous phase was recovered and extracted twice with one volume of chloroform–isoamyl alcohol (24:1, v/v. Nucleic acids in the aqueous phase were precipitated by the addition of 0.7 volumes of isopropanol and 0.1 volume of sodium acetate 3M pH 4.8, gently mixed and incubated over night at -20°C. The nucleic acids were then pelleted by centrifugation at 13,000 rpm for 30 min and washed with 70% ethanol, dried and resuspended in 30 to 100 µl of sterile deionized water.

5.3. DNA extraction from enrichment cultures for metagenomic analyses

Thirty millilitres of the crude oil enrichment culture (Section 7.3.) were mixed with extraction buffer 2X (200 mM EDTA pH8 and 200 mM Tris-HCl pH8) with proteinase K and lysozyme (0.1 mg ml^{-1} and 1 mg ml^{-1}, respectively) and then incubated at 37°C for 1 h in a horizontal shaker at 900 rpm (Shaker ST3). After this treatment, 1% SDS was added, the sample was then gently mixed and incubated at 50°C and 900 rpm for 1 h. The samples were frozen in liquid nitrogen and thawed immediately in a water bath at 65°C for 10 min. This freeze–thawing step was repeated three times and then the sample was incubated at 100ºC for 1 min. The nucleic acids were extracted twice with one volume of phenol–chloroform–isoamyl alcohol (25:24:1, v/v). The mixture was shaken and centrifuged at 13,000 rpm for 4 min (Eppendorf 5415R). The aqueous phase was recovered and extracted twice with one volume of chloroform–isoamyl alcohol (24:1, v/v. Nucleic acids in the aqueous phase were precipitated by the addition of 0.6 volumes of isopropanol gently mixed and incubated at 4ºC for 30 min.

The nucleic acids were then pelleted by centrifugation at 13,000 rpm for 25 min at 4ºC, washed with 70% ethanol, dried and resuspended in sterile deionized water.

Between five to ten micrograms of the purified DNA was used for direct 454 pyrosequencing in GATC Biotech AC (Germany) and 16S rDNA gene clone library construction.

5.4. 16S rRNA gene clone libraries construction

16S rRNA genes were amplified using the universal primers for *Bacteria* GM3F (5'-AGAGTTTGATCMTGGC-3') and GM4R (5'-TACCTTGTTACGACTT-3') (Muyzer et al., 1995) and the Ex taq polymerase kit (Takara) following the manufacturer's instructions. The PCR reaction was carried out in 50 µl of reaction (final volume) using 1µl of template (10-100 ng) and following standard conditions: 30 cycles (denaturation at 94ºC for 30 s, annealing at 50ºC for 1 min, extension at 72ºC for 2 min) preceded by 3 min denaturation at 94ºC and followed by 10 min extension at 72ºC. PCR amplicons (3µl) were run by electrophoresis on 1 % agarose gels (Agarose D1 medium EEO, Pronadisa) and stained with ethidium bromide in order to detect positive amplification. The bands were visualized in a Syngene GBox gel documentation system (Imgen Technologies). The obtained PCR products were purified using a PCR purification kit (Qiagen).

Clone libraries were constructed using the pGEM-T Easy Vectors System (Promega), according to the manufacturer's recommendations. Positive colonies were screened for unique inserts by PCR with the M13 primer pair (M13F: 5'-GTTTTCCCAGTCACGAC-3'; M13R: 5'-CAGGAAACAGCTATGA-3'). Purified PCR products were sequenced by the Genomex DNA Sequencing Service (www.genomex.com) using the GM3F primer.

The plasmids of positives clones were extracted and measured with Hoescht fluorescent dye. The concentration of the plasmid/PCR product was adjusted to 0.075 pM in 6 µl by dilution with sterile water. The sequencing reaction was performed by PCR amplification in a final volume of 10 µl using 0.05 pM of plasmid, 4 pM of primer, and 1 to 3 µl of Big Dye Terminators premix, according to Applied Biosystems protocol. After heating to 98°C for 5 min, the reaction was cycled as follows: 30-40 cycles of 30s at 96°C, 30s at 55°C, and 4 min at 60°C (9700 thermal cycler AB). Removal of excess of Big Dye Terminators was performed by ethanol precipitation. The samples were dried

in a vacuum centrifuge, dissolved in 10 µl of formamide, loaded onto an Applied Biosystems 3730 sequencer and run for 2 h.

5.5. 16S rRNA gene sequence analyses and phylogenetic tree construction

16S rRNA gene sequences were corrected using Sequencher 4.8 software (Gene Codes Corp.). The RDP chimera-check program (Cole et al., 2009) was used to predict chimerical clones. Sequences were automatically aligned and manually corrected using the ARB software package (Ludwig et al., 2004) against the aligned sequence dataset of the ARB-SILVA project (Pruesse et al., 2007). SILVA is a secondary database from the European Nucleotide Archive (ENA) that contains an updated selection of quality checked and automatically aligned rRNA sequences. In this study were used the databases 98- (Chapters 1 and 2) and 108-small subunit reference database (SSURef), containing only sequences above 1.200 bases (www.arb-silva.de).

Manually curate partial sequences were inserted into a previously reconstructed neighbor joining tree of representative complete sequences using the ARB-parsimony tool with a 40% filter generated from complete sequences. Phylogenetic inference of full length 16 rRNA gene sequences was estimated by maximum likelihood methods.

The sequences were grouped into OTUs (Operational Taxonomic Units), assuming that one OTU included sequences with similarity values equal to or higher than 97% (Zaballos et al., 2006). Alternatively, and in order to simplify the calculations, it was decided to identify sequence clades that produced biologically meaningful units (called operational phylogenetic units, OPUs; (Rosselló-Móra and López-López, 2008). An OPU was considered as each single unique phylogenetic clade in the tree only composed by clones, and based on the latest updated 16S rRNA gene database, instead of being limited by a numerical threshold (López-López et al., 2010). Actually, they may also be referred to as the "operational phylogenetic-based microbial populations" formulated for ecological purposes (Pernthaler and Pernthaler, 2005).

Nucleotide sequences from Chapter 1 and 2 were submitted to the GenBank database under accession numbers **FJ949236** to **FJ949449** and **HQ400766** to **HQ400941**. Nucleotide sequences from Chapter 3 are pending of submission to the database.

5.6. Taxonomic classification of 16S rRNA and 23S rRNA gene fragments in the metagenome

In order to retrieve the 16S rRNA and 23S rRNA gene fragments obtained by direct pyrosequencing, unassembled reads were processed by the bioinformatics pipeline of the SILVA project (Pruesse et al., 2007). Reads shorter than 100 nucleotides and with more than 2% ambiguities or 2% homopolymers were removed. The remaining reads were imported into the ARB software for further analysis. Fragments with 100–500 aligned bases within the 16S rRNA gene boundaries and 300–600 aligned bases within the 23S rRNA gene boundaries, were added to the guide trees of the small subunit (SSU) and large subunit (LSU) datasets of the SILVA Reference (Ref) release 104 by using the ARB Parsimony Tool (Yilmaz et al., 2011).

Taxonomic assignments were based on membership of the fragments to the existing clades of the SILVA taxonomy, as represented by the guide trees of the high quality SILVA Ref datasets (Pruesse et al., 2007).

5.7. Taxonomic and functional metagenomic analysis

Gene prediction was carried out using the Glimmer3 and Metagene software (http://www.cbcb.umd.edu/software/glimmer/,(Noguchi et al., 2006). Batch cluster analysis of metagenome sequences was performed with the GenDB v2.2 system (Meyer et al., 2003) by collecting for each predicted open reading frame (ORF) observations from similarity searches against sequences at SwissProt (Bairoch et al., 2004), KEGG (Kanehisa et al., 2008), COGs (Tatusov et al., 2001), genomesDB databases (Richter et al., 2008), and protein family databases as Pfam (Finn et al., 2008). Predicted protein-coding sequences were automatically annotated by the software MicHanThi (Quast, 2006). The MicHanThi software predicts gene functions using a fuzzy logic-based approach based on similarity searches using the NCBI-non redundant (including Swiss-Prot) and InterPro database (Hunter et al., 2009). Furthermore, manual annotation and data mining were performed by using JCoast, version 1.6 (Richter et al., 2008).

To highlight the phylogenetic consistency, all proteins were searched for similarity by BLAST analysis for the phylogenetic distribution of best hits against genomesDB. Genome DB is a composite database built from the proteome FASTA files obtained

from the National Center for Biotechnology Information (NCBI) Reference Sequences database (RefSeq) for all fully sequenced bacterial and archaeal genomes. In addition, taxonomic and contextual information was parsed from the NCBI Entrez Genome Project database.

To identify potential metabolic pathways, genes were searched for similarity against the KEGG (Kyoto Encyclopedia of Genes and Genomes) and COGs (Clusters of Orthologous Groups of proteins) databases. KEGG and COGs annotation schemes contain categories of metabolic functions organized in multiple hierarchical levels. KEGG analysis maps enzymes onto known metabolic pathways, while COGs uses evolutionary relations (orthologs: connected through vertical evolutionary descent) to group functionally related genes. In both approaches, a match was counted if the similarity search resulted in an expectation value below $1e^{-40}$. The expectation value describes the number of hits that can be expected by chance when searching a database of a particular size. It decreases exponentially as the score of the match increases. When the expectation value is closer to zero the match is more significant. In order to corroborate the automatic function annotation of interesting ORFs, the amino acidic sequences were compared with those at Swiss-Prot and Pfam. Swiss-Prot is a manually annotated and reviewed section of the UniProt Knowledgebase (UniProtKB) that represents a high quality annotated and non-redundant protein sequence database, which brings together experimental results, computed features, and scientific conclusions (Bairoch et al., 2004). On the other hand, Pfam is a comprehensive collection of protein domains and families, represented as multiple sequence alignments and as profile hidden Markov models (Finn et al., 2008)

5.8. Quantification of total cell numbers by DAPI staining

DAPI (4´, 6-diamidino-2-phenylindole) is a fluorescent DNA-intercalating dye that binds to negatively charged molecules such as polyphosphate. DAPI forms highly fluorescent complexes with double stranded DNA by binding preferentially to AT-rich regions (Eriksson et al., 1993).

For DAPI-staining the fixed sediment (4% formaldehyde, 4 °C) was 10-fold diluted with PBS 4X. The samples were subject to ultrasounds at different times (from 1 to 20 min) (AP Selectra Ultrasonic, 40 KHz, 200 W) in order to detached and disaggregate the cells

from the sediment particles. Maximum cell numbers were obtained after 5 min ultrasounds, as revealed by cell counting after DAPI-staining. The treatment of the samples with ultrasounds has been demonstrated to not alter the results obtained using different staining procedures (Manini and Danovaro, 2006).

The sediment was filtered (0.22 µm, 16 mm Isopore GTTP, Millipore) and filter sections were stained with DAPI (1 µg ml^{-1}) for 90 sec and further washed in distilled water. Filters were immersed in absolute ethanol (6 sec) in order to dehydrate the cells and distain the filter tissue to avoid background color. Samples were mounted with citifluor solution (Citifluor Ltd.) onto microscope slides and stored at -20ºC.

The stained samples were examined using a fluorescence microscope (Axio imager.A1, Zeiss) with UV laser and the filter set 49 (G 365, FT 395, BP 445/50, Zeiss). The maximum excitation and emission of DAPI bound to dsDNA were 358 and 461 nm, respectively. Counts are reported as means calculated from 15 randomly chosen microscope fields corresponding to approximately 600 DAPI-stained cells. Fifteen microscope fields of 1,200 μm^2 were the optimum number of fields with the lowest standard deviation. Counting more than 15 fields did not produced significant modifications in means and standard deviations.

5.9. Fluorescence in situ *hybridization (FISH)*

Five milliliters of the supernatant obtained during cell extraction were fixed with 4% formaldehyde for 6 h at 4 °C and centrifuged at 13, 000 rpm g for 15 min. The pellet was resuspended in PBS 4X:ethanol (1:1) and stored at -20 ºC. A subset of 30 µL were diluted in PBS 4X, sonicated (3 pulses of 3 s at 84 µm amplitude, Bandelin Sonoplus), and subsequently filtered. Filter sections were hybridized and DAPI-stained (Snaidr et al., 1997). The hybridization was carried out using both, monolabeled and horseradish peroxidase (HRP)-labeled probes. The probes used in this study are listed in Table 1.

5.9.1. FISH using monolabeled oligonucleotide probes

Filter sections were placed onto glass slides (up to five filter sections could be placed onto one slide for simultaneous hybridization with the same probe) and covered with 20 µl of the hybridization solution (0.9 M NaCl, 20 mM Tris-HCl, 0.01% SDS, 5.5 ng μl^{-1} each probe and formamide (Aldrich) [the % depends on the probe, see Table 1]).

Hybridization vessels were prepared by placing a piece of blotting paper soaked with the remaining hybridization buffer (around 2 ml) into a 50 ml polyethylene tube. The slide was placed into the hybridization vessels (in a horizontal position) and incubated for 2 h at 46ºC. After the incubation period, the slides were quickly transferred into 50 ml of pre-warmed washing buffer (20 mM Tris-HCl, NaCl [concentration depending on % formamide used in the hybridization buffer, see Table A.1], 5 mM EDTA and 0.01% SDS) and incubated in a water bath at 48ºC for 15 min. Subsequently the filter sections were placed into a Petri dish with MilliQ water for several seconds and then air-dried on blotting paper.

Finally, the filter sections were DAPI stained as explained before and stored at -20ºC.

The oligonucleotide probes were labeled with a Cy3 fluorochrome (Thermo Hybaid, Interactiva Division).

Table 1. Oligonucleotide probes used for fluorescence *in situ* hybridization of microbial 16S rDNA.

Probe	Specificity	Sequence (5'-3')	Position in *E. coli*	Label	FA [%][a]	Reference
NON338	Antisense of EUB338	ACTCCTACGGGAGGCAGC	338-355	Cy3/HRP	10	(Wallner et al., 1993)
EUB338 I-III	Most *Bacteria*	**Mixture of probes EUB338 I, II and III**				
EUB338 I	Most *Bacteria*	GCTGCCTCCCGTAGGAGT	338-355	Cy3/HRP	35	(Amann et al., 1990)
EUB338 II	*Planctomycetales*	GCAGCCACCCGTAGGTGT	338-355	Cy3/HRP	35	(Daims et al., 1999)
EUB338 III	*Verrucomicrobiales*	GCTGCCACCCGTAGGTGT	338-355	Cy3/HRP	35	(Daims et al., 1999)
ARCH915	Most *Archaea*	GTGCTCCCCCGCCAATTCCT	915-935	Cy3/HRP	35	(Raskin et al., 1994)
DELTA495 a-c[b]	*Deltaproteobacteria*	**Mixture of probes DELTA495 a, b and c**				
DELTA495a	Most *Deltaproteobacteria* and most *Gemmatimonadetes*	AGTTAGCCGGTGCTTCCT	495-512	Cy3/HRP	35	(Lücker et al., 2007)
DELTA495b	Some *Deltaproteobacteria*	AGTTAGCCGGCGCTTCCT	495-512	Cy3/HRP	35	(Lücker et al., 2007)
DELTA495c	Some *Deltaproteobacteria*	AATTAGCCGGTGCTTCCT	495-512	Cy3/HRP	35	(Lücker et al., 2007)

[a] Formamide concentration in hybridization buffer; [b] Probes DELTA495(a-c) were used together with the unlabeled competitor probes cDELTA495(a-c) (Lücker et al., 2007). Details of oligonucleotide probes are also available at ProbeBase (http://www.microbial-ecology.net/probebase/).

5.9.2. Catalyzed reporter deposition (CARD-FISH)

CARD-FISH was performed as previously described (Ishii et al., 2004; Pernthaler and Pernthaler, 2007). As the probes were labeled with horseradish peroxidase (HRP) (Biomers, Germany), a permeabilization step was necessary in order to allow the diffusion of such a large molecule into the whole fixed cell. To avoid cell loss during cell wall permeabilization, filters were embedded in 0.2% low melting-point agarose (Nusieve GTG Agarose, Cambrex Bio Science Rockland, Inc). The agarose was boiled and let it cool down to 35-40°C. One drop of agarose, big enough to cover a filter of 1.7 cm i.d., was placed in the surface of a Petri dish with the filter face-down over it. After 5 s in contact with the agarose, the filter was dried for 10 min at 46°C.

Endogenous peroxidases were inactivated by incubating the samples with 0.15 % of H_2O_2 in methanol during 30 min at RT. Subsequently, the filters were washed with MilliQ water and 96% ethanol and air dried.

The permeabilization was carried out by incubating the filter sections 60 min in a lysozyme solution (10 mg ml^{-1} in 0.05 M EDTA, pH 8.0; 0.1M Tris-HCl, pH 8.0) and 2 min in a proteinase K solution (10 µg ml^{-1} in 50 mM EDTA, pH 8.0; 100 mM Tris-HCl, pH 8.0; 500 mM NaCl) at 37°C. After the incubation the filters were washed with MilliQ water.

Filter sections were placed into a reaction vial of 0.5 ml (10 to 20 sections per vial) containing 300 µl of hybridization buffer (0.9 M NaCl, 20 mM Tris-HCl, pH 7.5; 10% dextran sulphate, 0.02% SDS, formamide [the % depends on the probe, see Table 1], 1% Blocking Reagent [Boehringer, Mannheim, Germany]) and 1 µl of probe working solution (50 ng μl^{-1}). The filters were incubated at 46 °C for 2-3 h. The washing buffer was freshly prepared in a 50 ml tube (5 mM EDTA, pH 8.0; 20 mM Tris-HCl, pH 7.5; NaCl [concentration depending on % formamide used in the hybridization buffer, see Table A.1], 0.01% SDS) and pre-warmed. After incubation the filters were transferred to the washing buffer and incubated at 48°C for 5 min. Without let the filter sections dry they were transferred to PBS 1X and incubate for 15 min at RT. The excess of liquid in the filters was removed with blotting paper (without letting them dry).

Four hundred microliters of amplification buffer (PBS 1X, 0.1% Blocking Reagent, 2 M NaCl, 10% dextran sulphate) were mixed with fresh H_2O_2 solution (0.15% in PBS 1X) in a ratio of 100:1. Then, 1 µl of the fluorescently labeled tyramide (1 mg dye ml^{-1}) was added, well mixed and kept in the dark. The filters were dipped into the amplification

mix in the way that the filter sections face-up on the wall tube not touching between each other. The filters were incubated at 46°C during 20 min in the dark.

The excess of liquid was removed using blotting paper and the filters were incubated in PBS 1X at RT for 10 min in the dark. The filters were then washed in excess MilliQ during 1-5 min and 96% ethanol (~5 min), and let completely air dried in the dark before counterstaining with DAPI.

5.9.3. Cells quantification by fluorescence microscopy

Cells were quantified using a fluorescence microscope (Axio imager.A1, Zeiss).

The filter set used for FISH with monolabeled oligonucleotide probes was the HQ:Cy3 (AF analysentechnik; HQ 545/30, Q 570 lp, HQ610/75) while for CARD-FISH was the 38 (Zeiss; BP470/40, FT495, BP 525/50). Hybridization with probe NON338 (Cy3 and HRP-label) was performed as a negative control. Counts are reported as means calculated from 15 randomly chosen microscope fields corresponding to approximately 600 DAPI-stained cells. Over 500 DAPI-stained cells should be counted per hybridized filter piece to reduce the counting error to less than 5% (Pernthaler et al., 2002).

6. Statistical diversity indexes

The PAST software v1.82b was used to compute the statistical diversity indexes in the sequence dataset. The Shannon-Wiener diversity index (*H*) is commonly used to characterize species diversity in a community and accounts for both abundance and evenness of the species (OTUs or OPUs) present. The formula used was as follows:

$$H = -\sum\left(\frac{ni}{nt}\right)Ln\left(\frac{ni}{nt}\right)$$

where *ni* is the number of sequences of a particular OTU and *nt* is the total number of sequences. The Shannon-Wiener diversity index varies from 0 (communities with only a single taxon) to 4 (communities with many taxa, each with few individuals).

Dominance-D index was estimated as follows:

$$D = \sum\left(\frac{ni}{nt}\right)^2$$

As in the S-W index, *ni* represents the number of sequences of a particular OTU and *nt* is the total number of sequences. The D index varies from 0 (no dominant OTU or OPU) to 1 (100% of the sequences belonging to one OTU or OPU).

The coverage of the sample was estimated through the Good's coverage, calculated as follows:

$$C = 1 - \left(\frac{ni}{nt} \right)$$

where *ni* is the number of OTUs observed exactly once, and *nt* is the total number of sequences (Esty, 1986).

Rarefaction curves were performed using the Analytic Rarefaction 1.3 available at http://www.uga.edu/~strata/software. Rarefaction curves plot the total number of individuals counted with repeated samplings versus the total number of species (OTUs or OPUs) found in those samplings. The result is a curve that increases steeply at first and then gradually levels off. The point at which it levels off is the point where additional sampling is yielding no additional information about the number of species.

The comparison of the values obtained by FISH, DAPI and SRR analysis were performed by using the Student's *t* test ($P > 0.05$) on the averaged values.

7. Culture dependent approaches

7.1. Artificial seawater medium for the cultivation of SRB

Artificial seawater medium (ASW) was prepared in a special vessel (Figure 5) by mixing the reagents listed in Table 2, following the protocol described by Widdel and Bak (Widdel and Bak, 1992).

The medium was autoclaved and when its temperature decreased to approximately 80°C, the headspace of the flask was flushed with N_2 at a pressure of 100 mbar for 5 min. After flushing, the screw caps were tightly closed to produce a slight overpressure and the medium was let to cool down. After cooling, the gas connection was changed to N_2/CO_2 (9:1) and the solutions listed in Table 3 were added. The pH of the medium was adjusted to 7.0-7.3 by adding 1M H_2SO_4 or 1 M N_2CO_3 when necessary. The medium was distributed in sterile bottles and kept in the dark at RT.

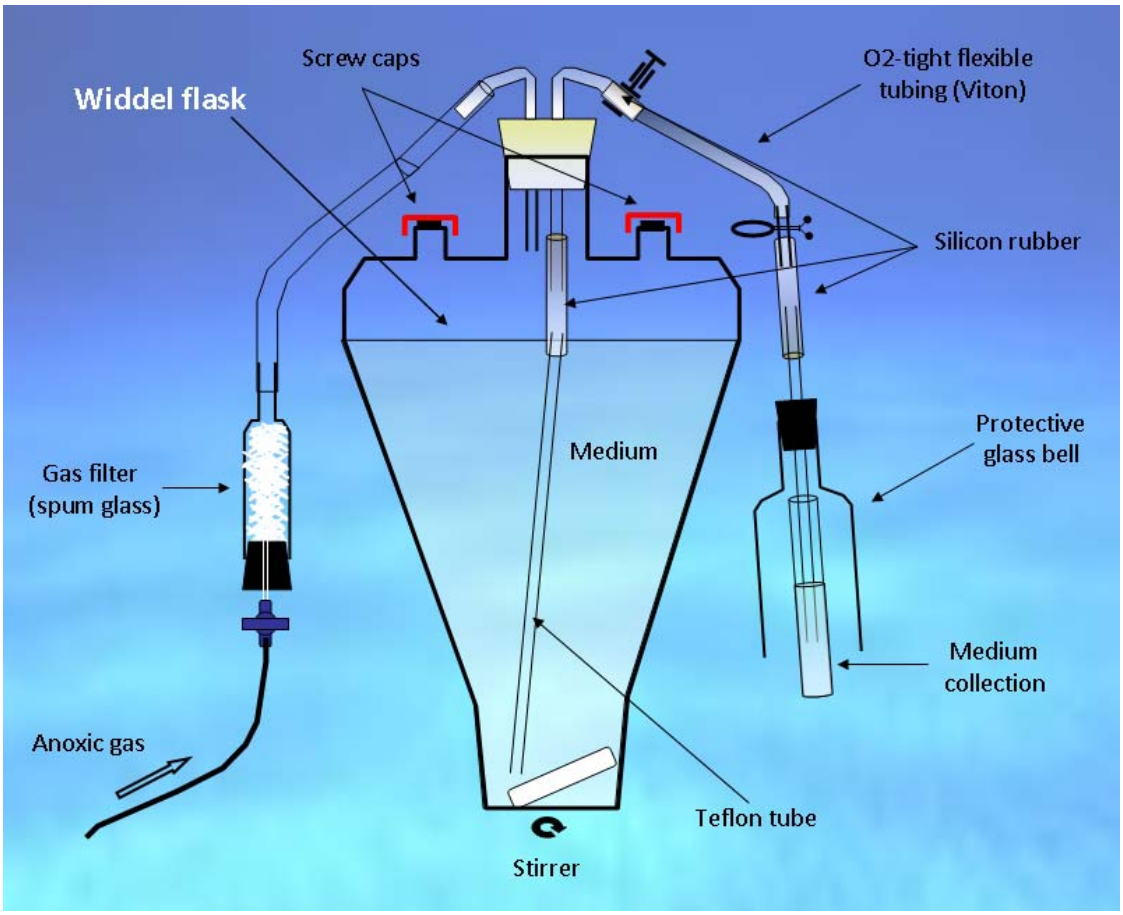

Figure 5. Schematic representation of a Widdel flask.

Table 2. ASW medium composition.

Reagent	Final concentration (mM)	g
NaCl	451	26.4
$MgCl_2.6H_2O$	28	5.6
$MgSO_4.7H_2O$	28	6.8
$CaCl_2.2H_2O$	10.1	1.47
KCl	8.9	0.66
KBr	0.8	0.09
MilliQ H_2O	Until 1000 ml	

Table 3. Additional reagents of the ASW medium.

Reactive	Add (ml)
1M $NaHCO_3$	30
4M NH_4Cl	1
1.1M KH_2PO_4	1
Trace elements solution*	1
Selenite-tungstate solution*	1
Vitamin solution*	1
Thiamin solution*	1
B_{12} solution*	1
Rivoflavin solution*	1
0.6M Na_2S	1
1M H_2SO_4**	0.65
Dithionite	Add 30 mg

* Preparation explained in Tables A.2, 3 and 4 (Annex).
** Instead of H_2SO_4, 30 mM FeOOH and 30 mM (final concentration), were added as electron acceptors to the media for the cultivation of iron and manganese-reducing bacteria, respectively.

7.2. Most probable number dilution series

For the MPN approach, 10 ml of ASW was dispensed into 15 ml tubes. In this case the addition of sodium sulphide (Na_2S) to the medium was replaced by the addition of an acid–washed iron nail in each tube that served to mildly reduce the culture medium and allowed the detection of growth by the precipitation of FeS (Figure 6) (Cifuentes et al., 2003).

Ten cm^3 of untreated, vegetated, naphthalene- and crude oil-amended sediment (from the 13 to 19 cm depth in samples from September 25th) were collected under oxygen free gas flow and diluted in 90 ml of ASW medium without electron donor. MPN tube series were inoculated anaerobically in 10-fold dilution steps.

Electron donors were then added at the following concentrations: 10 mM sodium acetate; 5 mM each of sodium lactate; pure hydrogen by flushing into the headspace of the tubes to saturate the gas phase; naphthalene and anthracene as crystals of 1 to

1.5 mg; crude oil was added as a single drop containing 1 to 1.5 mg. The cultures were incubated at 22 ºC for 4 months in dark.

To increase the statistical accuracy of the test, 3 tubes were inoculated from each dilution. After incubation, the pattern of positive and negative tubes was recorded, and the MPNs of organisms per cm^3 of the original sediment were calculated according to standard procedures (Blodgett, 2006). The highest positive MPN dilutions were chosen for 16S rDNA analysis.

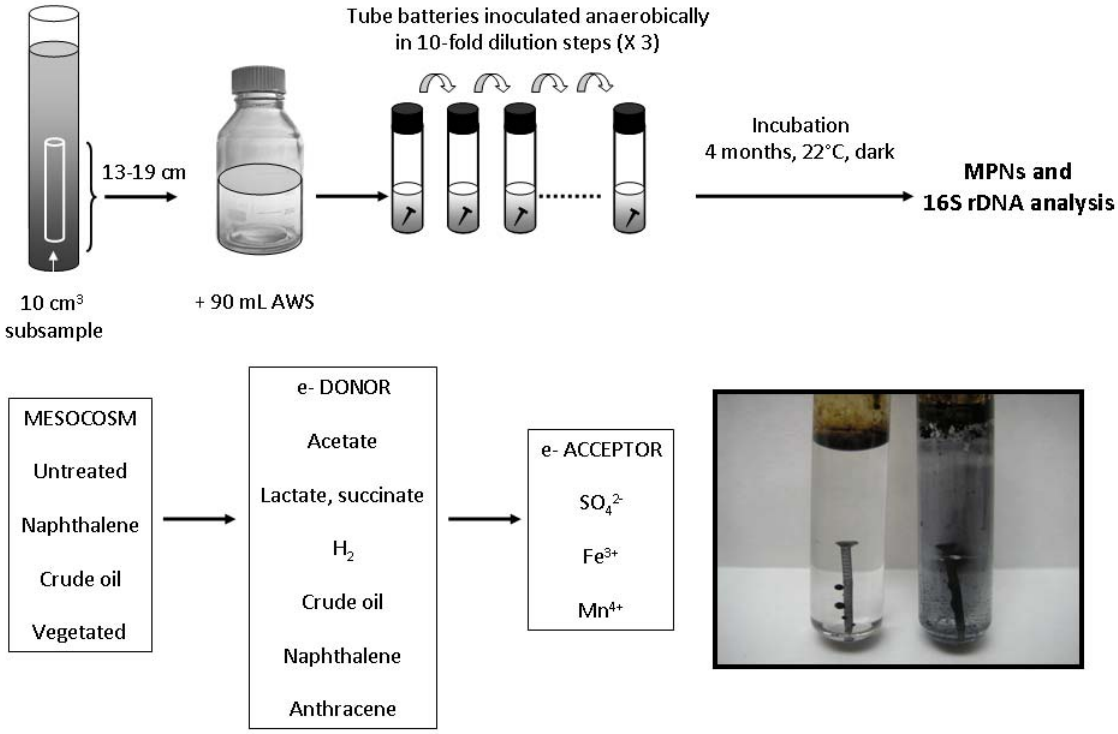

Figure 6. MPN cultivation procedure. The picture represents an example of positive growth reported by precipitation of FeS on a culture amended with crude oil (left tube) in comparison with a control culture incubated without inoculum (right tube).

7.3. Establishment of hydrocarbon-degrading enrichment cultures

Sediment from 2 to 12 cm depth of a sediment core contaminated with naphthalene (3 years) was used as inoculum. A 20 ml aliquot was carefully mixed with 10 ml of ASW containing 28 mM sulphate. Five millilitres of this mixture were inoculated into 100 ml 8-corners bottles containing 55 ml of ASW medium and 1 ml of light crude oil from Casablanca (Morocco) under CO_2/N_2 gas flow. The bottles were placed upside down

and in oblique position, avoiding the contact of the hydrocarbon with the rubber stopper, and incubated at 28ºC and 50 rpm. In order to obtain a sediment-free enrichment culture, two subsequent transfers (10% inoculum, v/v) were carried out when the sulphide concentration in the medium reached 12-15 mM. In a forth transfer, sediment free enrichment culture was inoculated by triplicate. Cell numbers and sulphide production were monitored along the incubation, and degradation of crude oil constituents was analyzed at the end of the growth.

In order to detect the growth with alternative electron donors and acceptors, incorporated within the inoculum or the crude oil, several control cultures (negative, abiotic, and sulphate free, Figure 7) were set up and incubated simultaneously.

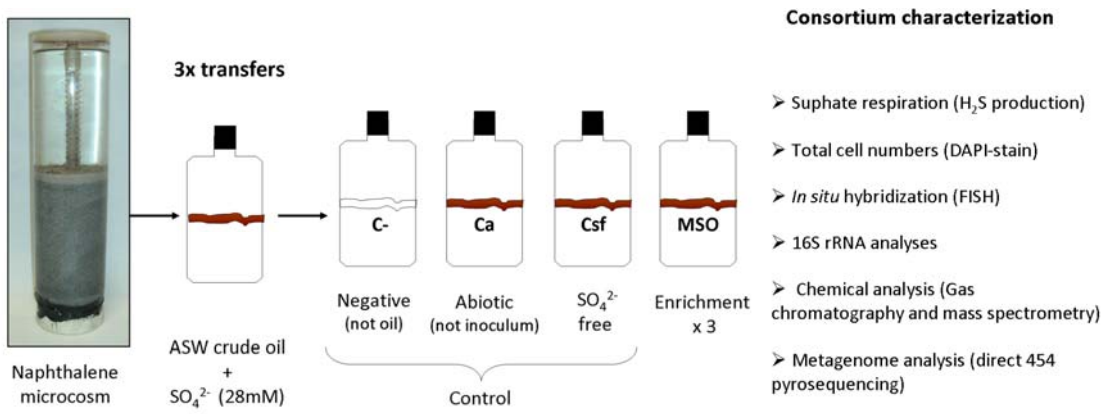

Figure 7. Experimental procedure for the enrichment and characterization of crude oil-degrading consortia.

When the sulphide concentration reached 13-15 mM, each replicate culture was divided into several aliquots:

- Ten millilitres of each replicate were collected, mixed with the other replicates (30 ml in total), and processed for total DNA extraction as explained in Section 5.3. This DNA was used for direct 454 pyrosequencing and 16S rDNA gene clone library construction (Section 5.4.).
- One millilitre of each culture was fixed in 4% formaldehyde-PBS 4X for the DAPI/FISH procedure (Section 5.8.).
- Five millilitres were separated for chemical analysis (GC-MS and ICR-FT-MS, Sections 8.2 and 8.3).

7.4. *Quantification of the sulphide production in the enrichment cultures*

Dissolved sulphide in the enrichment cultures was determined spectrophotometrically as a colloidal solution of copper sulphide as described before (Cord-Ruwisch, 1985). The method is based in the following reaction:

$$CuSO_4 + H_2S \rightarrow CuS + H_2SO_4$$

The culture medium (100 µl) was added to 4 ml of acidic copper reagent (5 mM Cu SO_4, 50 mM HCl) and gently mixed by inversion (2 s). The reaction causes a brownish precipitation of CuS that was measured with a spectrophotometer (U-2900, Hitachi) at 480 nm wavelength.

Calibration curve was determined by plotting the optical density (OD) values determined from known concentrations of Na_2S. The standards were prepared by appropriated dilution of titrated 1M Na_2S in anoxic MilliQ water. The calibration curve was linear in the range from 0 to 20 mM sulphide.

8. Analytical chemistry

8.1. Quantification of naphthalene in sediments by high performance liquid chromatography

Naphthalene was extracted from the sediment using solid-phase extraction (SPE) in C_{18} resin, as described previously (Sarrazin et al., 2006). The samples were oven dried at 35°C before the extraction. A sediment sample of 5 g was introduced into a 50 ml glass flask, and 20 ml of acetone were added. The flask was ultrasonicated during 30 min (AP Selectra Ultrasonic, 40 KHz, 200 W). The mixture was vigorously shaken and let it set for 30 min. Ten millilitres of the liquid extract were collected into a 10 ml glass tube after filtration of the overlaying solvent using a 9.0 cm GF/C glass microfiber filter (Whatman International). Subsequently, 25 ml of water were added to the filtrate. C_{18} Bon Elute cartridges (Varian) were conditioned before use by passing 5 ml of acetone and 5 ml of a solvent constituted by 40% of acetone in water. The extraction solution

was then passed through the C_{18} resin at a flow of rate of 2 ml min^{-1}. After the sample loading, the cartridge was air dried for 15 min. The analytes were eluted from the cartridge by passing 1 ml of acetone 3 times. Before each elution the resin had to be impregnated for 10 min with acetone. Two millilitres of methanol was aspired through the resin in order to complete the naphthalene recuperation. The purified elute was collected in a 5 ml volumetric flask and adjusted with methanol before RP-HPLC analysis. Ultrapure water was obtained by using a MilliQ purification system (Millipore, Bedford, MA) and used in all the procedures.

High performance liquid chromatography (HPLC) analyses were performed with an Elite EZLaChrom LC (Hitachi, VWR) equipped with a pump, a degassing unit (L-2130), an autosampler (L-2200) and a fluorescence detector L 2485. Data acquisition and processing were carried out on Agilent *EZ* LaChrom Elite Software. Separation of the naphthalene was performed at 21 ºC on a C_{18} column (3 µm, 3.9 x 150 mm, Waters) connected to a pre-column (20 x 4 mm) containing a similar coating.

The elution profile, flow rate and fluorescence detection conditions were those previously described for the 16 EPA PAHs (Sarrazin et al., 2006). The mobile phase of the HPLC system consisted of acetonitrile (Solvent A) and water (Solvent B). Different proportions A:B were used during the analysis. The separation started with a linear gradient from 65:35 to 100% acetonitrile in 25 min that was maintained isocratic during 15 min to finally re-establish the initial conditions with a linear gradient to 65:35 in 1 min. These conditions were held during 20 min before a new injection. The total flow rate of the mobile phase was 1 ml min^{-1}, the temperature in the column was 21ºC and the sample volume injected was 25 µL. The excitation and emission wavelengths were 280 nm and 340 nm respectively.

Working standard solutions were prepared by appropriate dilutions of naphthalene (Sigma-Aldrich) in acetone:methanol (3:2; v/v), while calibration curves were established by injecting an appropriate amount of standard solutions at different concentrations.

The determination of recovery yields was performed by adding a defined quantity (100 µg kg^{-1}) of naphthalene to three replicates of uncontaminated sediment and subsequent extraction.

Reproducibility was established by determining the standard deviation of three independent measurements and detection limits were calculated as three times the standard deviations of the blanks.

8.2. Gas chromatography

Total petroleum hydrocarbons (TPHs) in the residual crude oil were obtained by column chromatography of the culture organic extracts (Vila et al., 2010).

8.2.1. Sample preparation

Five hundred millilitres of the culture were concentrated to dryness under vacuum, weighed, redissolved in n-hexane and applied to an SPE glass column (J.T. Baker) packed with 2.5 g of alumina (Merck, Darmstad, Germany) previously activated at 120 ºC. The saturated hydrocarbons were eluted with n-hexane, the aromatics with dichloromethane, and the resins with methanol. All the fractions were concentrated to dryness under vacuum and weighed. The saturated and aromatic fractions were redissolved in 1 ml of dichloromethane and 0.1 ml of each one were combined to obtain the TPHs. O-terphenyl (0.01 g L^{-1}) (Sigma-Aldrich Chemie) was added as an internal standard.

8.2.2. Total petroleum hydrocarbons analysis

GC-FID analyses were performed using a TRACE GC2000 (Thermo) gas chromatograph equipped with a FID. GC-MS analyses were performed in a Hewlett Packard HP5890 Series II gas chromatograph coupled to an HP5989 mass spectrometer. The GC chromatograph was equipped with DB5 capillary column (30 x 0.25mm i.d., J&W Scientific, Folsom, CA) with a 0.25-mm film thickness. The column temperature was held at 50 1C for 1 min and then increased to 320 ºC at 5 ºC min^{-1}, this final temperature being held for 10 min.

Injector, transfer line and detector temperatures were set at 290, 290 and 320 ºC, respectively. The samples (1 ml) were injected in splitless mode using helium as the carrier gas, at a flow rate of 1.1 ml min^{-1}. The extent of biodegradation of the 16 PAHs

included in the US EPA list of priority pollutants and alkyl PAHs was determined from the hopane-normalized peak areas of the target analytes compared with those obtained for the same compounds in the control samples. The peak areas of the analytes were measured in the GC-MS reconstructed ion chromatograms obtained using the molecular ion for the aromatics, *m/z* 85 for linear and branched alkanes, *m/z* 230 for the internal standard o-terfenil, and *m/z* 191 for the conservative internal biomarker 17a(H),21b(H)-hopane.

8.3. Ion cyclotron resonance Fourier transform mass spectrometry (ICR-FT-MS) analyses

This approach was used in order to provide evidence of complex modifications in the metabolite composition of the cultures supplemented with crude oil and PAHs. ICR-FTMS is a high resolution technique that allows the determination of the mass-to-charge ratio (m/z) of the polar molecules present in a sample with very high accuracy. Using an electrospray (ESI), the molecules are ionized and the ions are trapped in a magnetic field with electric trapping plates where they are excited to a larger cyclotron radius (circular movement of ions in a strong magnetic field, Figure 8) by an oscillating electric field perpendicular to the magnetic field. When the ion´s orbit is close enough to the detection electrodes, they induce an image current that is amplified and recorded, for all the ions simultaneously. The resulting signal, called free induction decay (FID) or interferogram (Figure 9), consists in a superposition of sine waves. Fourier transform decomposes that signal into its constituent frequencies giving a mass spectrum after calibration. FTICR-MS is a very useful technique for the analysis of complex mixtures since the resolution (narrow peak width) allows the detection of ions of similar mass to charge (*m/z*).

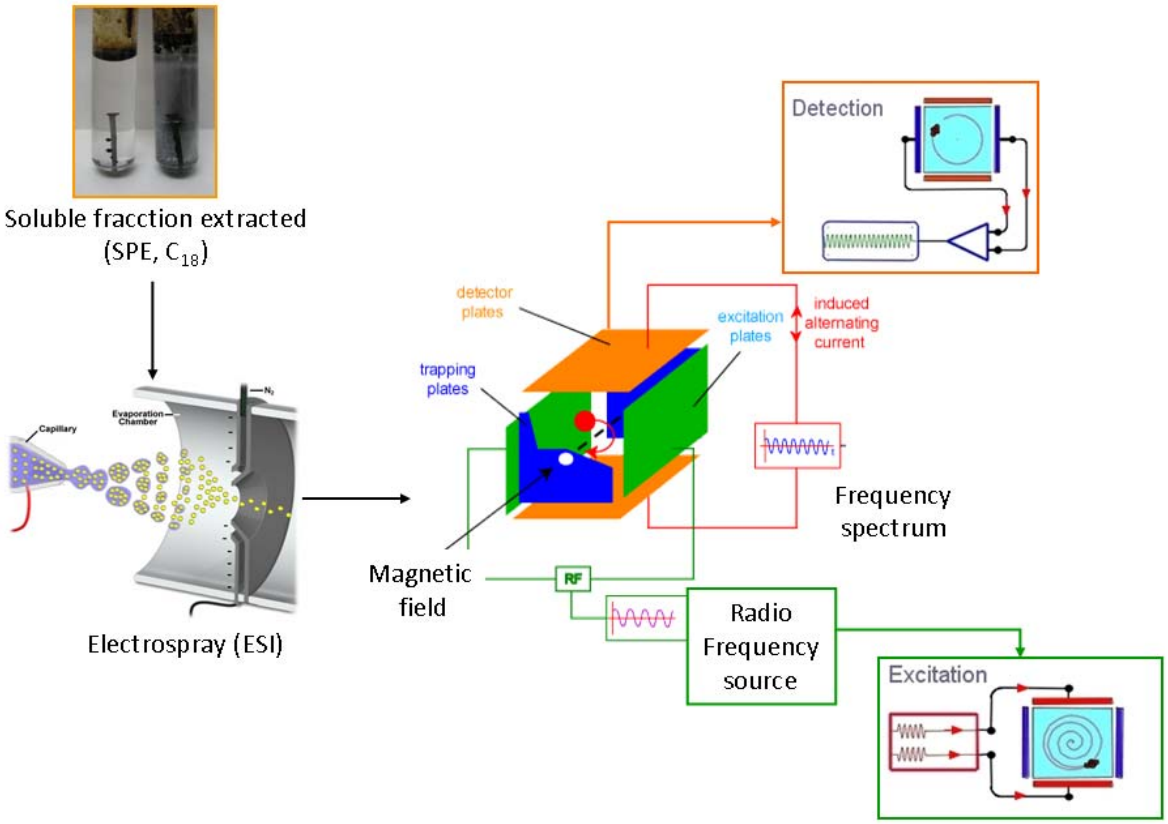

Figure 8. Schematic view of the ion cyclotron resonance Fourier transform mass spectrometry (modified from http://www.chm.bris.ac.uk/ and http://www.magnet.fsu.edu/).

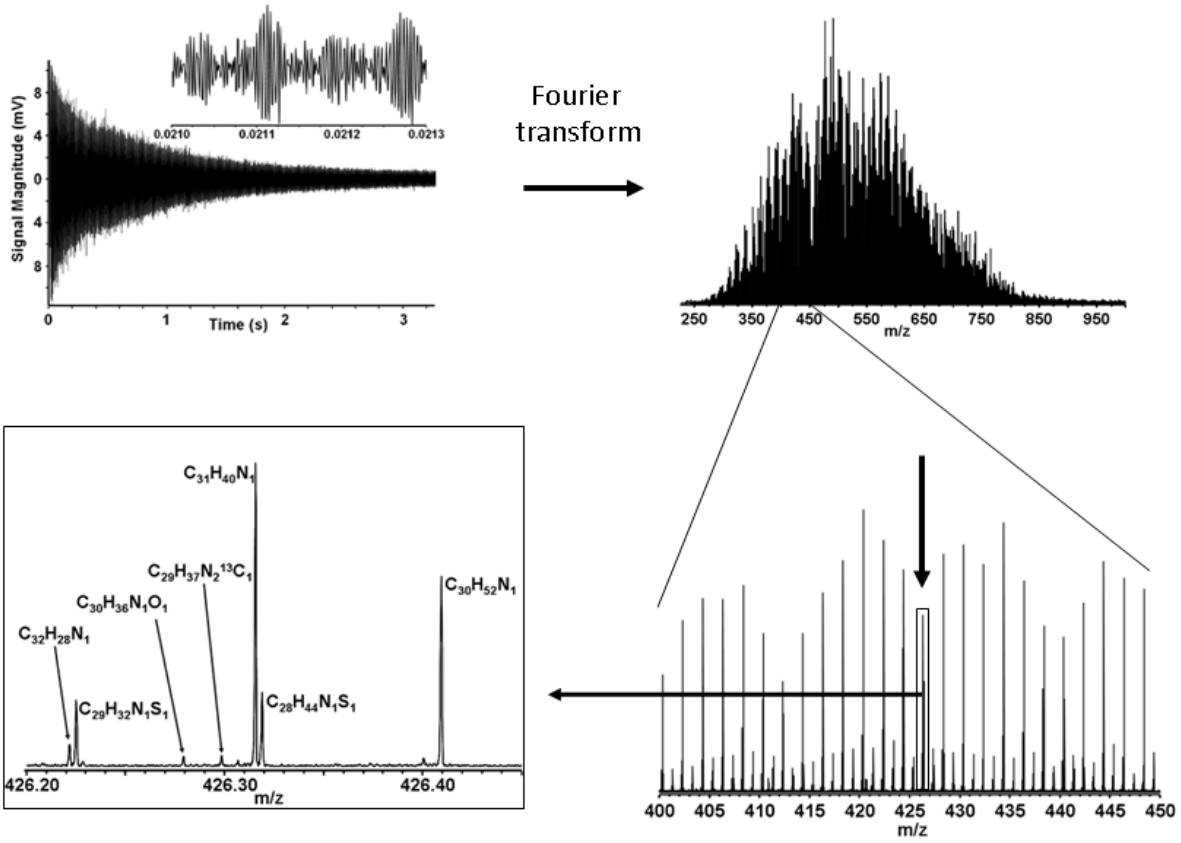

Figure 9. Fourier transform allows the translation of the resulting interterferogram into a mass spectrum.

8.3.1. Sample preparation

The soluble fraction of the cultures was extracted from one milliliter of the cultures supplemented with crude oil, naphthalene or anthracene (Schmitt-Kopplin et al., 2008). The samples were acidified with 10 µL 100% formic acid prior to solid phase extraction (SPE) in C18 cartridges (100 mg ml^{-1}; BakerBond). The cartridges were previously conditioned with 1 ml of methanol and 1 ml of acidified water (1% formic acid in water; v/v). After application of the sample, the columns were washed with acidified water and the analytes were eluted with 1 ml methanol. The original crude oil sample (100 mg) was also extracted and analyzed. For the crude oil degradation, four grown tubes of the highest dilution were randomly selected for their metabolite extraction. For anthracene and naphthalene degradation, two tubes of each metabolism were used for metabolite analysis.

8.3.2. Metabolite analysis

High-resolution mass spectra acquisition and data analysis were performed as previously described (Schmitt-Kopplin et al., 2008; Schmitt-Kopplin et al., 2010a). High-resolution mass spectra were acquired with a Bruker (Bremen, Germany) SOLARIX Fourier transform ion cyclotron resonance mass spectrometer, equipped with a 12-Tesla superconducting magnet. Ionization was performed in negative-ion modus. Samples were introduced into the APOLLO II microelectrospray source from Bruker at a flow rate of 120 µL h^{-1} with a nebulizer gas pressure of 20 psi (138 kPa) and a drying gas pressure of 15 psi (103 kPa) at 200 °C (Agilent sprayer). Spectra were first externally calibrated on clusters of arginine (1 mg l^{-1} in methanol) and internal calibration was systematically done with the presence of fatty acids reaching accuracy values lower than 0.10 ppm in routine day to day measurements. The spectra were acquired with a time domain of 4 megaword in the mass range of 100–2000 *m/z* for a peak resolution >500,000 at *m/z* 400, reaching 1,000,000 at *m/z* 250. Three hundred scans were accumulated for each sample. Elemental formulas were calculated for each peak in batch mode by an in-house–written software tool (Schmitt-Kopplin et al., 2010b). In conjunction with an automated theoretical isotope pattern comparison, the generated formulas were validated by setting sensible chemical constraints (N rule; O:C ratio ≤ 1; H:C ratio ≤ 2n þ 2; element counts: C ≤ 100, H ≤ 200, O ≤ 80, N ≤ 3, S ≤ 3) and mass accuracy window (set at < 0.2 ppm). Final formulas were generated and classified into groups containing CHO, CHNO, CHOS, or CHNOS. Based on these groups of *m:z* ratios, specific mass spectra could be reconstructed (Schmitt-Kopplin et al., 2010b).

8.3.3. Interpretation of the mass spectra: the van Krevelen diagram

The interpretation of mass spectra obtained from complex mixtures of organic compounds as crude oil (with more than ten thousand signals) is an arduous task. But already in 1950, Dirk van Krevelen (van Krevelen, 1950) suggested the use of a graphical-statistical method for the study of the structure and the reaction processes of coal that can also applied to crude oil samples. That method consists in a rectangular diagram in which the O/C atomic ratios calculated from the elementary

composition of the molecules are plotted in the x-axis while the H/C atomic ratios are plotted in the y-axis (Figure 10).

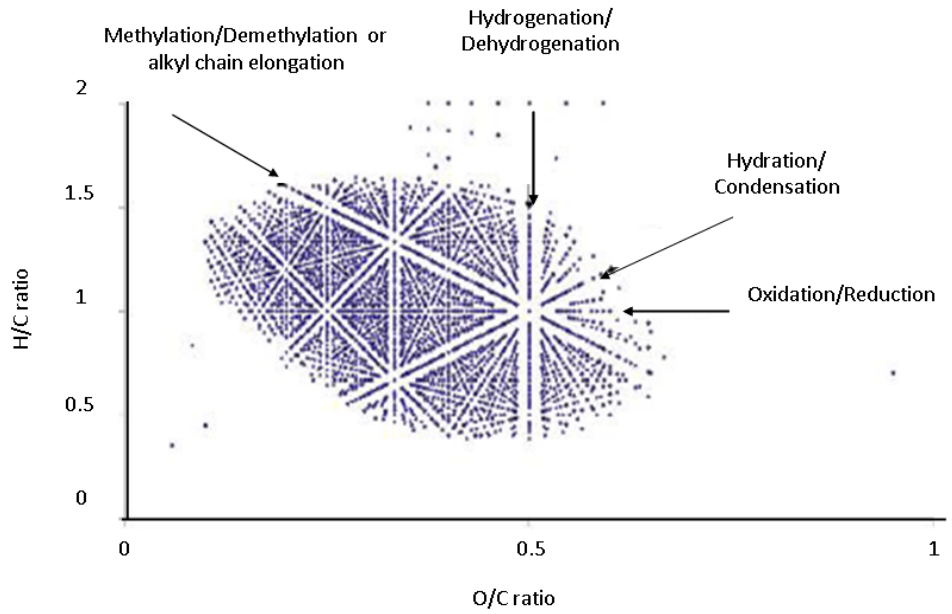

Figure 10. van Krevelen diagram for elemental data calculated from the ultrahigh resolution mass spectrum. Distinctive lines in the plot representing chemical reactions are noted (modified from Kim et al., 2003).

Each molecular formula is represented as a point. The diagram can be extended to three dimensions when the N/C or S/C atomic ratios are included. The H/C ratio separates compounds according to their degree of unsaturation while the O/C ratio separates compounds according to O classes (Meija, 2006). In the diagram, the data are distributed in the form of a pattern due to the fact that the elementary compositions of the variety of peaks differ from each other by quantized ratios of the elements C, H and O. Trends along the lines can be indicative of reaction that involves loss or gain of elements in a specific molar ratio (van Krevelen, 1950). As can be observed in the Figure 9 there are four clear line trends representing reactions as methylation/demethylation,hydrogenation/dehydrogenation, hydration/dehaydration, oxidation/reduction or carboxilation (Kim et al., 2003).

9. References

Amann, R.I., Binder, B.J., Olson, R.J., Chisholm, S.W., Devereux, R., and Stahl, D.A. (1990) Combination of 16S rRNA-targeted oligonucleotide probes with flow cytometry for analyzing mixed microbial populations. *Appl. Environ. Microbiol.* **56**: 1919-1925.

Bairoch, A., Boeckmann, B., Ferro, S., and Gasteiger, E. (2004) Swiss-Prot: juggling between evolution and stability. *Brief Bioinform* **5**: 39-55.

Blodgett, R. (2006) Most Probable Number from serial dilutions. *Bacteriological analytical manual online. U.S. food and drug administration (http://www.fda.gov/Food/ScienceResearch/LaboratoryMethods/BacteriologicalAnalyticalManualBAM/ucm109656.htm)*.

Blott, S.J., and Pye, K. (2001) GRADISTAT: a grain size distribution and statistics package for the analysis of unconsolidated sediments. *Earth Surf. Proc. Land.* **26**: 1237-1248.

Cifuentes, A., Antón, J., De Wit, R., and Rodríguez-Valera, F. (2003) Diversity of bacteria and archaea in sulphate-reducing enrichment cultures inoculated from serial dilution of *Zostera noltii* rhizosphere samples. *Environ. Microbiol.* **5**: 754-764.

Cole, J.R., Wang, Q., Cardenas, E., Fish, J., Chai, B., Farris, R.J. et al. (2009) The Ribosomal Database Project: improved alignments and new tools for rRNA analysis. *Nucleic Acids Res.* **37**: D141-145.

Cord-Ruwisch, R. (1985) A quick method for the determination of dissolved and precipitated sulfides in cultures of sulfate-reducing bacteria. *J. Microbiol. Meth.* **4**: 33-36.

Daims, H., Bruhl, A., Amann, R., Schleifer, K.H., and Wagner, M. (1999) The domain-specific probe EUB338 is insufficient for the detection of all Bacteria: development and evaluation of a more comprehensive probe set. *Syst. Appl. Microbiol.* **22**: 434-444.

Erftemeijer, P.L.A., and Koch, E.W. (2001) Sediment geology methods for seagrass habitat. *In* Global Seagrass research methods. Short, F. T, and Coles, R. G. (eds.). Elsevier Science B.V. Amsterdam, NED. pp. 345-367.

Eriksson, S., Kim, S.K., Kubista, M., and Norden, B. (1993) Binding of 4',6-diamidino-2-phenylindole (DAPI) to AT regions of DNA: evidence for an allosteric conformational change. *Biochemistry* **32**: 2987-2998.

Esty, W.W. (1986) The efficiency of Good's nonparametric coverage stimator. *Ann. Stat.* **14**: 1257-1260.

Ferdelman, T.G., Fossing, H., Neumann, K., and Schulz, H.D. (1998) Sulfate reduction in surface sediments of the south-east Atlantic continental margin between 15º 38' S and 27º 57'S (Angola and Namibia). *Limnol. Oceanogr.* **44**: 650-661.

Finn, R.D., J., T., Mistry, J., Coggill, P.C., Sammut, S.J., Hotz, H.-R. et al. (2008) The Pfam protein families database. *Nucleic Acids Res.* **36**: D281-D288.

Franco, M.A., Vinas, L., Soriano, J.A., de Armas, D., Gonzalez, J.J., Beiras, R. et al. (2006) Spatial distribution and ecotoxicity of petroleum hydrocarbons in sediments from the Galicia continental shelf (NW Spain) after the Prestige oil spill. *Mar. Pollut. Bull.* **53**: 260-271.

García-Martinez, M., López-López, A., Calleja, M.L., Marbà, N., and Duarte, C.M. (2008) Bacterial community dynamics in a seagrass (*Posidonia oceanica*) meadow sediment. *Estuar. Coast.* **32**: 276-286.

Ishii, K., Mussmann, M., MacGregor, B.J., and Amann, R.I. (2004) An improved fluorescence *in situ* hybridization protocol for the identification of bacteria and archaea in marine sediments. *FEMS Microbiol. Ecol.* **50**: 203-212.

Jørgensen, B.B. (1978) A comparison of methods for the quantification of bacterial sulfate reduction in coastal marine sediments II. Calculation from mathematical models. *Geomicrobiol. J.* **1**: 29-47.

Jørgensen, B.B., and Fenchel, T. (1974) The sulfur cycle of a marine sediment model system. *Mar. Biol.* **24**: 189-201.

Kallmeyer, J., Ferdelman, T.G., Weber, A., Fossing, H., and Jorgensen, B.B. (2004) A cold chromium distillation procedure for radiolabeled sulfide applied to sulfate reduction measurements. *Limnol. Oceanogr. Methods.* **2**: 171-180.

Kanehisa, H., Akira, M., Goto, S., Hattori, M., Hirakawa, Itoh, M. et al. (2008) KEGG for linking genomes to life and the environment. *Nucleic Acids Res.* **36**: D480–D484.

Kim, S., Kramer, R.W., and Hatcher, P.G. (2003) Graphical method for analysis of ultrahigh-resolution broadband mass spectra of natural organic matter, the van Krevelen diagram. *Anal. Chem.* **75**: 5336-5344.

López-López, A., Yarza, P., Richter, M., Suárez-Suárez, A., Antón, J., Niemann, H., and Rosselló-Móra, R. (2010) Extremely halophilic microbial communities in anaerobic sediments from a solar saltern. *Environ. Microbiol. Rep.* **2**: 258–271.

Lücker, S., Steger, D., Kjeldsen, K.U., MacGregor, B.J., Wagner, M., and Loy, A. (2007) Improved 16S rRNA-targeted probe set for analysis of sulfate-reducing bacteria by fluorescence *in situ* hybridization. *J. Microbiol. Methods.* **69**: 523-528.

Ludwig, W., Strunk, O., Westram, R., Richter, L., Meier, H., Yadhukumar et al. (2004) ARB: a software environment for sequence data. *Nucleic Acids Res.* **32**: 1363-1371.

Manini, E., and Danovaro, R. (2006) Synoptic determination of living/dead and active/dormant bacterial fractions in marine sediments. *FEMS Microbiol. Ecol.* **55**: 416-423.

Meija, J. (2006) Mathematical tools in analytical mass spectrometry. *Anal. Bioanal. Chem.* **385**: 486-499.

Meyer, F., Goesmann, A., McHardy, A.C., Bartels, D., Bekel, T., Clausen, J. et al. (2003) GenDB--an open source genome annotation system for prokaryote genomes. *Nucleic Acids Res.* **31**: 2187-2195.

Muyzer, G., Teske, A., Wirsen, C.O., and Jannasch, H.W. (1995) Phylogenetic relationships of *Thiomicrospira* species and their identification in deep-sea hydrothermal vent samples by denaturing gradient gel electrophoresis of 16S rDNA fragments. *Arch. Microbiol.* **164**: 165-172.

Nogales, B., Moore, E.R., Abraham, W.R., and Timmis, K.N. (1999) Identification of the metabolically active members of a bacterial community in a polychlorinated biphenyl-polluted moorland soil. *Environ. Microbiol.* **1**: 199-212.

Noguchi, H., Park, J., and Takagi, T. (2006) MetaGene: prokaryotic gene finding from environmental genome shotgun sequences. *Nucleic Acids Res.* **34**: 5623-5630.

Orfila, A., Jordi, A., Basterretxea, G., Vizoso, G., Marbà, N., Duarte, C.M. et al. (2005) Residence time and *Posidonia oceanica* in Cabrera Archipelago National Park, Spain. *Continental Shelf Research* **25**: 1339-1352.

Pernthaler, A., and Pernthaler, J. (2005) Diurnal variation of cell proliferation in three bacterial taxa from coastal North Sea waters. *Appl. Environ. Microbiol.* **71**: 4638-4644.

Pernthaler, A., and Pernthaler, J. (2007) Fluorescence *in situ* hybridization for the identification of environmental microbes. *Methods Mol. Biol.* **353**: 153-164.

Pernthaler, A., Pernthaler, J., and Amann, R. (2002) Fluorescence *in situ* hybridization and catalyzed reporter deposition for the identification of marine bacteria. *Appl. Environ. Microbiol.* **68**: 3094-3101.

Pruesse, E., Quast, C., Knittel, K., Fuchs, B.M., Ludwig, W., Peplies, J., and Glöckner, F.O. (2007) SILVA: a comprehensive online resource for quality checked and aligned ribosomal RNA sequence data compatible with ARB. *Nucleic Acids Res.* **35**: 7188-7196.

Quast, C. (2006) MicHanThi—Design and implementation of a system for the prediction of gene functions in genome annotation projects. Universität Bremen, Diploma work.

Raskin, L., Stromley, J.M., Rittmann, B.E., and Stahl, D.A. (1994) Group-specific 16S rRNA hybridization probes to describe natural communities of methanogens. *Appl. Environ. Microbiol.* **60**: 1232-1240.

Richter, M., Lombardot, T., Kostadinov, I., Kottmann, R., Duhaime, M.B., Peplies, J., and Glockner, F.O. (2008) JCoast - a biologist-centric software tool for data mining and comparison of prokaryotic (meta)genomes. *BMC Bioinformatics* **9**: 177.

Rosselló-Móra, R., and López-López, A. (2008) The last common denominator: species or operational taxonomic units? *In* Accessing uncultivated microorganisms: from the environment to organisms and genomes and back. Zengler, K. (ed.). Washington, DC: ASM Press. pp. 117-130.

Sarrazin, L., Diana, C., Wafo, E., Pichard-Lagadec, V., Schembri, T., and Monod, J. (2006) Determination of polycyclic aromatic hydrocarbons (PAHs) in marine, brackish, and river sediments by HPLC, following ultrasonic extraction. *J. Liq. Chrom. & Rel. Technol.* **29**: 69-85.

Schmitt-Kopplin, P., Englmann, M., Rossello-Mora, R., Schiewek, R., Brockmann, K.J., Benter, T., and Schmitz, O.J. (2008) Combining chip-ESI with APLI (cESILI) as a multimode source for analysis of complex mixtures with ultrahigh-resolution mass spectrometry. *Anal. Bioanal. Chem.* **391**: 2803-2809.

Schmitt-Kopplin, P., Gelencser, A., Dabek-Zlotorzynska, E., Kiss, G., Hertkorn, N., Harir, M. et al. (2010b) Analysis of the unresolved organic fraction in atmospheric aerosols with ultrahigh-resolution mass spectrometry and nuclear magnetic resonance spectroscopy: organosulfates as photochemical smog constituents. *Anal. Chem.* **82**: 8017-8026.

Schmitt-Kopplin, P., Gabelica, Z., Gougeon, R.D., Fekete, A., Kanawati, B., Harir, M. et al. (2010a) High molecular diversity of extraterrestrial organic matter in Murchison meteorite revealed 40 years after its fall. *Proc. Natl. Acad. Sci. U S A* **107**: 2763-2768.

Snaidr, J., Amann, R., Huber, I., Ludwig, W., and Schleifer, K.H. (1997) Phylogenetic analysis and *in situ* identification of bacteria in activated sludge. *Appl. Environ. Microbiol.* **63**: 2884-2896.

van Krevelen, D.W. (1950) Graphical-statistica method for the study of structure and reaction processes of coal. *Fuel* **XXIX**: 269-284.

Vila, J., Maria Nieto, J., Mertens, J., Springael, D., and Grifoll, M. (2010) Microbial community structure of a heavy fuel oil-degrading marine consortium: linking microbial dynamics with polycyclic aromatic hydrocarbon utilization. *FEMS Microbiol. Ecol.* **73**: 349-362.

Wallner, G., Amann, R., and Beisker, W. (1993) Optimizing fluorescent *in situ* hybridization with rRNA-targeted oligonucleotide probes for flow cytometric identification of microorganisms. *Cytometry* **14**: 136-143.

Widdel, F., and Bak, F. (1992) Gram – negative mesophilic sulfate – reducing bacteria. *In* The Prokaryotes. Balows, A., Trüper, HG., Dworkin, M., Harder, W. and Schleifer, K.-H. (eds.) 2nd ed., Vol. IV. Springer, NY. pp. 3352-3378.

Yilmaz, P., Kottmann, R., Pruesse, E., Quast, C., and Glockner, F.O. (2011) Analysis of 23S rRNA genes in metagenomes - a case study from the Global Ocean Sampling Expedition. *Syst. Appl. Microbiol.* **34**: 462-469.

Zaballos, M., López-López, A., Øvreås, L., Bartual, S.G., D'Auria, G., Alba, J.C. et al. (2006) Comparison of prokaryotic diversity at offshore oceanic locations reveals a different microbiota in the Mediterranean Sea. *FEMS Microbiol. Ecol.* **56**: 389-405.

Zhou, J., Bruns, M.A., and Tiedje, J.M. (1996) DNA recovery from soils of diverse composition. *Appl. Environ. Microbiol.* **62**: 316-322.

Chapter 1: Relevant environmental features of the ecosystem

1. Introduction

The Mediterranean Sea is characterized by relatively warm, salty and oligotrophic waters. These characteristics are a reflection of the Mediterranean climate and the enclosed nature of the basin (Duarte *et al.*, 1999). The irradiance over the area, 20% greater than at similar latitudes in the Atlantic Ocean (Bishop and Rossow, 1991), leads to a high evaporation rate that coupled to the scarce water inflow and low precipitation, result in an increased salinity (3.6 – 3.9%) in comparison to the Atlantic Ocean (3.3-3.7%) (Laubier, 2005).

The coastal seafloor surrounding the Balearic Islands is mainly constituted by carbonated sand flats that physically support the most important primary producer in this marine ecosystem, the endemic dominant, reef-building seagrass *Posidonia oceanica* (Gómez-Pujol *et al.*, 2007). The sediments are primarily composed by bioclastic material as foraminifera, shell fragments of gastropods and bivalves mainly related to the presence of *P. oceanica* (Duarte and Chiscano, 1999).

In this chapter, the most relevant ecological features of the sedimentary ecosystem are described in terms of physico-chemical features, microbial diversity, *in situ* abundances, and the usage of different electron donors and acceptors by the microbial culturable fraction. The data obtained in this study were compared to those previously reported in non-oligothrophic regions.

2. Results and discussion

2.1. Environmental features

The hydrodynamic conditions at Alcúdia Bay (North of Mallorca island) are marked by low tides, currents influenced by northern winds that dominated most of the year and a fast renewal of the water body from the open sea each 20h (Figure 1). Sand transport due to the intense water forces is relatively high, and strongly influenced the surface dynamics of the sediment.

The most relevant physico-chemical characteristics of the sediment (e.g. density, porosity, granulometry, OM content, sulphate concentration) were investigated. The results, summarized in Table 1, were in the same range than those previously described in similar sandy sediments from the Mediterranean region (Danovaro, 1996b; Holmer *et al.*, 2003; Calleja *et al.*, 2007).

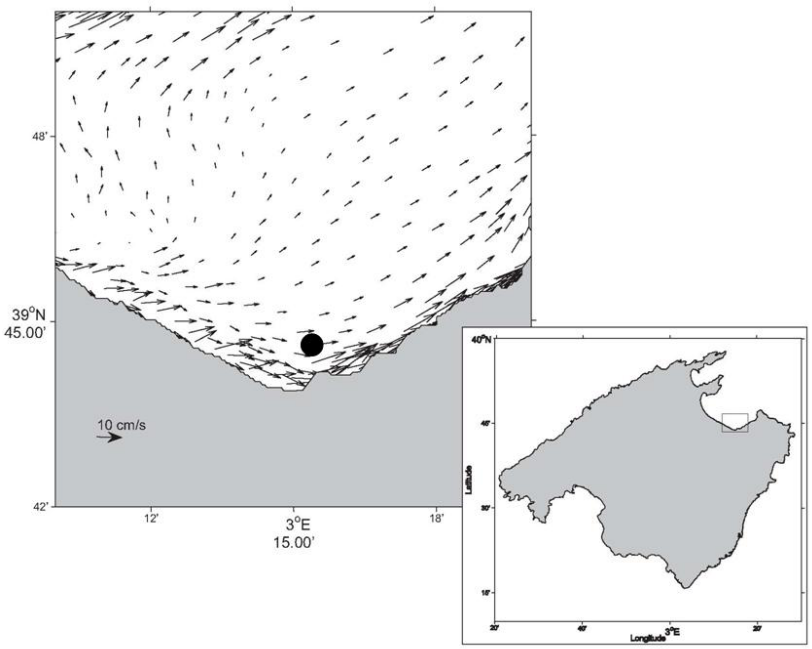

Figure 1. Water circulation model showing the vertically averaged velocities of the currents in the area of study (sampling site marked with a black dot).

Table 1. Geographic and physico-chemical characteristics of the sampling site.

Environmental features	
Geographic location	Alcúdia Bay, Mallorca, Spain
(latitude; longitude)	39º 52,1' N; 3º 08,7' E
Collection date	June 2006
Water depth	12 m
Temperature*	21ºC
Sediment type	Bare, carbonated (Biogenic), sandy
Granulometric classification	99.1 ± 0.2% fine sand
	164.8 ± 4.9 µm grain size
Density	1.5 ± 0.02 g cm^{-3}
Porosity	0.44 ± 0.02 g cm^{-3} (29%)
Total OM	1.7 ± 0.2% DW
Pore water sulphate concentration	26.8 ± 0.7 mM

* Bottom water

The sediment consisted in a porous matrix (29%) of fine sand (164.8 ± 4.9 µm) carrying a low OM content (1.7 ± 0.2% DW). However, a large microbial biomass was observed, which contrasted with the oligotrophic character of the Mediterranean Sea.

Total cell numbers, as determined by DAPI staining and epifluorescence microscopy, averaged 1.2 (± 0.05) x 10^9 cells cm^{-3} sediment (mean ± SD, n = 3) and were in the same range than previously reported in other coastal sandy sediments from richer areas as the German Wadden Sea (Llobet-Brossa *et al.*, 1998; Musat *et al.*, 2006), the Atlantic Ocean (Epstein and Rossel, 1995) or the sediments associated to the rizosphere of *P. oceanica* (García-Martinez *et al.*, 2008) (Table 2).

Moreover, the microbial abundances detected at the Balearic sediments (García-Martinez *et al.*, 2008 and this study) were even comparable to those reported in forestry soils (4 x 10^7 cells g^{-1}) and strongly contradicted the established assumption of sandy sediments being geochemical deserts that harbor no life. In the case of an oligotrophic environment as the Mediterranean Sea, this fact is remarkable as it might suggest an evolutionary microbial adaptation to low nutrient availability or the predominance of autotrophic metabolisms. However, it should not be ignored the reported fast exchange of substrates between the water column and the upper layers of sands (Huettel and Rusch, 2000) which might lead to an underestimation of the actual OM content in sediments as those from the Mediterranean Sea. Hence, more research would be necessary in order to determine the real rate of organic carbon input in this environment and its relation with the observed large microbial biomass.

Table 2. Microbial abundances in different environments.

Environmental sample	Total cell number (10^8) cm^{-3}	Total cell number (10^8) g^{-1} DW	Geographic location	Reference
Marine sandy sediment	12	8	Alcúdia Bay (IB, ES)	This study
	2-8		Tuckerton (NJ, USA)	(Rusch *et al.*, 2003)
	6-12		Artificial beach Wadden Sea (DE)	(Llobet-Brossa *et al.*, 1998)
	10		Massachusetts Bay (USA)	(Epstein and Rossel, 1995)
		4-8	Tokyo Bay (JP)	(Kuwae and Hosokawa, 1999)
	0.4-1.6		Königshafen Bay (DE)	(Rusch *et al.*, 2001)
	30		Wadden Sea (DE)	(Musat *et al.*, 2006)
		0.14-0.84	Kane'ohe Bay (Hawaii, USA)	(Sorensen *et al.*, 2007; Sørensen *et al.*, 2007)
		0.24	Ancona harbor (IT)	(Luna *et al.*, 2002)
Associated to seagrass		9-49	Cabrera National Park (IB, ES)	(García-Martinez *et al.*, 2008)
		0.83-5.8	Ligurian Sea (IT)	(Danovaro, 1996b, a)
		5.12-332	Ligurian Sea (IT)	(Danovaro *et al.*, 1994)
Marine muddy sediment	17-64		Wadden Sea (DE)	(Mussmann *et al.*, 2005)
		43	Ancona harbor (IT)	(Luna *et al.*, 2002)
		27	Tokyo Bay (JP)	(Kuwae and Hosokawa, 1999)
	17-54		Weser estuary (DE)	(Llobet-Brossa *et al.*, 2002)
Seawater	0.001-0.01		Ebro Delta (ES)	(Duarte and Vaqué, 1992)
	0.0015-0.006		NW Mediterranean Sea (BCN, ES)	(Gasol *et al.*, 1998)
	0.001-0.008		Ise Bay (JP)	(Naganuma, 1997)
Fresh water	0.01-0.015		Cabiúnas Lagoon (BR)	(Furtado, 2001)
	0.008-0.012		Lake Stechlin (DE)	(Furtado, 2001)
	0.016-0.026		Dagow (DE)	(Furtado, 2001)
	0.015-0.17		Horn Point (MD, USA)	(Shiah and Ducklow, 1995)
Forest soil		0.4		(Richter and Markewitz, 1995)
Cultivated and grassland soils		20		(Paul and Clark, 1989)

2.2. Bacterial phylogenetic affiliation revealed by the 16S rDNA

Considering the heterogeneity of natural environments, three 16S rRNA gene clone libraries were constructed from three independent sediment samples. From each library, 75 clones were randomly selected and sequenced. However, the data were treated as a single experiment. The 214 partial sequences were grouped into 140 OTUs (Operational Taxonomic Units) and 109 OPUs (Operational Phylogenetic Units). The

mean identity within each OPU was 93.5% (± 4.7 SD), with a minimum identity of 81%. It is difficult to interpret what the sequence diversity of a given clade means in terms of naturally occurring species populations (Konstantinidis and DeLong, 2008) but OPUs may be equalized to genera, and in some cases families, from the taxonomic point of view (Yarza *et al.*, 2008).

Rarefaction curves, Good's coverage values and diversity indexes were calculated for the assigned OTUs and OPUs (Table 3 and Figure 2). A considerable degree of bacterial diversity, as confirmed by Shannon-Weiner indexes over 4 and Dominance-D values close to 0, indicated that no OTU or OPU predominated in the community. Also, the Good's coverage values (0.6 to 0.7 for OPUs) and the rarefaction curves indicated that additional effort would be necessary to fully cover the sediment's diversity.

Table 3. Statistical indexes computed with data from the 16S rRNA gene clone libraries.

	Bacteria		***Deltaproteobacteria***	
	OTUs*	**OPUs**	**OTUs***	**OPUs**
Number of sequences	214		41	
Good's coverage value	0.44	0.66	0.29	0.61
Number of taxa	140	109	34	26
Shannon-Weiner index	4.49	4.23	3.45	3.13
Dominance-D value	0.02	0.03	0.04	0.05

* Clustered at 97% identity.

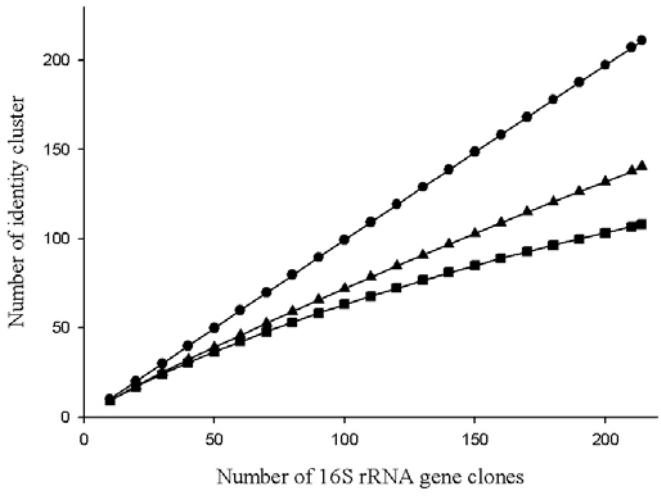

Figure 2. Rarefaction curves of the bacterial 16S rRNA gene clones. The curves were plotted as OTUs at 100% (dots) and 97% (triangles) sequence identity *versus* the number of 16S rRNA gene clones analyzed. The number of OPUs *versus* the number of 16S rRNA gene clones is also shown (squares).

Despite of our limited sequencing effort, we identified a high abundance of diverse uncultured lineages previously found in marine sediments (Musat *et al.*, 2006; Sørensen *et al.*, 2007), and in the rhizosphere of *P. oceanica* (García-Martinez *et al.*, 2008). The phylogenetic affiliations are listed in Table 4 and Table A.5. (Annex). The most frequently retrieved bacterial phylum was *Proteobacteria* (45.9% of the OPUs and 60.3% of the clones), mostly represented by *Deltaproteobacteria* (23.9% of the OPUs and 19.2% of the clones), *Gammaproteobacteria* (14.7% of the OPUs and 33.2% of the clones) and *Epsilonproteobacteria* (5.5% of the OPUs and 6.5% of the clones), in agreement with similar studies (Ravenschlag *et al.*, 1999; Musat *et al.*, 2006; Polymenakou *et al.*, 2009).

Table 4. Phylogenetic affiliation and frequencies of the bacterial phylotypes contained in the 16S rDNA clone libraries.

Phylogenetic affiliation	clone Nr	OUT Nr	OPU Nr	% OPUs
Deltaproteobacteria	41	34	26	23.9
Gammaproteobacteria	71	24	16	14.7
Alphaproteobacteria	3	2	2	1.8
Epsilonproteobacteria	14	6	6	5.5
Acidobacteria	10	9	6	5.5
Chaldithrix	1	1	1	0.9
Clostridiales	5	4	3	2.8
Fusobacteria	8	2	2	1.8
Planctomycetes	8	8	6	5.5
Verrucomicrobia	4	3	3	2.8
Lentisphaerae	2	2	2	1.8
Acidimicrobiaceae	2	2	1	0.9
Chloroflexi	16	14	11	10.1
Sphingobacteriaceae	4	4	4	3.7
Unclassified	25	25	20	18.3

Within the class *Deltaproteobacteria*, where about 80% of the known SRB species are included (Muyzer and Stams, 2008), over 50% of the OPUs (56% of the clones) were related to the family *Desulfobacteraceae*, while the rest were mainly related to unclassified *Deltaproteobacteria* (34% of the OPUs and 31.7% of the clones) (Figure A.1 and Table A.5). *Desulfobacteraceae*, the most represented family in the clone library, has been observed to thrive in other sandy (Musat *et al.*, 2006) or muddy sediments (Mussmann *et al.*, 2005) as well. Less frequently retrieved sequences

affiliated with *Syntrophobacteraceae*, *Desulfobulbaceae* and *Bacteriovorax* (3.85%, 3.85% and 7.7% of the OPUs, respectively).

2.3. In situ *quantification of the potential sulphate-reducing bacteria fraction*

Deltaproteobacteria made up a major fraction of those *Bacteria* that could be identified by fluorescence *in situ* hybridization, averaging 3.7 (± 0.2) x 10^8 cells cm^{-3} sediment, which was equivalent to 85% of the EUB338I-III detected cells (4.4 ± 0.2 x 10^8 cells cm^{-3} sediment).

The values were in the same range than previously reported in the microbiota associated to the rizosphere of *P. oceanica* (García-Martinez *et al.*, 2008) and even to those reported at the Wadden Sea (Llobet-Brossa *et al.*, 2002). However, the comparison is based on hybridizations using different set of probes and therefore the different specificity of the oligonucleotides must be taken into account. Despite of this fact, the high abundance of *Deltaproteobacteria,* in both bare and vegetated sediments at the Balearic Islands, evidenced the potential importance of this group in the oxidation of deposited OM through sulphate respiration in the Mediterranean Sea.

FISH detection efficiencies with the probe mixture EUB338I-III were low (29% of total cells), but comparable to those determined in other coastal sediments (26 to 39% in (Pernthaler *et al.*, 2002), 13-35% in (Bühring *et al.*, 2005). However, the large fraction of undetectable cells can not solely be explained by the low sensitivity of FISH, as the use of the more sensitive technique CARD-FISH yielded just 10% higher detection rates. Considering that the percentage of FISH-detectable *Archaea* was only 8.1% (± 1), approximately half of the DAPI counts were either impermeable to the probes, with a ribosomal content below the threshold of CARD-FISH, non hybridizable, or dead. Also, Pernthaler and colleagues (2002) determined relatively low CARD-FISH detection rates (mean 63%) in shallow subsurface layers of Wadden Sea sediments.

Natural bacterial assemblages display different metabolic levels and vital states. For a long time it has been assumed that all bacteria stained by fluorochromes were alive, but nowadays it is recognized that only a portion of aquatic bacteria is alive and actively growing, while a large fraction is dormant or dead (Luna *et al.*, 2002 and

references therein). During the last years some studies attempted to determine bacterial dead fractions in marine sediments reporting from 30 to 70% of dead cells of the total cell counts (Luna *et al.*, 2002; Manini and Danovaro, 2006). Those percentages might explain the low hybridization efficiencies obtained in this and other studies, and suggest the necessity of a combined use of DAPI-stain and FISH with other methods for the assessment of membrane integrity (e.g. propidium iodide or ethidium homodimer-2 stains).

2.4. Most probable number of culturable sulphate-, iron- and manganese-reducing bacteria in bare and vegetated sandy sediments

Viable counts of sulphate-reducing bacteria were determined by most probable number (MPN) serial dilution. Lactate, acetate, and H_2 were used as substrates (see Experimental Procedures). As it is well known that some sulphate reducers can couple carbon oxidation to the reduction of metals as Fe(III) or Mn(IV) (Coleman *et al.*, 1993), the abundance of culturable Fe- and Mn- reducers was also estimated by this approach (Table 5).

Table 5. MPNs of culturable sulphate-, Fe(III)- and Mn(IV)-reducing bacteria, in bare and vegetated sediment (associated to the rizosphere of *P. oceanica*) growing with different electron donors and acceptors.

	MPN 10^3 cells cm^{-3} sediment (95% confidence interval)								
e- donors	**Acetate**			**Lactate**			**H_2**		
e- acceptors	**SO_4^{2-}**	**Fe(III)**	**Mn(IV)**	**SO_4^{2-}**	**Fe(III)**	**Mn(IV)**	**SO_4^{2-}**	**Fe(III)**	**Mn(IV)**
Bare	10	0.2	0.03	2.3	0.4	0.2	10	0.2	0.02
Vegetated	8	0.2	0.01	6.2	0.8	0.2	16	0.2	0.03

In every case, the numbers accounted for less than 0.1% of the total cells determined by DAPI, in accordance with the fact that only a few members of natural communities grow *in vitro* using conventional cultivation techniques (Amann *et al.*, 1995).

SRB using acetate (complete oxidizers) and H_2 (autotrophs) largely dominate (1 x 10^4 cells cm^{-3} sediment in both) over lactate-oxidizers that accounted 2.3 x 10^3 cultivable

cells cm^{-3} sediment. The results supported former evidences of acetate and H_2 being the most important electron donors for sulphate respiration in marine sediments (Sørensen *et al.*, 1981). Llobet-Brossa and colleagues (2002) described a similar trend in muddy sediments of the German Wadden Sea despite of its higher OM content (11.6% OM) and also reported abundances of acetate- and H_2-utilizing SRB one order of magnitude higher than those of lactate-oxidizers.

The sediment associated to the rizosphere of *P. oceanica* hosted 3 times more lactate oxidizers (6.3×10^3 cultivable cells cm^{-3}) than the bare sediment. The values were also higher than those using acetate or H_2 as electron acceptors. Vegetated sediments, as deposits of released biomass from seagrasses and their epiphytic communities, are richer in nutrients than the bare sediments. Actually, the sediments associated to the rizosphere of *P. oceanica* contained 5 times more OM (10.3%) as it was described in a previous study in a close location at the Balearic Islands (García-Martinez *et al.*, 2008).

In agreement with previous observations in sediments at different locations, alternative electron acceptors as Fe(III) and Mn(IV) were of secondary importance in both types of sediment (Canfield *et al.*, 1993). Iron and manganese supported the growth of only a few hundreds of cells per cubic centimetre of sediment. The higher MPN were obtained with Fe(III) and lactate (400 cells cm^{-3} sediment) as electron acceptor and donor respectively.

3. References

Amann, R.I., Ludwig, W., and Schleifer, K.H. (1995) Phylogenetic identification and *in situ* detection of individual microbial cells without cultivation. *Microbiol. Rev.* **59**: 143-169.

Bishop, J.K.B., and Rossow, W.B. (1991) Spatial and temporal variability of global surface solar irradiance. *J. Geophys. Res.* **96**: 16839–16858.

Bühring, S.I., Elvert, M., and Witte, U. (2005) The microbial community structure of different permeable sandy sediments characterized by the investigation of bacterial fatty acids and fluorescence *in situ* hybridization. *Environ. Microbiol.* **7**: 281-293.

Calleja, M.L., Marbà, N., and Duarte, C.M. (2007) The relationship between seagrass (*Posidonia oceanica*) decline and sulfide porewater concentration in carbonated sediments. *Estuar. Coast. Mar. Sci.* **73**: 583-588.

Canfield, D.E., Jorgensen, B.B., Fossing, H., Glud, R., Gundersen, J., Ramsing, N.B., Thamdrup, B., Hansen, J.W., Nielsen, L.P., and Hall, P.O. (1993) Pathways of organic carbon oxidation in three continental margin sediments. *Mar. Geol.* **113**: 27-40.

Coleman, M.L., Hedrick, D.B., Lovley, D.R., White, D.C., and Pye, K. (1993) Reduction of Fe(III) in sediments by sulphate-reducing bacteria. *Nature* **361**: 436-438.

Danovaro, R. (1996a) Detritus-Bacteria-Meiofauna interactions in a seagrass bed (*Posidonia oceanica*) of the NW Mediterranean. *Mar Biol* **127**: 1-13.

Danovaro, R. (1996b) Detritus-Bacteria-Meiofauna interactions in a seagrass bed (*Posidonia oceanica*) of the NW Mediterranean. *Mar. Biol.* **127**: 1-13.

Danovaro, R., Fabiano, M., and Boyer, M. (1994) Seasonal changes of benthic bacteria in a seagrass bed (*Posidonia oceanica*) of the Ligurian Sea in relation to origin, composition and fate of the sediment organic matter. *Mar. Biol.* **119**: 489-500.

Duarte, C.M., and Vaqué, D. (1992) Scale dependence of bacterioplankton patchiness. *Mar. Ecol. Prog. Ser.* **84**: 95-100.

Duarte, C.M., and Chiscano, C.L. (1999) Seagrass biomass and production: a reassessment. *Aquat. Bot.* **65**: 159-174.

Duarte, C.M., Agustí, S., Kennedy, H., and Vaqué, D. (1999) The Mediterranean climate as a template for Mediterranean marine ecosystems: the example of the northeast Spanish littoral. *Prog. Oceanogr.* **44**: 245-270.

Epstein, S.S., and Rossel, J. (1995) Enumeration of sandy sediment bacteria: search for optimal protocol. *Mar. Ecol. Prog. Ser.* **117**: 289-298.

Furtado, A.L.S. (2001) Bacterial abundance, biomass and production in a Brazilian coastal lagoon and in two German lakes. *An. Acad. Bras. Ci.* **73**: 39-49.

García-Martinez, M., López-López, A., Calleja, M.L., Marbà, N., and Duarte, C.M. (2008) Bacterial community dynamics in a seagrass (*Posidonia oceanica*) meadow sediment. *Estuar. Coast.* **32**: 276-286.

Gasol, J.M., Doval, M.D., Pinhassi, J., Calderón-Paz, J.I., Guixa-Boixareu, N., Vaqué, D., and Pedrós-Alió, C. (1998) Diel variations in bacterial heterotrophic activity and growth in the northwestern Mediterranean Sea. *Mar. Ecol. Prog. Ser.* **164**: 107-124.

Gómez-Pujol, L., Orfila, A., Cañellas, B., Álvarez-Ellacuria, A., Méndez, F.J., Medina, R., and Tintoré, J. (2007) Morphodynamic classification of sandy beaches in low energetic marine environment. *Mar. Geol.* **242**: 235-246.

Holmer, M., Duarte, C.M., and Marbà, N. (2003) Sulfur cycling and seagrass (*Posidonia oceanica*) status in carbonate sediments. *Biogeochemistry* **66**: 223-239.

Huettel, M., and Rusch, A. (2000) Transport and degradation of phytoplankton in permeable sediment. *Limnol. Oceanogr.* **45**: 534–549.

Konstantinidis, K., and DeLong, E.F. (2008) Genomic patterns of recombination, clonal divergence and environment in marine microbial populations. *ISME J.* **2**: 1052-1065.

Kuwae, T., and Hosokawa, Y. (1999) Determination of abundance and biovolume of bacteria in sediments by dual staining with 4',6-diamidino-2-phenylindole and acridine orange: relationship to dispersion treatment and sediment characteristics. *Appl. Environ. Microbiol.* **65**: 3407-3412.

Laubier, L. (2005) Mediterranean Sea and humans. Inproving a conflictual partnership. *In* The Mediterranean Sea. Saliot, A. (ed.). *In* Handbook of Environmental Chemistry (Vol 5). Springer-Verlag Berlin Heidelberg. p.p. 3-27.

Luna, G.M., Manini, E., and Danovaro, R. (2002) Large fraction of dead and inactive bacteria in coastal marine sediments: comparison of protocols for determination and ecological significance. *Appl. Environ. Microbiol.* **68**: 3509-3513.

Llobet-Brossa, E., Rossello-Mora, R., and Amann, R. (1998) Microbial Community Composition of Wadden Sea Sediments as Revealed by Fluorescence *In Situ* Hybridization. *Appl. Environ. Microbiol.* **64**: 2691-2696.

Llobet-Brossa, E., Rabus, R., Böttcher, M.E., Könneke, M., Finke, N., Schramm, A., Meyer, R.L., Grötzschel, S., Rosselló-Móra, R., and Amann, R. (2002) Community structure and activity of sulfate-reducing bacteria in an intertidal surface sediment: a multi-method approach. *Aquat. Microb. Ecol.* **29**: 211-226.

Manini, E., and Danovaro, R. (2006) Synoptic determination of living/dead and active/dormant bacterial fractions in marine sediments. *FEMS Microbiol. Ecol.* **55**: 416-423.

Musat, N., Werner, U., Knittel, K., Kolb, S., Dodenhof, T., van Beusekom, J.E., de Beer, D., Dubilier, N., and Amann, R. (2006) Microbial community structure of sandy intertidal sediments in the North Sea, Sylt-Romo Basin, Wadden Sea. *Syst. Appl. Microbiol.* **29**: 333-348.

Mussmann, M., Ishii, K., Rabus, R., and Amann, R. (2005) Diversity and vertical distribution of cultured and uncultured Deltaproteobacteria in an intertidal mud flat of the Wadden Sea. *Environ. Microbiol.* **7**: 405-418.

Muyzer, G., and Stams, A.J. (2008) The ecology and biotechnology of sulphate-reducing bacteria. *Nat. Rev. Microbiol.* **6**: 441-454.

Naganuma, T. (1997) Abundance and Production of Bacterioplankton along a Transect of Ise Bay, Japan. *J. Oceanogr.* **53**: 579-583.

Paul, E.A., and Clark, F.E. (1989) Soil microbiology and biochemistry (Killham, K. ed.). Academic Press, San Diego, CA.

Pernthaler, A., Pernthaler, J., and Amann, R. (2002) Fluorescence *in situ* hybridization and catalyzed reporter deposition for the identification of marine bacteria. *Appl. Environ. Microbiol.* **68**: 3094-3101.

Polymenakou, P.N., Lampadariou, N., Mandalakis, M., and Tselepides, A. (2009) Phylogenetic diversity of sediment bacteria from the southern Cretan margin, Eastern Mediterranean Sea. *Syst. Appl. Microbiol.* **32**: 17-26.

Ravenschlag, K., Sahm, K., Pernthaler, J., and Amann, R. (1999) High bacterial diversity in permanently cold marine sediments. *Appl. Environ. Microbiol.* **65**: 3982-3989.

Richter, D.D., and Markewitz, D. (1995) How deep is soil? *Bioscience* **45**: 600-609.

Rusch, A., Forster, S., and Huettel, M. (2001) Diatoms and Detritus in an Intertidal Sandflat Subject to Advective Transport across

the Water-Sediment Interface. *Biogeochemistry* **55**: 1-27.

Rusch, A., Huettel, M., Reimers, C.E., Taghon, G.L., and Fuller, C.M. (2003) Activity and distribution of bacterial populations in Middle Atlantic Bight shelf sands. *FEMS Microbiol. Ecol.* **44**: 89-100.

Shiah, F.-K., and Ducklow, H.W. (1995) Multiscale variability in bacterioplankton abundance, production, and specific growth rate in a temperate salt-marsh tidal creek. *Limnol. Oceanogr.* **40**: 55-66.

Siokou-Frangou, I., Christaki, U., Mazzocchi, M.G., Montresor, M., Ribera d'Alcalá, M., Vaqué, D., and Zingone, A. (2010) Plankton in the open Mediterranean Sea: a review. *Biogeosciences* **7**: 1543–1586.

Sørensen, J., Christensen, D., and Jorgensen, B.B. (1981) Volatile fatty acids and hydrogen as substrates for sulfate-reducing bacteria in anaerobic marine sediment. *Appl. Environ. Microbiol.* **42**: 5-11.

Sorensen, K.B., Glazer, B., Hannides, A., and Gaidos, E. (2007) Spatial structure of the microbial community in sandy carbonate sediments. *Mar Ecol Prog Ser* **346**: 61-74.

Sørensen, K.B., Glazer, B., Hannides, A., and Gaidos, E. (2007) Spatial structure of the microbial community in sandy carbonate sediments. *Mar. Ecol. Prog. Ser.* **346**: 61-74.

Yarza, P., Richter, M., Peplies, J., Euzeby, J., Amann, R., Schleifer, K.H., Ludwig, W., Glockner, F.O., and Rossello-Mora, R. (2008) The All-Species Living Tree project: A 16S rRNA-based phylogenetic tree of all sequenced type strains. *Syst. Appl. Microbiol.* **31**: 241-250.

Chapter 2: Response of sulphate-reducing bacteria to an artificial oil spill in coastal Mediterranean marine sediment

1. Introduction

Small-scale laboratory experiments (e.g. microcosms and culture dependent approaches) provide invaluable insights in the field of microbial hydrocarbon degradation, as they facilitate the monitorization of biological processes and give statistic robustness. However, these approaches lack sufficient environmental realism (variables and scale) to permit confident predictions about real-world situations (Reilly, 1999). Thus, a combination of *in vitro* and *in situ* experimental approaches is essential for the evaluation of the fate and effects of xenobiotic chemicals as crude oil over environmental communities.

In situ mesocosm experiments might be considered as windows to the ecosystems, as they introduced ecological realism and allow accessing and taking into account a broader range of physicochemical, biological, and toxicological variables instead of parameters that can be controlled to some extent. Therefore, *in situ* mesocosm experiments were performed in order to study the response of sulphate-reducing bacteria inhabiting Mediterranean marine sediments to crude oil contamination, or a heavy contamination with naphthalene as a model of polycyclic aromatic hydrocarbon. This chapter describes the changes in the microbial community caused by the contamination as reported by a combination of *in situ* quantification, cultivation approaches and the measurement of metabolic activity rates.

2. Results and discussion

2.1. Rationale of the experiment

The experiment consisted of three mesocosms, each one enclosing about 150 L of sediment, installed on bare sandy sediment (see Experimental Procedures). Two mesocosms were artificially contaminated with naphthalene and crude oil respectively, while a third mesocosm of untreated sediment served as a control. Due to the fact that at this depth the seafloor may be exposed to significant sand transport,

most of the study was concentrated in the layer below 13 cm in order to ensure stability of the physical structure of the sediment, and to guarantee permanent anaerobic conditions during the experiment. The experiment was set up at the end of June 2006 when the bottom water temperature was 21ºC. The results presented here were obtained from triplicate samples after 23 and 92 days incubation.

2.2. Changes in the microbial abundance after hydrocarbon contamination

The changes in the total number of cells (DAPI-stained), *Bacteria* (hybridized with probe EUB338I-III) and *Deltaproteobacteria* (hybridized with probe DELTA495a-c) were monitored after 23 and 92 days of exposition to the hydrocarbons and compared to the natural trend observed in the untreated sediment (Figure 1 and Table 1).

At the beginning of the experiment (June 24th, 2006), the untreated sediment accounted 1.2 (± 0.05) x 10^9 cells cm^{-3} (mean ± SD, n = 3) while in late September, the total cell number doubled to 2.2 (± 0.4) x 10^9 coinciding with a rise of bottom water temperature from 21ºC to 24ºC. A correlation between microbial abundance and temperature has already been observed in other similar sediment systems (Danovaro *et al.*, 1994; Llobet-Brossa *et al.*, 2002; Burke *et al.*, 2003). Besides, this trend might be also stimulated by the spring bloom of primary producers, which leads to a deposition of diatoms during July and August, increasing the availability of organic matter in the sediment (Lasternas *et al.*, 2011).

Contrary, hydrocarbon contamination prevented the natural rise in cell abundance as the values in both hydrocarbon exposed mesocosms were significantly lower than in the untreated sediment at the end of the experiment. As can be observed in Figure 1, total cell numbers remained without significant changes through the experiment after crude oil contamination. This attenuation might be related to the high toxicity of most hydrocarbons, which is generally related to effects in the fluidity of the cell membrane. Hydrocarbons may accumulate in the lipid bilayer causing disruption and changes in the permeabilization, therefore compromising the viability of the cells (Heipieper and Martínez, 2010).

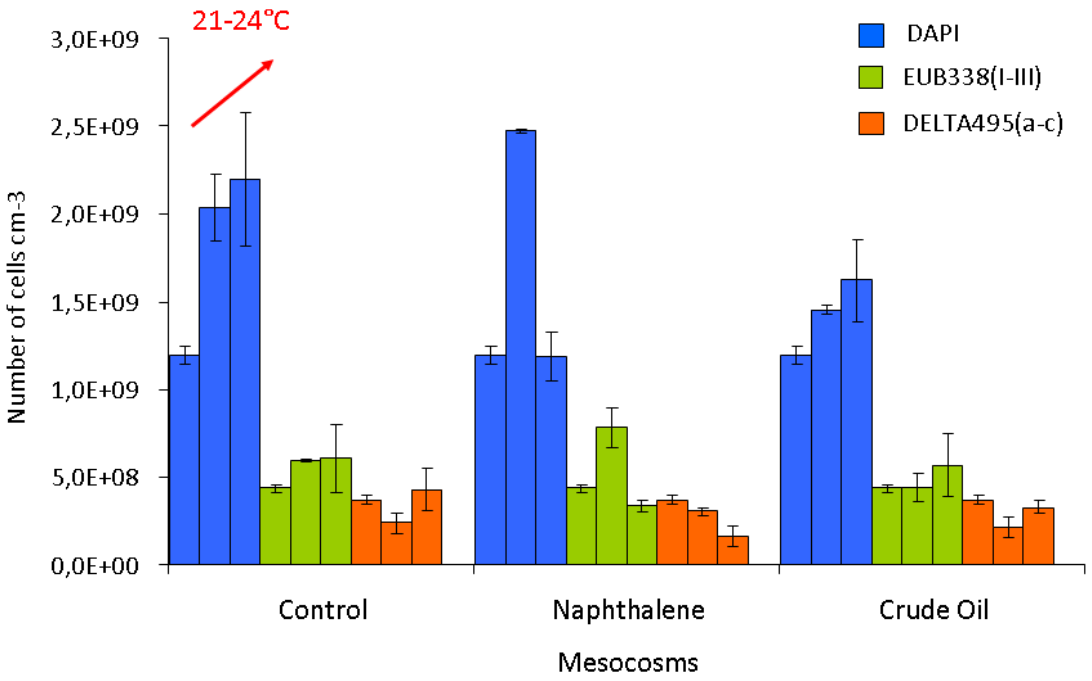

Figure 1. Total cell counts (DAPI) and relative abundance of *Bacteria* (EUB338I-III) and *Deltaproteobacteria* (DELTA495a-c) in the mesocosms during the three months of the experiment.

Despite of this negative effect of crude oil contamination, FISH approaches did not report significant changes in the abundances of detectable *Bacteria.* Even, deltaproteobacterial-related organisms made up a major fraction of those *Bacteria* that could be identified by FISH, as they maintained a sufficient ribosomal content to be detected. This fact must not be hastily associated to their ability for hydrocarbon degradation, but suggests an inherent adaptation of a fraction of the autochthonous communities to endure the presence of hydrocarbons in their environment.

On the other hand, the input of naphthalene in the sediment did not affect immediately the abundance of cells. As in the untreated mesocosm, total cell numbers doubled from June to July. However, it decreased to initial values in September. This delayed effect might be explained by the low solubility of naphthalene in water (0.24 mM at 25°C) and therefore its slow diffusion in the sediment. Naphthalene contamination reduced the bacterial and deltaproteobacterial abundances by 1.2 and 2.3 times, respectively, after 3 months of incubation.

Table 1. Total cell counts and relative abundance of *Bacteria* and *Deltaproteobacteria* in the mesocosms during the three months experiment.

Mesocosms	Total cell numbers 10^9 cells cm^{-3} ± SD, n = 3			Fluorescence *in situ* hybridization 10^8 cells cm^{-3} (% of total cells)											
				Bacteria probes EUB338I-III						*Deltaproteobacteria* probes DELTA495a-c					
	Jun*	Jul*	Sep*	Jun		Jul		Sep		Jun		Jul		Sep	
Untreated	**1.2** ± 0.05	**2.0** ± 0.2	**2.2** ± 0.4	**4.4** ± 0.2	(40)	**5.9** ± 0.1	(30)	**6.1** ± 2.0	(31)	**3.7** ± 0.2	(31)	**2.4** ± 0.6	(12)	**4.3** ± 1.2	(20)
Naphthalene		**2.5** ± 0.01	**1.2** ± 0.1			**7.8** ± 1.1	(32)	**3.4** ± 0.4	(29)			**3.1** ± 0.2	(12)	**1.6** ± 0.6	(17)
Oil		**1.5** ± 0.03	**1.6** ± 0.2			**4.4** ± 0.8	(30)	**5.7 ±** 1.9	(36)			**2.1** ± 0.6	(15)	**3.3** ± 0.4	(20)

* **Jun**=June, 0 days; **Jul**=July, 23 days; **Sep**=September, 92 days incubation.

2.3. In situ *sulphate reduction rates (SRR)*

The metabolic activity of SRB was determined by means of sulphate-reduction rate estimations after 92 days of hydrocarbon exposure.

The integrated SRR (as the sum of the averaged rates of all horizons) in the untreated sediment was 0.32 ± 0.26 mmol m^{-2} d^{-1}, whereas in the sediments exposed to naphthalene and crude oil it increased 3 and 2.6 times (0.97 ± 0.3 and 0.85 ± 0.5 mmol m^{-2} d^{-1}), respectively. As can be observed from the vertical profiles (Figure 2.A.), while the SRR slightly decreased in depth at the untreated sediment, the contaminated mesocosms exhibited evident peaks at 11 and 9 cm below the surface in naphthalene- and crude oil- amended sediments, respectively.

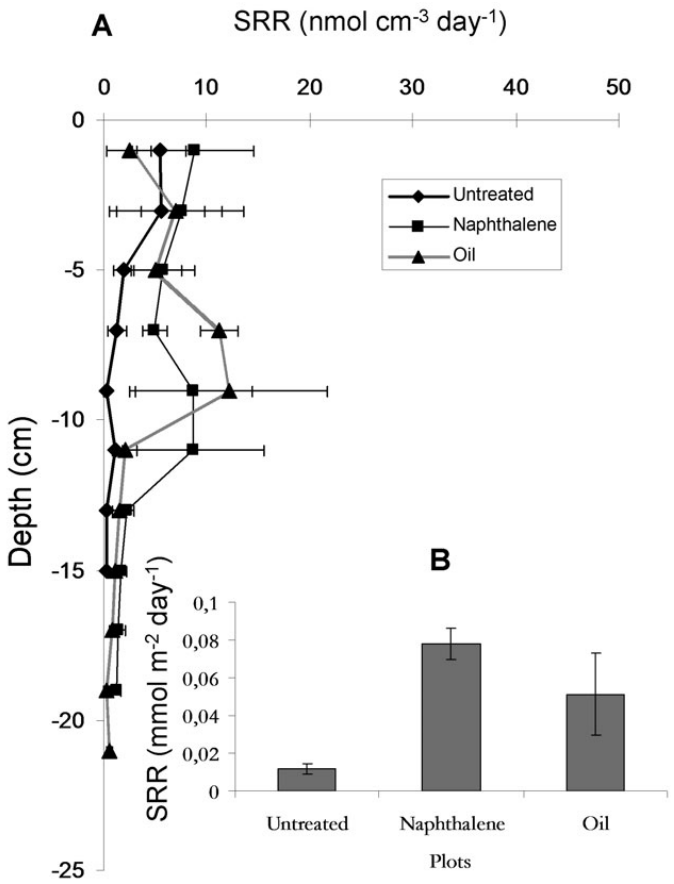

Figure 2. A. Vertical profile of sulfate reduction rates in the experimental plots after 92 days incubation with the hydrocarbons and in the untreated sediment. Values are means (± SD, n = 3). **B**. Integrated values of the rates in the studied layer of the sediment.

Unfortunately, the *a priori* selection of the horizon in the study (13 to 19 cm depth) was below the SRR peaks in both treatments. However, the selected layer also showed quantifiable differences (Figure 2.B.) since the addition of hydrocarbons enhanced the SRR about five fold in comparison with the undisturbed sediments. The integrated SRR in the untreated sediment at the studied layer (0.012 ± 0.004 mmol m^{-2} d^{-1}) was enhanced to 0.078 ± 0.014 and 0.051 ± 0.04 mmol m^{-2} d^{-1} in the naphthalene and crude oil mesocosms, respectively (Student's *t* test: /*t*/ = 5.06, *p* = 0.05, *df* = 4).

In combination with the results obtained by FISH, the increased SRR after hydrocarbon contamination pointed out to a metabolic stimulation of the autochthonous SRB.

2.4. Naphthalene quantification

Naphthalene concentration in the sediment served as an indicator of hydrocarbons diffusion from the inserts to the sediment. Naphthalene was chosen as a model PAH and due to its reduced solubility in water (0.24 mM at 25°C).

The untreated sediments contained a basal naphthalene concentration of 8.35 ± 0.53 µg kg^{-1} (mean and SD, n = 3) that did not vary significantly along the experiment (Figure 3). In the naphthalene-amended sediments, its concentration increased only slightly (2 times, 15.06 ± 1.5 µg kg^{-1}) during the first 23 days of incubation, but almost 4 times (33.25 ± 4.66 µg kg^{-1}) after 92 days. The slow diffusion from the pipettes to the sediment explains the delayed response of the microbial community observed by fluorescence hybridizations. On the other hand, the crude oil-amended plot showed a gradual increase in the naphthalene concentration to 2 times (17.82 ± 4.3 µg kg^{-1}) and 2.6 times (20.8 ± 6.9 µg kg^{-1}) after 23 days and 92 days of incubation, respectively.

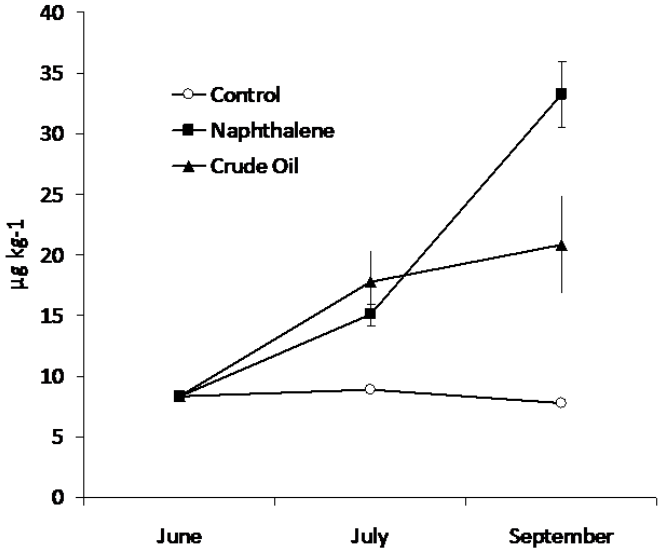

Figure 3. Estimated naphthalene concentration in the mesocosms along the experiment.

2.5. Changes in the SRB culturability due to hydrocarbon contamination

MPN series were used to quantify possible changes in the culturability of SRBs inhabiting the sediment after 92 days of exposure to the hydrocarbons. Different substrates were tested as putative electron donors (i.e. acetate, lactate, hydrogen, crude oil, naphthalene and anthracene) with sulphate as an electron acceptor. Positive growth was obtained in all the substrates tested (Table 2). As stated before, the most abundant SRBs in the untreated sediment were those using acetate or hydrogen as substrates (1 x 10^4 cells cm^{-3} sediment), but surprisingly those growing with crude oil (2 x 10^4 cells cm^{-3}) accounted for the largest cultivable fraction. Less abundant were the anthracene (9 x 10^3 cells cm^{-3}) and naphthalene (1.2 x 10^2 cells cm^{-3}) oxidizers. The exposure to contaminants significantly enhanced the number of cultivable organisms growing with all the electron donors. The increment was of 1 and 2 orders of magnitude in the naphthalene- and crude oil-amended sediments, respectively. The highest MPN (93 x 10^4 cells cm^{-3}) was obtained with acetate from the crude oil-amended mesocosm. Unfortunately, in both contaminated plots the abundance of crude oil oxidizers was underestimated, since we inoculated these metabolic types just up to the dilution 10^{-5}, and all tubes turned positive. However, in both cases more than 11 x 10^4 cells cm^{-3} sediment could be determined. The high proportion of SRBs growing with crude oil as an electron donor suggested that some components of the mixture

might serve as primary substrates for growth, either by full or partial mineralization, rendering an increased sulphide concentration in the tubes.

From the highest MPN positive dilutions of each culture condition, ten 16S rRNA gene partial sequences were analyzed (176 sequences in total). Most of them (82%) were related to known SRBs that could be classified in four main deltaproteobacterial families: *Desulfobulbaceae*, *Desulfuromonadaceae*, *Desulfovibrionaceae* and *Desulfobacteraceae* (Figure 4 and Figures A.1.).

We observed a high retrieval frequency of *Desulfobulbaceae*- (92 to 96.5% id) and *Desulfuromonadaceae*- (95.5 to 98% id) related sequences from the naphthalene-amended mesocosm, and *Desulfovibrionaceae*-related sequences (90 to 96% id) from crude oil-amended sediment, in the cultures supplemented with hydrocarbons. From the three families, only *Desulfovibrio* has been suggested as hydrocarbons (alkanes) oxidizer but its ability to degrade them has not yet been proven *in vitro* (Aeckersberg, 1991). Therefore, an additional effort is required to confirm their degrading capabilities and to prove their putative role in hydrocarbon contaminated sediments.

On the other hand, *Desulfobacteraceae,* despite of being a family with several previously described hydrocarbon degraders (Widdel *et al.*, 2010), dominated in only three cultures, although these were always supplemented with aromatic hydrocarbons as electron donors (naphthalene culture from naphthalene-amended sediment and both naphthalene and anthracene cultures from untreated sediment). Most of the retrieved sequences were closely related to aromatic and aliphatic hydrocarbon degraders as strain PL12 (97.5% id), *o*XyS1 (97% id), and the species *Desulfotignum toluenicum* and *Desulfobacula toluolica* (93% id).

Table 2. Most probable numbers of cultivable SRB from the mesocosms growing with different electron donors.

Mesocosms	Most Probable Numbers 10^4 cells cm^{-3} sediment (95% confidence interval)											
	Acetate		Lactate		H_2		Oil		Naphthalene		Anthracene	
Untreated	1	(0.18-4.2)	0.23	(0.047-0.92)	1	(0.18-4.2)	2	(0.4-7.1)	0.012	(0.003-0.042)	0.9	(0.21-2.6)
Naphthalene	11	(1.8-41)	4.60	(0.9-20)	24	(4.2-100)	>11	(4.2)	0.072	(0.013-0.180)	2.4	(0.42-10)
Oil	93	(18-420)	11	(1.8-41)	38	(8.7-110)	>11	(4.2)	0.150	(0.045-0.420)	11	(1.8-41)

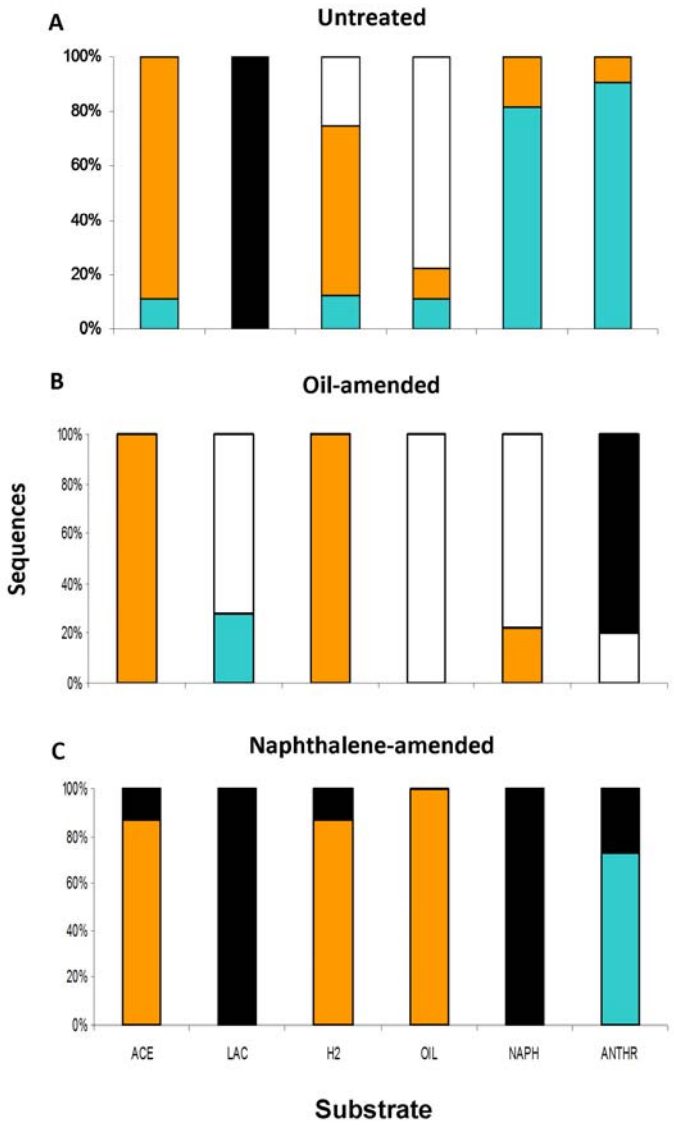

Figure 4. Relative percentages of SRB 16S rDNA sequences retrieved from cultures supplemented with different electron donors: ACE, acetate; LAC, lactate; H2, hydrogen; OIL, crude oil; NAPH, naphthalene or ANTHR, anthracene. A. Untreated mesocosm; B. oil-amended mesocosm, C. naphthalene-amended mesocosm. *Desulfobulbaceae* (orange), *Desulfuromonadaceae* (black), *Desulfovibrionaceae* (white) and *Desulfobacteraceae* (blue).

2.6. Evidence of crude oil and PAH degradation by the SRB cultures

Complex modifications in the polar metabolite composition of the cultures growing with crude oil and PAHs under sulfidogenic conditions were determined by high resolution mass spectrometry (ICR-FT-MS). The spectra obtained rendered more than ten thousand signals for each sample that were converted into CHO (C: carbon; H:

hydrogen; O: oxygen), CHOS (S: sulphur), CHNO (N: nitrogen) and CHNOS elementary compositions. O/C and H/C atomic ratios from each signal were calculated and plotted in van Kravelen diagrams (Figures 5 and 6) for the visualization of metabolite profiles and their comparison under different incubation conditions.

The original Prestige crude oil contained a high diversity of heterocyclic compounds with low O/C and H/C atomic ratios. The most abundant structures were sulphurated, nitrogenated and hydroxylated aromatic compounds (NOSs) (Figure 5.A.). However, when the crude oil was abiotically incubated in AWS medium, the diversity of oxygen-containing aromatic and aliphatic compounds increased significantly (Figure 5.B.), possibly due to hydrolysis. Besides, most nitrogen-containing compounds present in the original crude oil loss aromaticity while incorporating oxygen. Therefore, abiotic reactions might contribute to the increase in the diversity and abundance of available substrates for bacterial metabolism.

Bacterial crude oil utilization was evidenced by the appearance of new molecules, not present in the controls, exclusively formed during the biotic incubation in crude oil (Figure 5.C.). The hundreds of new nitrogen-, oxygen- and sulphur-containing compounds detected, both aromatic and aliphatic, might be produced by partial modification of the original substrates. Remarkably, a conspicuous increment of fatty acid-like structures was also observed (dense region of blue points in Figure 5.D.). The production of fatty acids during the anaerobic degradation of alkanes has been previously described in several SRB isolated strains (So and Young, 1999; So *et al.*, 2003).

Evidences of PAHs metabolization (e.g. naphthalene and anthracene) were also revealed by the appearance of a new set of molecules after biotic incubation (Figure 6.B). As happened with the crude oil, the abiotic incubation of PAHs produced an increased in the diversity of polar compounds in the medium. However, this increment was more obvious when the PAHs where incubated in the presence of SRB. Bacterial growth produced the appearance of hydroxylated, carboxylated and hydrogenated polyaromatic substances (lower part of the diagram H/C<1). Unfortunately, any of the metabolic intermediates proposed for the anaerobic degradation of naphthalene

(Meckenstock *et al.*, 2004) could be detected by this infusion approach in the MPN cultures.

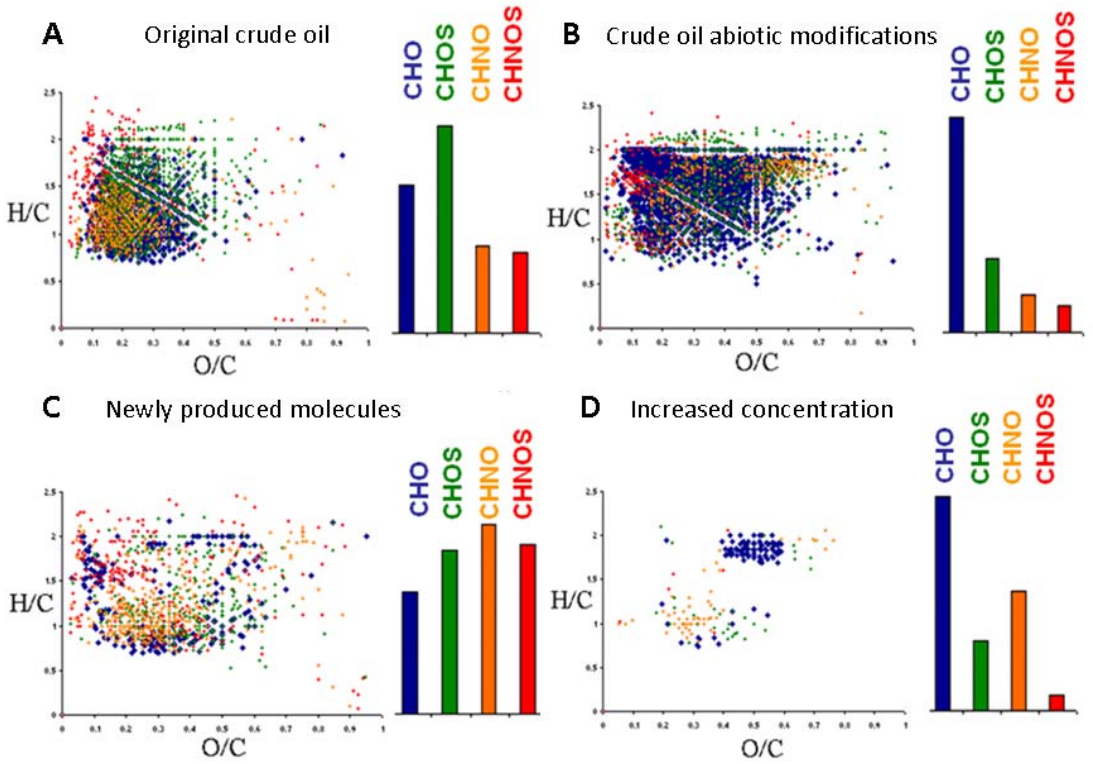

Figure 5. van Krevelen representation of the mass spectral data of the polar fraction of the crude oil extracted from MPN samples. On the right of the diagrams the relative abundances of the CHO, CHOS, CHON and CHNOS are shown. **A.** Original crude oil **B.** Abiotic incubation **C**. New molecules obtained after biotic incubation. **D.** Molecules with increased signal after biotic incubation.

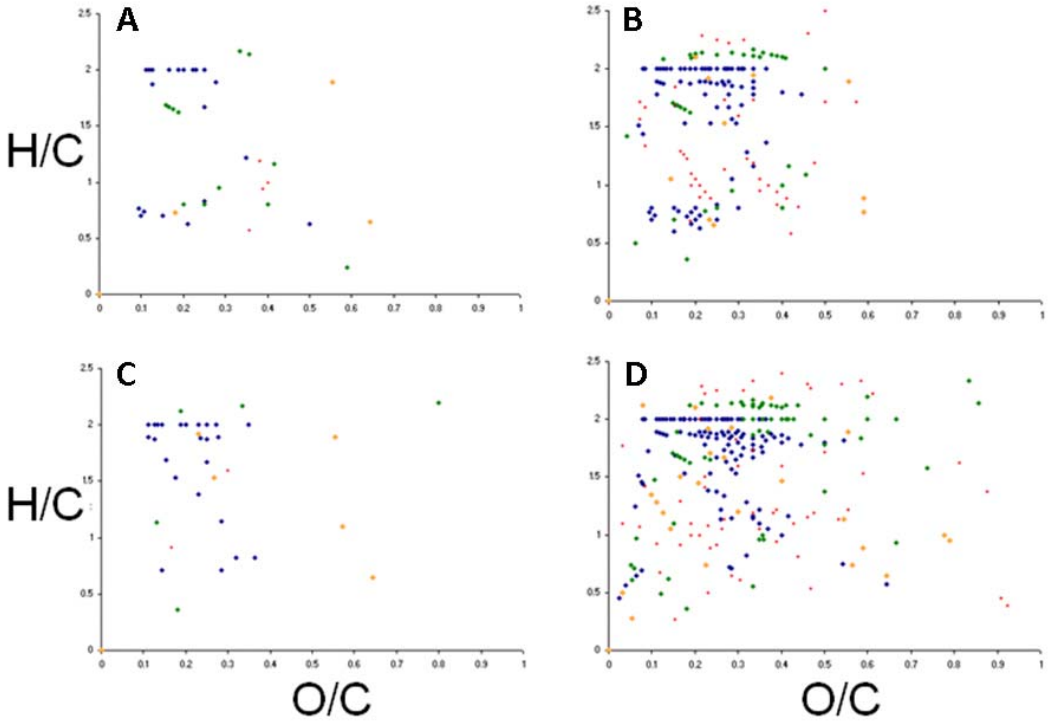

Figure 6. van Krevelen representation of the mass spectral data of the polar fraction extracted from MPN cultures growing with PAHs. **A.** Naphthalene abiotic incubation; **B.** Naphthalene biotic incubation; **C.** Anthracene abiotic incubation; **D**. Anthracene biotic incubation. The color of the points indicates the elemental compositions: CHO (blue), CHOS (green), CHNO (orange), CHNOS (red).

3. References

Aeckersberg, F. (1991) Anaerobic oxidation of saturated hydrocarbons to CO_2 by new type of sulfate-reducing bacterium. *Arch. Microbiol.* **156**: 5-14.

Burke, D.J., Hamerlynck, E.P., and Hahn, D. (2003) Interactions between the salt marsh grass *Spartina patens*, arbuscular mycorrizal fungi and sediment bacteria during the growing season. *Soil Biol. Biochem.* **35**: 501-511.

Danovaro, R., Fabiano, M., and Boyer, M. (1994) Seasonal changes of benthic bacteria in a seagrass bed (*Posidonia oceanica*) of the Ligurian Sea in relation to origin, composition and fate of the sediment organic matter. *Mar. Biol.* **119**: 489-500.

Heipieper, H.J., and Martínez, P.M. (2010) Toxicity of hydrocarbons to microorganisms. In Handbook of hydrocarbon and lipid microbiology. Timmis, K. N. (ed). Berlin Heidelberg, DE: Springer-Verlag, pp. 1566-1573.

Lasternas, S., Tunin-Ley, A., Ibañez, F., Andersen, V., Pizay, M.-D., and Lemée, R. (2011) Short-term dynamics of microplankton abundance and diversity in NW Mediterranean Sea during late summer conditions (DYNAPROC 2 cruise; 2004). *Biogeosciences* **8**: 743-761.

Llobet-Brossa, E., Rabus, R., Böttcher, M.E., Könneke, M., Finke, N., Schramm, A. et al. (2002) Community structure and activity of sulfate-reducing bacteria in an intertidal surface sediment: a multi-method approach. *Aquat. Microb. Ecol.* **29**: 211-226.

Meckenstock, R.U., Safinowski, M., and Griebler, C. (2004) Anaerobic degradation of polycyclic aromatic hydrocarbons. *FEMS Microbiol. Ecol.* **49**: 27-36.

Reilly, T.J. (1999) The use of mesocosms in marine oil spill-ecological research and development. *Pure Appl. Chem.* **71**: 153-160.

So, C.M., and Young, L.Y. (1999) Initial reactions in anaerobic alkane degradation by a sulfate reducer, strain AK-01. *Appl Environ Microbiol* **65**: 5532-5540.

So, C.M., Phelps, C.D., and Young, L.Y. (2003) Anaerobic transformation of alkanes to fatty acids by a sulfate-reducing bacterium, strain Hxd3. *Appl Environ Microbiol* **69**: 3892-3900.

Widdel, F., Knittel, K., and Galushko, A. (2010) Anaerobic hydrocarbon-degrading microorganisms: an overview. *In* Handbook of hydrocarbon and lipid microbiology. Timmis, K. N. (ed). Berlin Heidelberg, DE: Springer-Verlag, pp. 1998-2021.

Chapter 3: First insights into the phylogeny and physiology of Mediterranean SRB hydrocarbon degraders

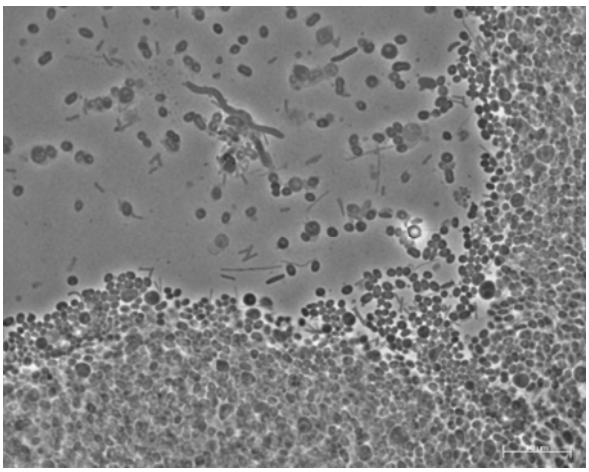

1. Introduction

Culturing remains an essential requirement to understand the role and physiology of microbes in the marine environment (Joint *et al.*, 2010). Culture-dependent techniques have shown to be selective, as the enrichment strategies often select opportunistic fast growing organisms under the specific conditions. However, the genomic, proteomic and metabolomic information retrieved from these organisms make up the basis for the development of metabolic models, functional annotation, and the determination of key enzymatic pathways, genes and metabolites, which may serve as biomarkers for the *in situ* monitorization of microbial activities as well as for the retrieval of not-yet-cultured organisms.

During the last two decades, significant information regarding the microbial phylogeny and biochemical pathways involved in the anaerobic oxidation of hydrocarbons has been obtained (reviewed in Boll and Heider, 2010; Widdel *et al.*, 2010; Fuchs *et al.*, 2011). Phylogenetically diverse microbes, belonging to *Archaea*, *Firmicutes*, *Alpha-*, *Beta-*, *Gamma-* and *Deltaproteobacteria*, have been brought into cultures (92 pure cultures and 24 enrichments) demonstrating that hydrocarbons may be used as carbon and energy sources by diverse physiological groups using a variety of electron acceptors (e.g. nitrate, iron, sulphate) (Widdel *et al.*, 2010).

Despite of a relatively small culture collection, unprecedented biochemical reactions involved in the activation of hydrocarbons have been observed (e.g. fumarate addition, hydroxylation and carboxylation). In the presence of oxygen, hydrocarbons are activated through a unique biochemical reaction involving enzyme-bound reactive oxygen species (e.g. mono- or dioxygenases) that enable the hydroxylation of hydrocarbons in exergonic reactions that overcome the high dissociation energies of their C-H bonds (Boll and Heider, 2010). However, as anaerobic bacteria cannot generate reactive oxygen species, alternative mechanisms involving enzyme radical species, and coupling of exergonic to endergonic partial reactions, become necessary. The activation strategy varies depending on the C–H bond dissociation energies of the substrate and the electron acceptor free energy yield (ΔG^{o}). Compounds with high C–H

bond dissociation energies (> 355 KJ mol^{-1}) are predominantly activated via fumarate addition (e.g. benzylsuccinate synthase activates toluene in the denitrifying *Thauera aromatica,* (Leuthner and Heider, 2000), while lower dissociation energies are overcame by hydroxylation with water (e.g. ethylbenzene dehydrogenase activates ethylbenzene in the denitrifying *Azoarcus* sp.; Kniemeyer and Heider, 2001).

The biodegradation of non-substituted aromatics with higher dissociating energies, such as benzene and naphthalene, is also possible under anaerobic conditions (Musat and Widdel, 2008; Musat *et al.*, 2009). Two different activating reactions, carboxylation and methylation, had been proposed based on ^{13}C-labeled substrate incorporation and the detection of metabolic intermediates (Zhang *et al.*, 2000; Annweiler *et al.*, 2002; Safinowski and Meckenstock, 2006). However, the enzyme involved in the critical activating step remains unknown (Boll and Heider, 2010).

Polar compounds (i.e. NOSs: nitrogen-, oxygen- and sulphur-containing molecules) present in the crude oil might also serve as electron donors and acceptors during crude oil degradation (Bak and Widdel, 1986; Lizama *et al.*, 1995; Annweiler *et al.*, 2002). More insights have been elucidated for the anaerobic degradation of nitrogen heterocyclic compounds than for those containing sulphur. The activation of nitrogen heterocyclic compounds, such as indole or quinoline and their methylated isomers, proceed via hydroxylation as the initial transformation step under nitrate- and sulphate-reducing conditions (Madsen and Bollag, 1989; Shranker and Bollag, 1990; Johansen *et al.*, 1997).

Despite of our increasing knowledge, little is known about the relevance of the proposed metabolic pathways in the degradation of crude oil by interacting microbial populations. By analogy to the degradation of organic matter (see General Introduction, Section 2.5), a closed interplay of populations with diverse metabolic capabilities might be fundamental for the mineralization of crude oil constituents in the marine environment. Individual bacterial species have a restricted complement of enzymes and an essential substrate for one bacterial species may be a metabolic by-product of another species. Besides, cell-to-cell communication (e.g. quorum sensing) can moderate the activity of a mixed population of bacteria and promote concerted actions that benefits to certain populations or even to the whole community (Joint *et*

al., 2010). In the marine environment, these interactions could make the difference between death and survival.

Therefore, the enrichment and characterization of complex degrading consortia in crude oil is essential for the detection and physiological characterization of cooperative degradation (e.g. mutualisms and syntrophy). Moreover, the possibility of isolating "not-yet-cultured" organisms might be enhanced by the cultivation of complex consortia on multi substrate media.

The high SRB viability detected by MPN in the Mediterranean sediments after crude oil contamination (see Chapter 2, Section 3.2.5.), encouraged us to perform an enrichment of a SRB crude-oil degrading consortium. The enrichment was attempted in artificial seawater medium (AWS) containing crude oil and sulphate as the only electron donor and acceptor, respectively. In order to gain knowledge about the phylogenetic and metabolic characteristics of the consortium, a combination of fluorescence microscopy (i.e. DAPI-staining and *in situ* hybridization with specific probes), metabolic rates measurements (i.e. SRR), chemical analysis (i.e. GC-MS and ICR-FT-MS) and phylogenetic and metagenomic approaches were undertaken.

2. Results and discussion

2.1. Establishment of hydrocarbon-degrading enrichment cultures

A sediment-free crude oil degrading SRB consortium (MSO) was enriched from Mediterranean naphthalene-amended sediment by incubation and subsequent transfers into crude oil-containing artificial seawater medium. As shown in Figure 1, sulphide production and total cell numbers were enhanced by the presence of crude oil in the medium. After 80 days of incubation, the sulphide concentration was 5 times higher than in the crude oil-free culture (C-) (13 and 2.5 mM, respectively) while the cell abundances doubled. Crude oil degradation by the MSO consortium was primarily driven by sulphate reduction. A minor contribution of alternative metabolic processes, based in electron donors and acceptors other than crude oil and sulphate (e.g.

autotrophy and fermentation), was evidenced by the significantly lower bacterial growth in the crude oil-free (C-) and sulphate-free (Cfs) controls.

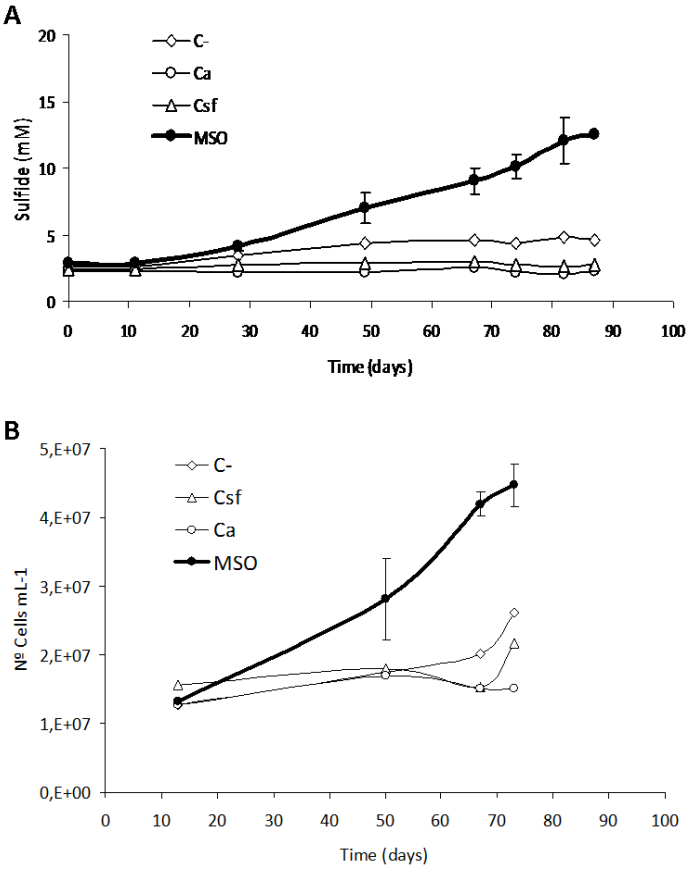

Figure 1. **A**. Anaerobic formation of sulphide during the incubation of sediment-free enrichment culture with crude oil as the only carbon source; **B**. Increase in the total number of cells (DAPI-stained) along the incubation time with crude oil. The incubation was carried out by triplicate (**MSO**) and three different controls were established in order to detect growth due to the use of other carbon sources (**C-:** crude-oil free culture; **Ca**: abiotic), or the use of electron acceptors other than sulphate (**Csf**: sulphate-free culture).

2.2. Evidences of bacterial growth based on crude oil degradation

The activity of the Mediterranean SRB consortium (MSO) over the different crude oil fractions was confirmed by a combination of GS-MS and ICR-FT-MS analysis of the residual crude oil recovered after 80 days of incubation. GC-MS analyses reported a substantial degree of weathering of the hydrocarbons due to abiotic reactions (Figure 2). However, the MSO consortium caused a further removal of both aliphatic and aromatic fractions. The biodegraded hydrocarbon fractions included C11-C28 linear

chain alkanes, branched alkanes (i.e. pristane and phytane) (Figure 2.A.) and two and three rings alkylated polycyclic aromatic hydrocarbons such as methylnaphthalene and methylphenanthrene (Figure 2.B.).

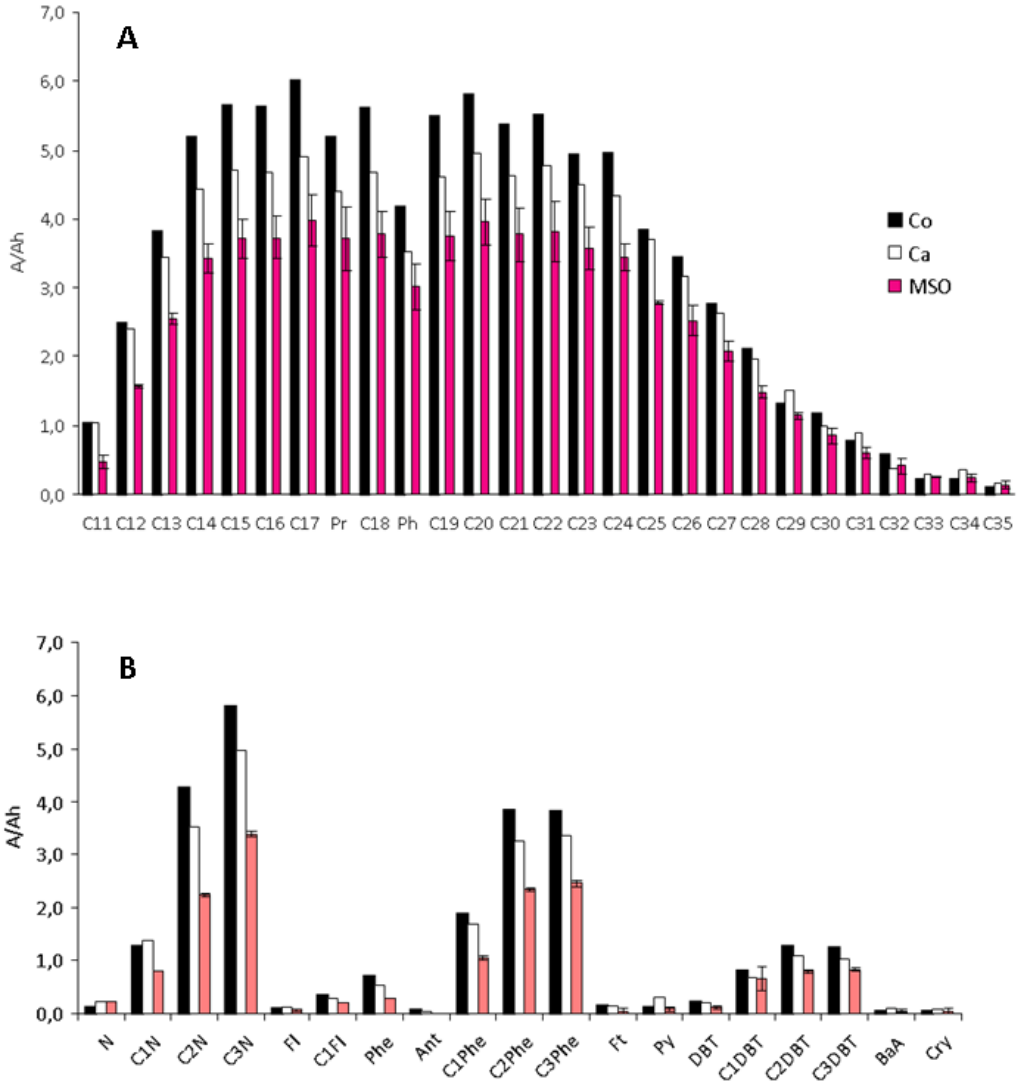

Figure 2. Relative distribution of aliphatic (**A**) and aromatic (**B**) hydrocarbons with respect to hopane (A/Ah) in the original oil (Co), abiotic control (Ca) and cultures of the MSO consortium after 80 days of incubation. The hopane is used as a conservative internal biomarker. C11 to C35 indicate the length of the *n*-alkanes; Pr: pristine, Ph: phytane, N: naphthalene; Fl: fluorene; Phe: phenanthrene; Ft: fluoranthene; Py: pyrene; DBT: dibenzothiophene; BaA: benzo(a)anthracene; Cry: chrysene; C1-, C2- and C3- indicate the number of methyl groups

The biological weathering of hydrocarbons was accompanied by the appearance of a new set of NOSs compounds, an increase in the diversity and abundance of

hydroxylated molecules, and the detection of key metabolic intermediates in the degradation of alkanes and methylated aromatic hydrocarbons.

The ICR-FT-MS indicated that the water-soluble metabolites varied from long aliphatic (C11-C26) to highly condensed molecules (H/C<1) and appeared exclusively under crude oil biotic incubation (Figure 3). In the van Krevelen diagram, the oxygen-containing molecules accumulated in the areas previously defined for polyphenolic compounds (e.g. lignin and tannin, (Reemstma, 2009) (Figure 3.D.). The increase in the abundance of phenolic metabolites during the anerobic bacterial growth suggested the occurrence of oxygen-independent hydroxylation processes. The hydroxylation of the methyl-group of methylphenols such us *p*-cresol (4-methylphenol) by water has been demonstrated in denitrifying and Fe(III)-reducing bacteria (Boll and Heider, 2010).

An increase in the signal of aliphatic compounds pointed out to the production of fatty acids during bacterial growth. These fatty acids might have a structural function (e.g. lipidic membrane), be used as surfactants (Muthusamy *et al.*, 2008), or correspond to metabolic intermediates. The anaerobic oxidation of alkanes to fatty acids had been reported under sulphate-reducing conditions (So and Young, 1999). The activation of alkanes via fumarate addition results in the formation of alkylsuccinate metabolites which are further processed via carbon-skeleton rearrangement, decarboxylation and β-oxidation (fatty acid metabolism involving acyl-CoA coenzymes) to CO_2 (Grundmann *et al.*, 2008; Callaghan *et al.*, 2011; Mbadinga *et al.*, 2011).

On the other hand, the increment in 3 and 4 fold of benzyl- and naphthylmethylene succinates respectively (key metabolic intermediates in the anaerobic degradation of toluene and methylnaphthalene) (Figure 4), pointed out to the activation of aromatic hydrocarbons via fumarate addition (Fuchs *et al.*, 2011). As the capability for the degradation of both, aliphatic and aromatic hydrocarbons in a single organism is not usually observed (Widdel *et al.*, 2010), these results might be related to a simultaneous enrichment of aliphatic and aromatic SRB degraders. However, the absence of more key aromatic intermediates (e.g. benzoyl-Coa and naphtoic acid) in the analyzed extracts, and the possibility of non-specific aromatic activation in the presence of alkanes as preferred substrates (Rabus *et al.*), suggested the occurrence of co-metabolic reactions.

Remarkably, the newly produced polar fraction was enriched in sulphur-containing compounds (Figure 3.C.). Sulphurated aliphatic molecules, characterized by H/C atomic ratios between 1.5 and 2, and O/C atomic ratios between 0.2 and 0.5, were related to proteins which might have structural or enzymatic functions (Reemstma, 2009). The high accumulation of sulphurated aromatic molecules (H/C<1) might correspond to metabolites generated during the partial modification of heterocycles such as thiophene and benzotiophene. Previous studies had shown that the anaerobic degradation of benzotiophene is possible under sulfidogenic conditions, and by co-metabolism in the presence of naphthalene (Annweiler *et al.*, 2001).

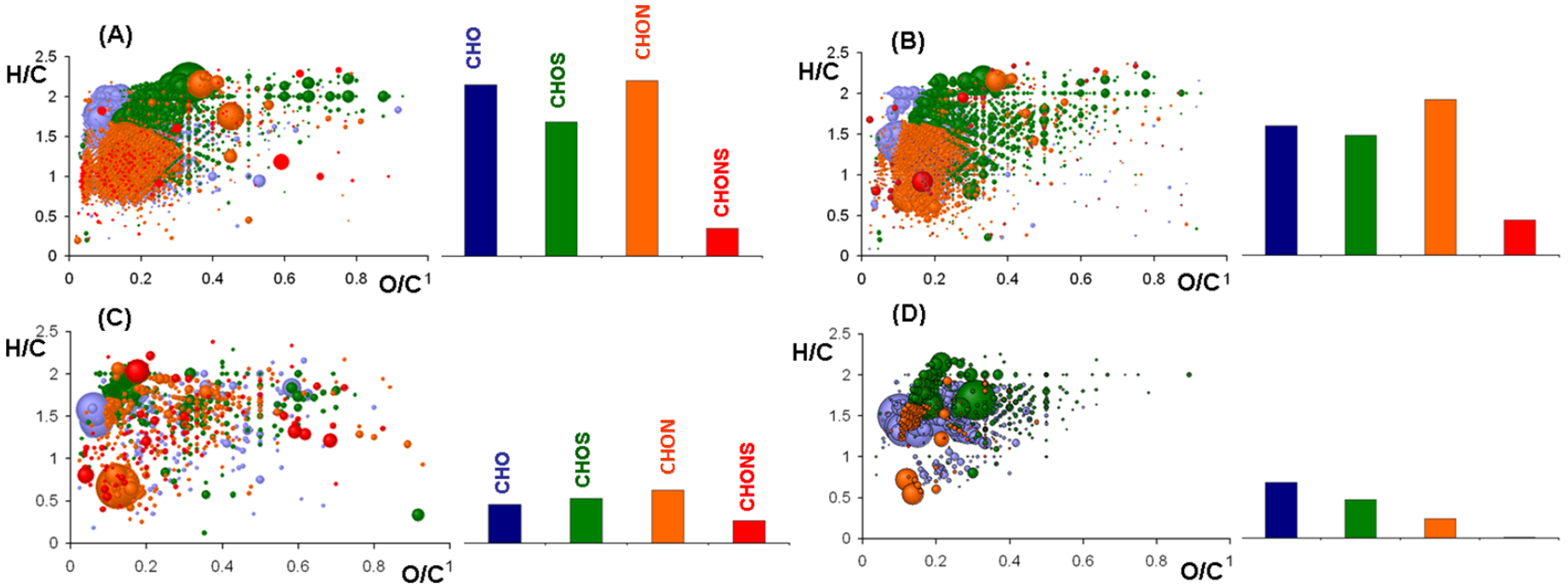

Figure 3. van Krevelen representation of the mass spectral data of the polar fraction of the crude oil extracted from the MOS consortium cultures. On the right of the diagrams the relative abundances of the CHO, CHOS, CHON and CHNOS are shown. **A.** Original crude oil, **B.** Abiotic incubation, **C**. New molecules obtained after biotic incubation, **D.** molecules with increased signal after biotic incubation.

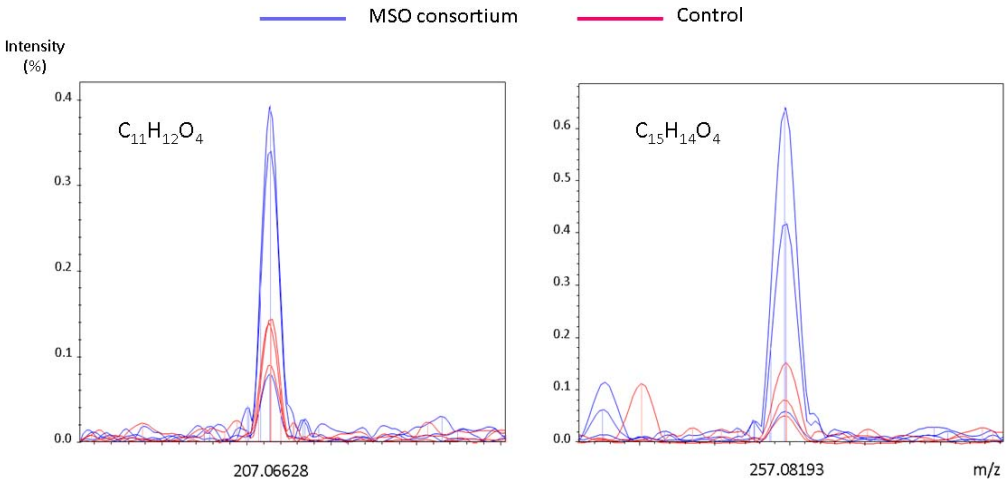

Figure 4. Mass spectra of benzylsuccinate ($C_{11}H_{12}O_4$) and naphthyl-2-methylene-succinate ($C_{15}H_{14}O_4$) showing their increased signal intensity in the MOS consortium culture (blue trace) in comparison with the controls (red trace).

2.3. Phylogenetic affiliation of the MSO consortium' members

The phylogenetic affiliation of the members of the MSO consortium was investigated by 16S rDNA amplification and FISH with specific bacterial and archaeal probes.

The resulting sediment-free SRB crude oil enrichment culture was dominated by rod- and filament-shaped cells (0.5 x 1.5 and 0.1 x 10 µm, respectively) (Figure 5). Sixty five percent of the cells were *Bacteria* while not archaeal signal was obtained by amplification neither by *in situ* hybridization.

Rod-shaped *Deltaproteobacteria* (hybridized with DELTA495a-c) made up the major fraction of EUB338I-III-detectable cells (90%) and a 65% of the DAPI-stained cells (Figure 6.A.). These cells contained refracting granules or inclusion bodies resembling those of polyhydroxyalkanoates (PHAs), commonly involved in bacterial carbon and energy reserve material. PHAs accumulated during times of oversupply with carbon sources (Jendrossek, 2009). Similar granules had being observed in other anaerobic hydrocarbon-degrading bacterium such as the denitrifying alkylbenzene-degrading strain EbN1 (Trautwein *et al.*, 2008).

A remarkable observation was that 14% of the DAPI-stained cells (40% of the non-EUB338-detectable), corresponding with the filamentous shape, did not hybridize with universal probes despite their abundance increased during growth on crude oil (Figure 6.B.).

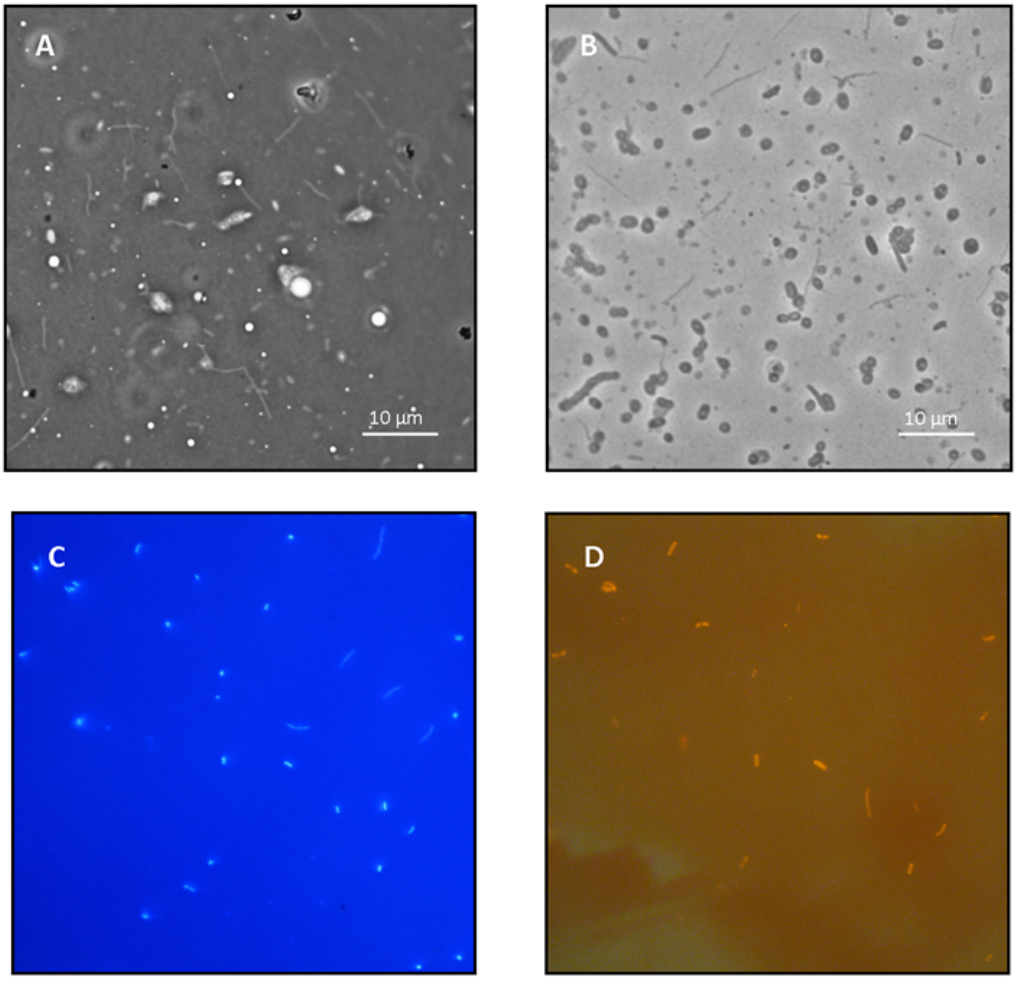

Figure 5. Microscopic display of cells in the MSO consortium growing with crude oil. **A**. Phase contrast micrograph of a crude oil drop; **B**. Phase contrast micrograph of the medium; C. Cells stained with DAPI; **D**. Cells hybridized with a *Deltaproteobacteria*-specific oligonucleotide probe (DELTA495a-c).

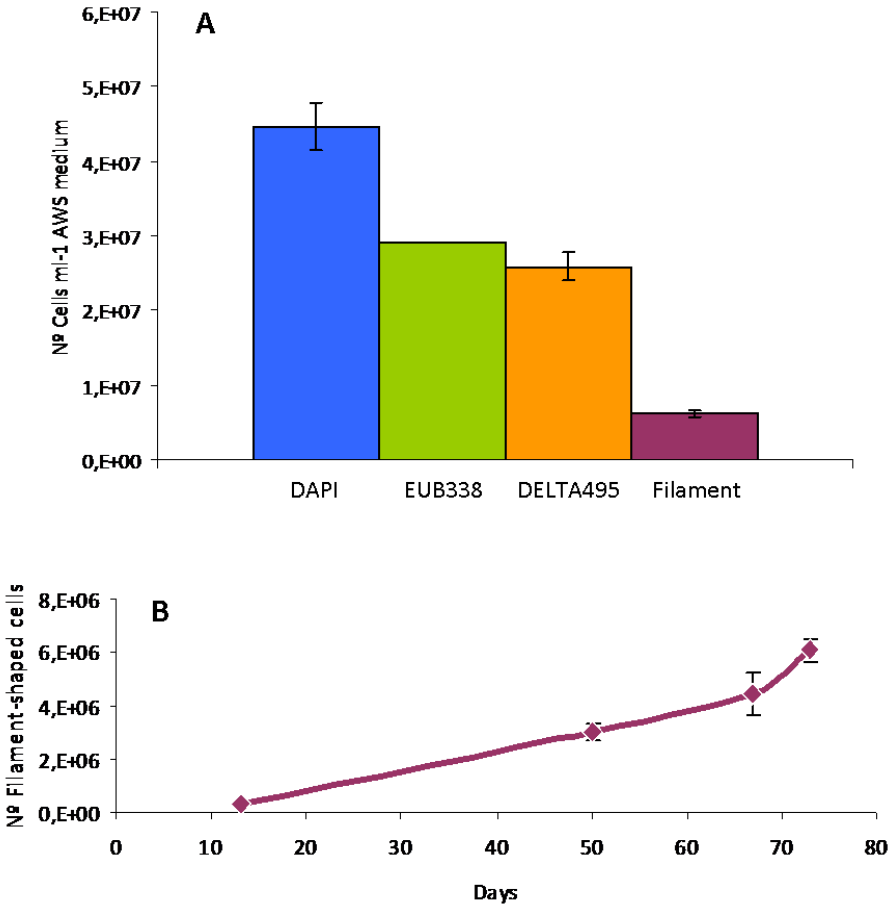

Figure 6. **A.** Total number of cells (DAPI), abundance of *Bacteria* (EUB338I-III) and *Deltaproteobacteria* (DELTA454a-c) determined by FISH. The "Filament" category represents the number of filament-shaped cells stained by DAPI. **B.** Increase in the number of filaments along the incubation in crude oil.

The analysis of 50 clones from the bacterial 16S rRNA gene clone library yielded a relatively high diversity of phylotypes. Fifty three percent of the sequences were closely related to sulphate-reducing *Desulfobacteraceae* (*Deltaproteobacteria*) previously described as hydrocarbon degraders, while the rest (47%) belonged to clades without hydrocarbon-degrading relatives (Figure 7).

The most frequently retrieved phylotype (45% of the total number of sequences) was 99% identical to strain PL12 (*Desulfabacteraceae*). This strain was first isolated from Kuwait marine sediment and it is able to completely oxidize *n*-hexane and *n*-decane to CO_2 (Higashioka *et al.*, 2009). Two other deltaproteobacterial phylotypes present in the clone library were affiliated to not-yet-cultured *Desulfobacteraceae*. Their sequence identity to other 16S rDNAs deposited at public databases was bellow the

genera threshold estimated from the LTP (94.9%, All Species Living Tree Project, Yarza *et al.*, 2008), what pointed out to their novelty within this family. Remarkably, their closest cultured relatives were hydrocarbon degrading SRBs such us strain NaphS2 (93% id, 6% of the total number of sequences), the only SRB naphthalene-oxidizer isolate (Galushko *et al.*, 1999), and *Desulfatibacillum alkenivorans* strain AK-01 (91% id, 2%), which is able to degrade C4 to C16 alkanes (Callaghan *et al.*, 2011).

On the other hand, the major fraction of non-deltaproteobacterial sequences affiliated with the candidate division OP3 (33%). Less represented sequences were related to *Epsilonproteobacteria*, *Firmicutes* and candidate division WS3 (8, 4 and 2% of the total number of sequences respectively).

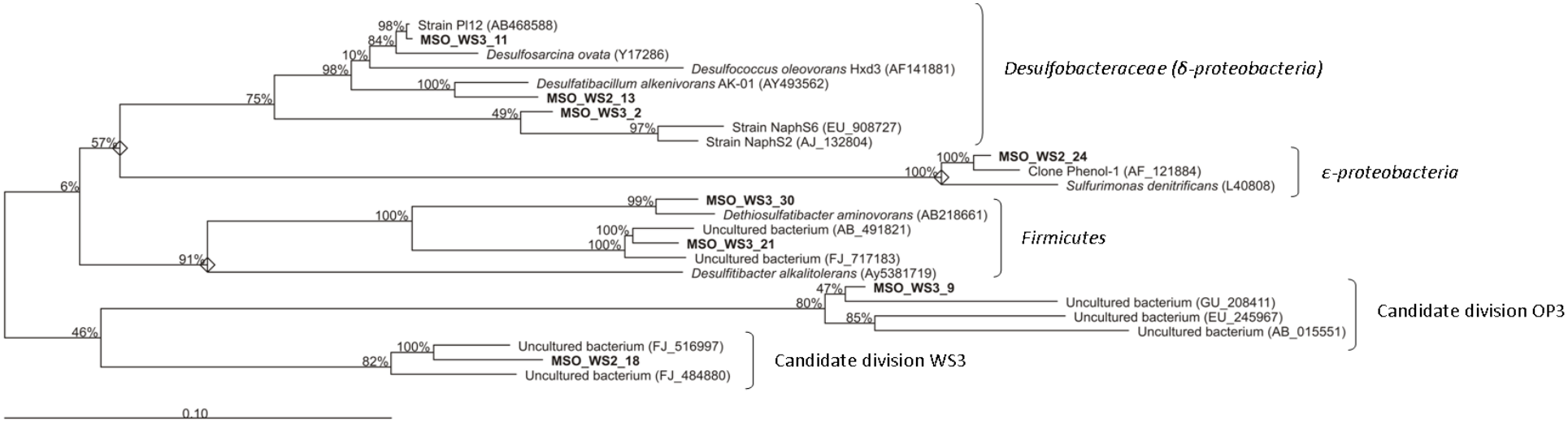

Figure 7. Phylogenetic affiliation of 16S rDNA sequences from the members of the MSO consortium (marked in bold). Phylogeny was inferred by maximum likelihood methods.

2.4. Metagenomic analyses of the MSO consortium

The genomic pool of the Mediterranean crude oil degrading consortium was analysed by means of a metagenomic approach applying 454-pyrosequencing technology. General features of the metagenome are listed in Table 1. The direct sequencing of isolated total community DNA resulted in 50. 000 reads with an average read length of 345 bp. Assembly of single reads resulted in the formation of 5. 088 contigs representing 14.3 Mbp of total DNA sequence. Considering an average genome size of 3.5 Mbp, the metagenomic library might represent raw sequences of approximately 4 prokaryotic genomes (Martin-Cuadrado *et al.*, 2007). Open reading frame (ORF) prediction lead to 11 Mbp of encoded information (77% coverage) comprising 17. 400 ORFs. Sixty four percent of these ORFs appeared in contigs with length ranging between 10. 000 and 126. 800 bp.

Table 1. General features of the MSO consortium metagenome.

Major features	Value
Number of reads	500. 000
Averaged length of sequence reads (bp)	345
Total length after assembly (Mbp)	14.3
Total coding (Mbp)	11
Nº Contigs	5. 088
Nº ORFs	17. 440
Coverage (%)	77

2.4.1. Phylogenetic affiliation of rRNA gene fragments retrieved by direct pyrosequencing

As pyrosequencing is not subjected to the same biases as gene amplification by PCR, the analyses of rDNA fragments retrieved by direct sequencing of total community DNA might complement the diversity studies based on 16S rDNA clone libraries. Unassembled reads from the MSO metagenome were processed in order to select sequences with rDNA identity (see Experimental Procedures, Section 5.6). A total of 121 (100-500bp) and 174 (300-600bp) rRNA gene fragments identified as 16S and 23S rDNA respectively, were classified into phylogenetic groups.

The phylogenetic diversity revealed by the rRNA sequences retrieved by direct pyrosequencing was coincident with the results obtained by the analyses of the 16S rRNA gene clone library, although the relative percentage of each phylotype varied. Ribosomal DNA fragments belonging to *Deltaproteobacteria* represented 55% and 59% of the total 16S and 23S rDNA sequences, respectively. As observed in the 16S rRNA clone library, other taxa were also present, although individually these groups did not represent more than 4 ± 3% of the total number of fragments (i.e. 7% *Chloroflexi*, 7% *Bacteroidetes*, 6% *Chlorobi*, 5% *Acidobacteria*, 5% *Firmicutes,* 2% candidate division OP3, 1% and candidate division WS3 and 1% *Epsilonproteobacteria*).

Most of the deltaproteobacterial sequences (93 and 97% of the 16S rDNA and 23S rDNA fragments, respectively) affiliated within the *Desulfobacteraceae* family (Figure 8). Sequences related to alkane-degrading SRBs (i.e. strains PL12 and AK-01) were the most represented in the metagenome (40 and 64% from the total number of 16S rDNA and 23S rDNA, respectively), while the relative abundance of sequences with similarity to naphthalene-degrading SRBs (i.e. strain NaphS2) accounted for around 30% of the sequences, a value ten fold higher than in the clone library.

Currently, 23S rDNA public databases accumulate a lower number of prokaryotic sequences than 16S rDNA archives (Yilmaz *et al.*, 2011). Thus, the phylogenetic affiliation based in these two biomarkers showed some discrepancies. For example, as 23S rDNA sequences belonging to strain PL12 were not present in the database, fragments from this organism might be assigned to strain AK-01 as the closest relative.

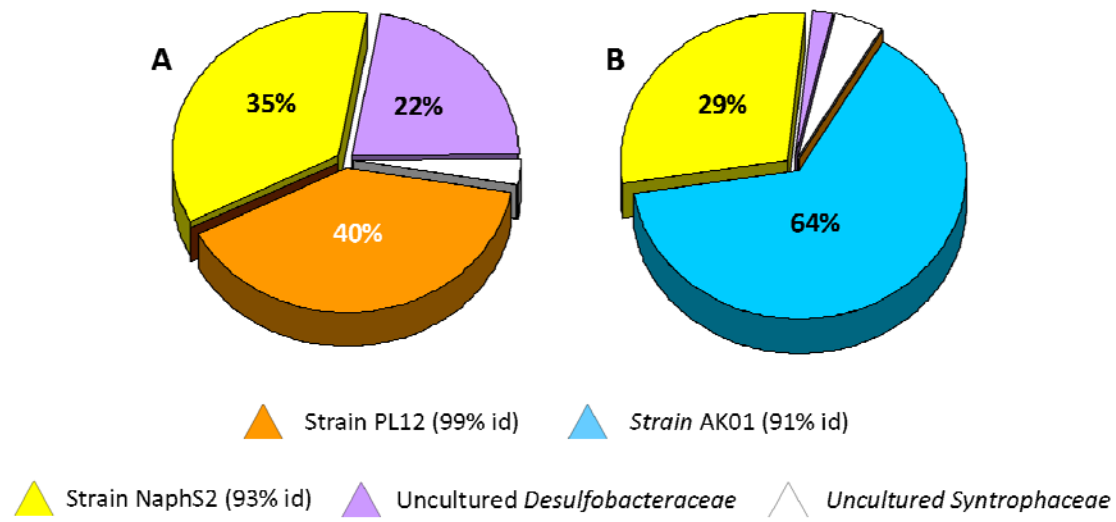

Figure 8. Deltaproteobacterial phylogenetic diversity retrieved by metagenomic approaches. **A.** 16S rDNA and **B**. 23S rDNA.

2.4.2. Phylogenetic affiliation of the predicted ORFs

To highlight the phylogenetic consistency, all ORFs were compared by BLAST analysis against genomesDB database. The phylogenetic affiliation at the domain level confirmed the dominance of bacterial genes and the absence of *Archaea.* At expectation values (e value) below $1e^{-05}$, 64% of the ORFs could be phylogenetically affiliated, but the rest could not be assigned to any domain due to the absence of orthology with sequences deposited in the databases. Notably, most of the unidentified ORFs assembled within the largest contigs, together with genes assigned to specific taxa suggesting the enrichment of not-yet-sequenced bacteria.

Thirty eight percent of the ORFs could be confidently classified (e values below $1e^{-40}$) (Figure 9). Most of these ORFs (70%) were related to *Deltaproteobacteria*, while the remaining 30% had best hits with other proteobacterial classes (e.i. 3.3% *Alpha-*, 3.3% *Beta-* and 8% *Gammaproteobacteria*) and phyla such as *Bacteroidetes* (6%), *Firmicutes* (5%) and *Chloroflexi* (< 5%). However, most of the ORFs related to taxa other than *Deltaproteobacteria* assembled within contigs with a high content of SRB-related genes.

Regarding the deltaproteobacterial ORFs, the phylogenetic affiliation was consistent with the information revealed by the rDNA analyses. Eighteen percent of the genes had best hits with sequences belonging to alkane-degrading SRBs such as strain AK-01

(10%) and *Desulfococcus oleovorans* (8.8%), and 17% were related to the naphthalene-degrading strain NaphS2. The rest of delaproteobacterial ORFs had best hits with non-hydrocarbon degrading SRB, such as *Desulfobacterium autotrophicum* (12%), *Desulfovibrio* sp. (3.7%) and *Syntrophobacter fumaroxidans* (3.5%).

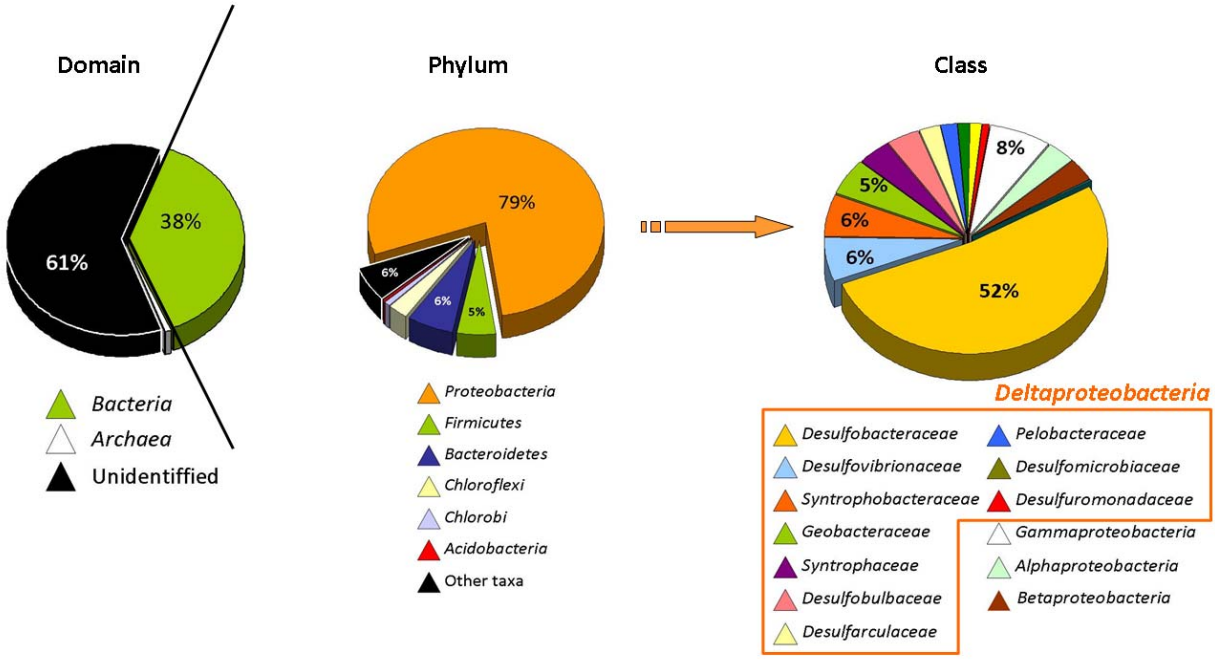

Figure 9. Phylogenetic affiliation of the predicted ORFs at expectation values below $1e^{-40}$.

2.4.3. Identification of phylogenetically relevant housekeeping genes

Universally conserved genes are typically present in single copies (SCGs) within genomes. This genes are subject to very low rates of indels (insertion/delection) and can be readily partitioned into synonymous and non-synonymous sites, which undergo very different rates and patterns of evolution. Such features allow the accurate alignment of homologues from divergent organisms and the differentiation of very closely related lineages (Santos and Ochman, 2004). Thus, conserved protein-coding regions can be used as a complement to the ribosomal DNA analyses in order to address the phylogenetic relationships of prokaryotes.

Up to 87 predicted ORFs had best hits with sequences from 43 different SCGs (Table A.6). Coinciding with former diversity analyses carried out in this study, most of the SCGs detected in the MSO metagenome belonged to hydrocarbon-degrading SRBs of the *Desulfobacteriaceae* family (83%). However, by this approach the percentage of SCGs sequences phylogenetically related to naphthalene degraders was higher than for alkane degraders (Figure 10). Sixty five percent of the SCGs had best hits with strain NaphS2 and *Desulfobacterium* sp. N47 (Selesi *et al.*, 2010), both naphthalene degraders, while only 18% were related to alkane degraders such as strain AK-01 and *Desulfococcus oleovorans.* The rest of SCGs were related to other *Deltaproteobacteria* (e.g. *Desulfobacterium autotrophicum* (Strittmatter *et al.*, 2009)) and phyla such as *Bacteroidetes* and *Firmicutes* (9.2%).

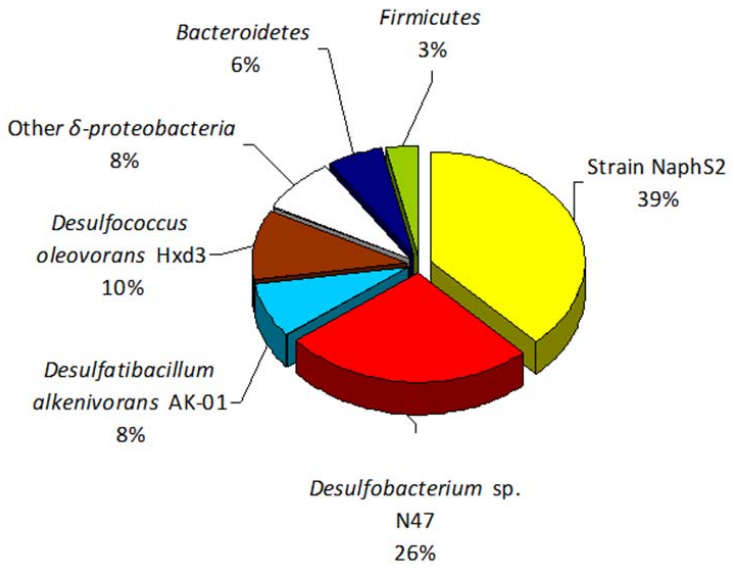

Figure 10. Phylogenetic affiliation of SCGs identified in the MSO metagenome.

2.4.4. Genetic pool and function prediction

Batch cluster analysis were performed using a set of gene calling programs based on similarity methods that collected functional information from several databases (e.g. KEGG, COG, SwissProt, Pfam). The function from 45% of the ORFs could be determined to some extent and classified into COG categories (expectation value below $1e^{-05}$) (Figure 11). Almost half of the COGs were related to metabolism, mainly of amino acids

and lipids, transport across the membranes, and energy production. The most represented functional group was that of transporters (6.3% of the predicted functions according to KEGG classification) and within it, ABC transporters were the most abundant (70.5% of the transporters).

COGs related to mechanisms of signal transduction, such as two-component regulatory system, represented 9.2% of the COGs. This system typically consists of membrane-bound histidine kinases and response regulators that facilitates the detection of specific environmental stimulus and mediate the cellular response through the differential expression of target genes (Skerker *et al.*, 2005).

On the other hand, 14.3% of the COGs were involved in genetic information processing, mainly replication, transcription and ribosome synthesis.

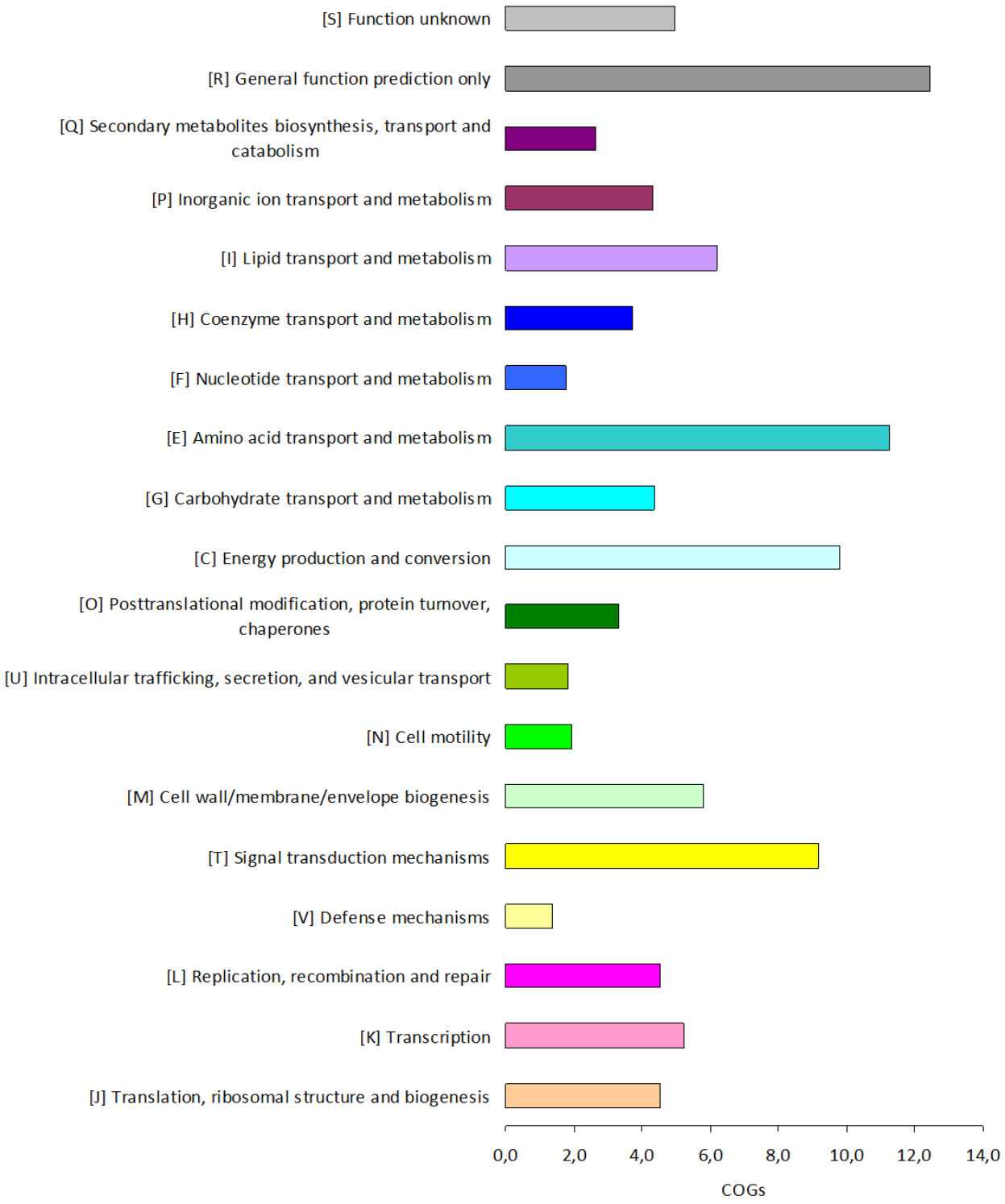

Figure 11. Distribution of COGs at expectation values below $1e^{-05}$.

2.4.4.1. Metabolic potential of the MSO consortium

In order to generate a meaningful manual annotation of the most relevant metabolic enzyme-coding genes, ORFs confidently associated to KEGG metabolic pathways (63% at expectation value below $1e^{-40}$) were sorted into protein families according to Pfam, the largest collection of protein families based on manual curated multiple sequence alignments (Finn *et al.*, 2008).

Fatty acids β-oxidation was by far the most represented metabolic pathway (Table 2 and Figure 12). Acyl-CoA dehydrogenase (FadE), which catalyzes the first step in the oxidation of fatty acids (conversion of acyl-CoA to enoyl-CoA, (Fujita *et al.*, 2007), accounted for 15.6% of the predicted metabolic functions, while enzymes involved in the subsequent reactions (i.e. FadB: enoyl-CoA hydratase/3-hydroxyacyl-CoA dehydrogenase and FadA: 3-ketoacyl-CoA thiolase), represented 4.4 and 1.5% of the predicted metabolic functions, respectively. Other enzyme-coding genes related to fatty acid biosynthesis and their transport across the membrane were also fairly abundant (e.g. FadD: acetyl-CoA synthetase and FabH: beta-ketoacyl-ACP synthase, 5.8 and 2%, respectively).

Besides, the detection of several alcohol and aldehyde dehydrogenases pointed out the capability of the MSO consortium for the degradation of alcohols and other organic compounds. This observation was consistent with the previous detection of these genes on the genome of the alkane-degrading strain AK-0 and its capability to grow on alkanols (So and Young, 1999; Callaghan *et al.*, 2011).

Although heterotrophy appeared to be the main metabolic strategy of the MSO consortium, genes related to chemolithoautotrophy were also present. Key enzymes from the Wood–Ljungdahl pathway, such us the bifunctional CO dehydrogenase/acetyl-CoA synthetase (CODH/ACS) and methylenetetrahydrofolate reductase accounted for 0.7 and 0.8% of the predicted metabolic functions. The Wood–Ljungdahl pathway, which has been also reported in strain AK-01 (Callaghan *et al.*, 2011), is involved in the synthesis of cellular carbon from CO_2 while gaining energy by coupling hydrogen oxidation to sulfate reduction (Ragsdale, 2008).

Table 2. Most abundant metabolic enzyme-coding genes according to KEGG classification ($1e^{-40}$).

Metabolism	Enzymes	Pfam	% KEGG-functions $1e^{-40}$
Fatty acids	Acyl-CoA dehydrogenases (FadE)	PF00441, PF02770, PF02771, PF08028	15,6
	Acetyl-CoA synthetase (ligase) (FadD)	PF00501, PF02629	5,8
	Enoyl-CoA hydratase/ Hydroxyacyl-CoA dehydrogenase (FadB)	PF00378, PF00725, PF02737	4,4
	Acetyl-CoA acetyltransferases (FadA)	PF02803, PF00108, PF01553	1,5
	Beta-ketoacyl-ACP synthase (FabH)	PF00109, PF02801, PF08541, PF08545	2
	FAD binding domain	PF01565	0,8
	Propionyl-CoA carboxyl transferase	PF01039	1
	Pyruvate synthase	PF01855	0,7
	Hydroxyglutaryl-CoA dehydratase	PF06050	0,6
	2Fe-2S iron-sulfur cluster binding domain	PF00111	0,5
	CoA-transferase	PF02515	0,9
	Fumarate lyase	PF00206	0,5
	Acetokinase	PF00871	0,4
	Methylmalonyl-CoA mutase	PF01642	0,9
Amino acids	Aminotransferase	PF00155, PF00202, PF00266, PF01063, PF01041	3,7
	Amino acid-binding ACT	PF01842	1,1
	Amino acid kinase	PF00696	0,9
	Carbamoyl-phosphate synthase	PF02786, PF00289	1,4
	Aspartate/ornithine carbamoyltransferase	PF02729	0,4
	3-deoxy-7-phosphoheptulonate synthase	PF00793	0,5
	Lon protease (S16)	PF05362	0,4
	Glutamine amidotransferase	PF00117, PF00310	1,6
	Glutamate ligase	PF02875, PF08245	1,4
	Asparagine synthase	PF00733	0,5
Carbohydrates	Glycosyl transferases	PF00534, PF00535, PF00912	1,7
	Transketolase	PF02779	0,5
	Pyruvate carboxylase	PF00682	0,5
	Phosphoglucomutase	PF02878	0,4
	Pyruvate formate lyase	PF02901	0,5
	Glycosyl hydrolases	PF00128	0,5
	Aconitase	PF00694	0,4
Nucleotides	Phosphoribosyl transferase	PF00156	0,7
	Adenylate and Guanylate cyclase	PF00211	0,7
	Nucleotidyl transferase	PF00483	0,6
	Methyltransferase	PF08241, PF01966	0,9
	Nucleotidyl transferase	PF00483	0,6
	tRNA synthetase	PF08264, PF00133	1
Alcohols	Alcohol dehydrogenase	PF00106, PF08240	2,9
	Iron-containing alcohol dehydrogenase	PF00465	0,5
	Zinc-binding alcohol dehydrogenase	PF00107	0,6
	Molydopterin dinucleotide binding protein	PF01568	0,5
	Molybdopterin oxidoreductas	PF00384	0,5
Aldehydes	Aldehyde ferredoxin oxidoreductase	PF02730, PF01314	2,2
	Aldehyde dehydrogenases	PF00171	0,8

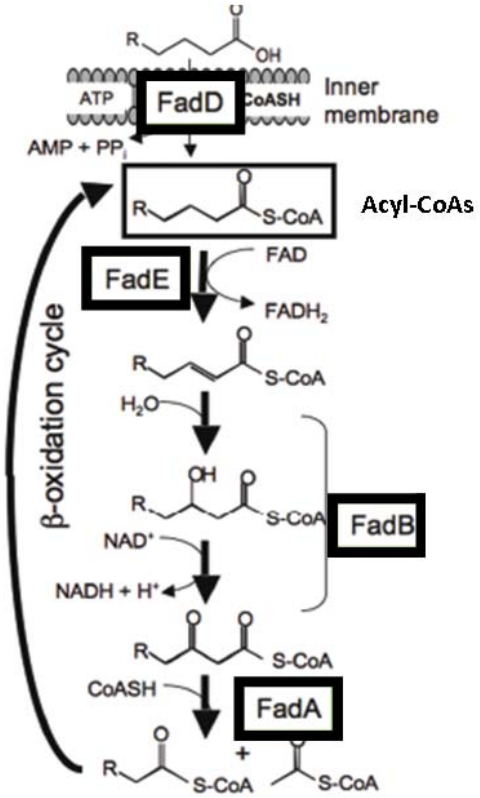

Figure 12. Overview of the reactions involved in the fatty acid β-oxidation. **FadA**: 3-ketoacyl-CoA thiolase (acetyl-CoA C-acyltransferase); **FadB:** enoyl-CoA hydratase/3-hydroxyacyl-CoA dehydrogenase; **FadE:** acyl-CoA dehydrogenase and **FadD:** acetyl-CoA synthetase (modified from Fujita *et al.*, 2007).

2.4.5. Genomic potential for the degradation of crude oil constituents

The MSO metagenome harbours a 7% of enzymatic functions that could be associated to pathways of degradation of hydrocarbons and xenobiotic polar organic compounds (Figure 13). Although the majority of these ORFs could also be associated to other central pathways (e.g. degradation of amino acids, lipids and carbohydrates), 12 ORFs were selected as they accumulate significant sequence identity to subunits of key enzymes involved in the anaerobic degradation of hydrocarbons (Table 3). These ORFs formed three independent clusters of genes that appeared in three of the longer contigs of the MSO metagenome:

i) **Contig OIL03** (90. 777 bp) contained a cluster of six ORFs with identity to several subunits of alkylsuccinate synthase (Ass), the glycyl radical enzyme involved in the anaerobic activation of alkanes via fumarate addition

(Mbadinga *et al.*, 2011). More details about this cluster are provided in Section 2.4.5.

ii) **Contig OIL09** (70. 096 bp): three ORFs were related to benzoyl-CoA reductase (Bcr), key enzyme involved in the ring reduction of benzoyl-CoA, central intermediate in the degradation of most aromatic hydrocarbons (Fuchs *et al.*, 2011).

iii) **Contig OIL42** (41. 683 bp): three ORFs were related to 4-hydroxybenzoyl-CoA reductase (4-HBCR), key enzyme in the anaerobic metabolism of hydroxylated aromatics (e.g. phenol, *p*-cresol, benzyl alcohol and 4-hydroxybenzoate) (Boll *et al.*, 2001). Due to mechanistic reasons, the aromatic ring of para-substituted aromatics cannot be reduced by Bcr. 4-HBCR removes the hydroxyl group from these para-substituted aromatics prior to ring dearomatization by Bcr (Boll *et al.*, 2001).

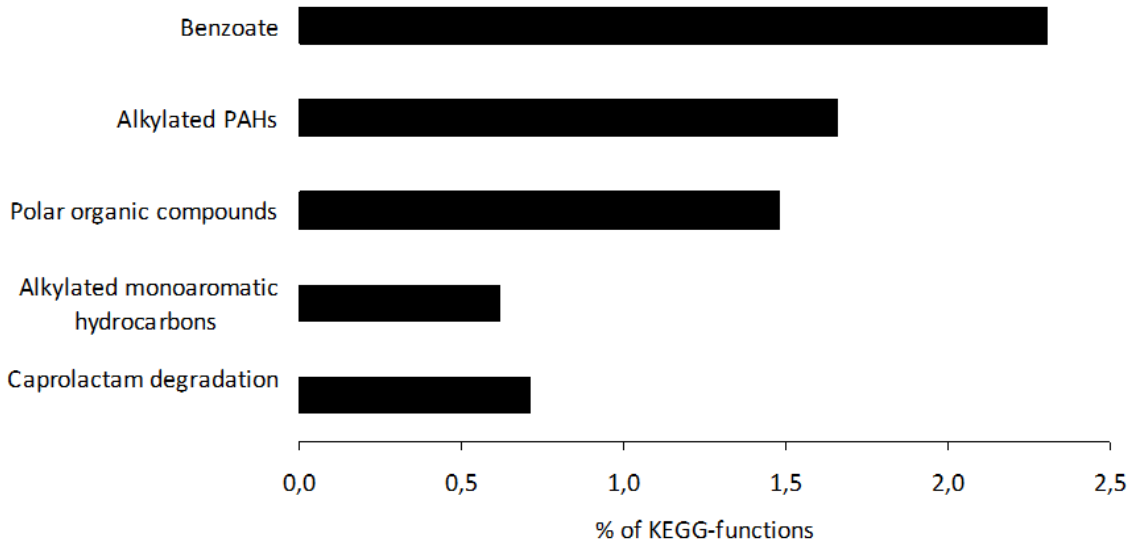

Figure 13. Distribution of functions related to the metabolism of xenobiotics according to KEGG at expectation values below $1e^{-40}$.

Table 3. Putative key enzymes in the anaerobic degradation of hydrocarbons that were detected in the MSO metagenome.

	Gene product	Locus	aa	kDa
Alkylsuccinate synthase	α-subunit (AssA)	OIL03_81	830	94.2
	β-subunit (AssB)	OIL03_83	128	14.2
	γ-subunit (AssC)	OIL03_80	54	6.0
	glycyl radical activating enzyme (AssD)	OIL03_77	329	37.4
	Chaperone (AssE)	OIL03_86	282	31.6
	Uncharacterized protein (MasE)	OIL03_82	73	8.3
Benzoyl-CoA reductase	Benzoyl-CoA reductase subunit	OIL09_52	425	47.2
	Benzoyl-CoA reductase activase	OIL09_53	257	27.2
	Benzoyl-CoA reductase subunit	OIL09_54	390	43.1
	4-Hydroxybenzoyl-CoA reductase, γ-subunit	OIL42_18	163	17.4
	4-Hydroxybenzoyl-CoA reductase, β-subunit	OIL42_19	292	30.7
	4-Hydroxybenzoyl-CoA reductase, α-subunit	OIL42_20	756	81.4

2.4.6. Main features of the alkylsuccinate synthase cluster in the MSO consortium

The fourth largest contig retrieved from the MSO metagenome (OIL03, 90. 777 bp), contained a cluster of genes with homology to several subunits of the *ass* operon from *D. alkenivorans* strain AK-01 (Callaghan *et al.*, 2011) and the denitrifying *Azoarcus* sp. strain HxN1 (Grundmann *et al.*, 2008) (Figure 14). This glycyl radical enzyme is a key player in the anaerobic degradation of aliphatic hydrocarbons. It is involved in the activation of *n*-alkanes via fumarate addition, the crucial reaction that facilitates the further biological attack of aliphatic chains. The gene product of OIL03_81 had best hits with the catalytic subunit of the alkylsuccinate synthase from strain AK-01 (78.2% identity with AssA) and strain HxN1 (71.5% identity with MasD). It also shared 37.4% identity with the α-subunit of the benzylsuccinate synthase (Bss), the analogue activating enzyme involved in the degradation of monoaromatic hydrocarbons (e.g. toluene, (Leuthner and Heider, 2000) (Figure 15).

Nine more ORFs flanked the putative *assA* gene in the MSO cluster. Five of them had best hits with subunits from strain AK-01 and strain HxN1, however their disposition in the cluster was substantially different (Figure 14). Downstream of *assA*, it was located OIL03_82, which product shared 60% identity with MasE. In strain HxN1, MasE has been postulated as the medium-size Ass subunit. This gene encodes for a protein containing a high number of cysteines, a common characteristic with the medium size

β-subunit of benzylsuccinate synthase (Grundmann *et al.*, 2008). The next gene product downstream (OIL03_83), had the best hit with AssB2 from strain AK-01 (54.4% identity) and MasB from strain HxN1 (44% identity), but currently, the function of this gene remains unknown.

Coinciding with the composition of both *ass* loci in strain AK-01, one chaperone-like protein (AssE, 76.6%) was found in the *ass* cluster of the MSO metagenome. This class of proteins is thought to be involved in the assembly, operation and disassembly of protein complexes (Neuwald *et al.*, 1999).

Upstream of AssA, OIL03_80 was 59.3% identical to AssC1 from strain AK-01 and 37% identical to BssC from *T. aromatica*. The protein encoded by *bssC* has been suggested to participate in the stabilization of the structure of the active site of BssA (Li *et al.*, 2009). Its iron-sulphur cluster appears to be essential for binding to BssA, what might serve as a linker between the α- and β-subunits of Bss.

All glycyl radical enzymes require an activase for the generation of the glycyl radical on the catalytic subunit of the enzyme. In the MSO cluster, a gene encoding a glycyl radical activating enzyme of the radical SAM superfamily was also found upstream of assA. OIL03_77 gene product was 53% identical to AssD from strain AK-01, 48% identical to the Mas activase (MasG, strain HxN1), and 39% identical to the activating enzyme BssD from *T. aromatica*.

Fatty acids derived from the oxidation of alkanes are oxidized to acetyl-CoA (even-numbered) and propionyl-CoA (odd-numbered) via β-oxidation (Callaghan *et al.*, 2011). Several β-oxidation genes were identified accompanying the *ass* cluster in OIL03 (Table 4).

Besides, three ORFs encoding outer membrane transport proteins were identified in OIL03. These were putative hydrocarbon transporters belonging to the FadL family. In *Pseudomonas putida* this proteins are encoded in TOL plasmids (toluene-degradation) and are concerned with transport of aromatic compounds such as toluene, *m*-xylene and benzyl alcohol (http://pfam.janelia.org/family/PF03349).

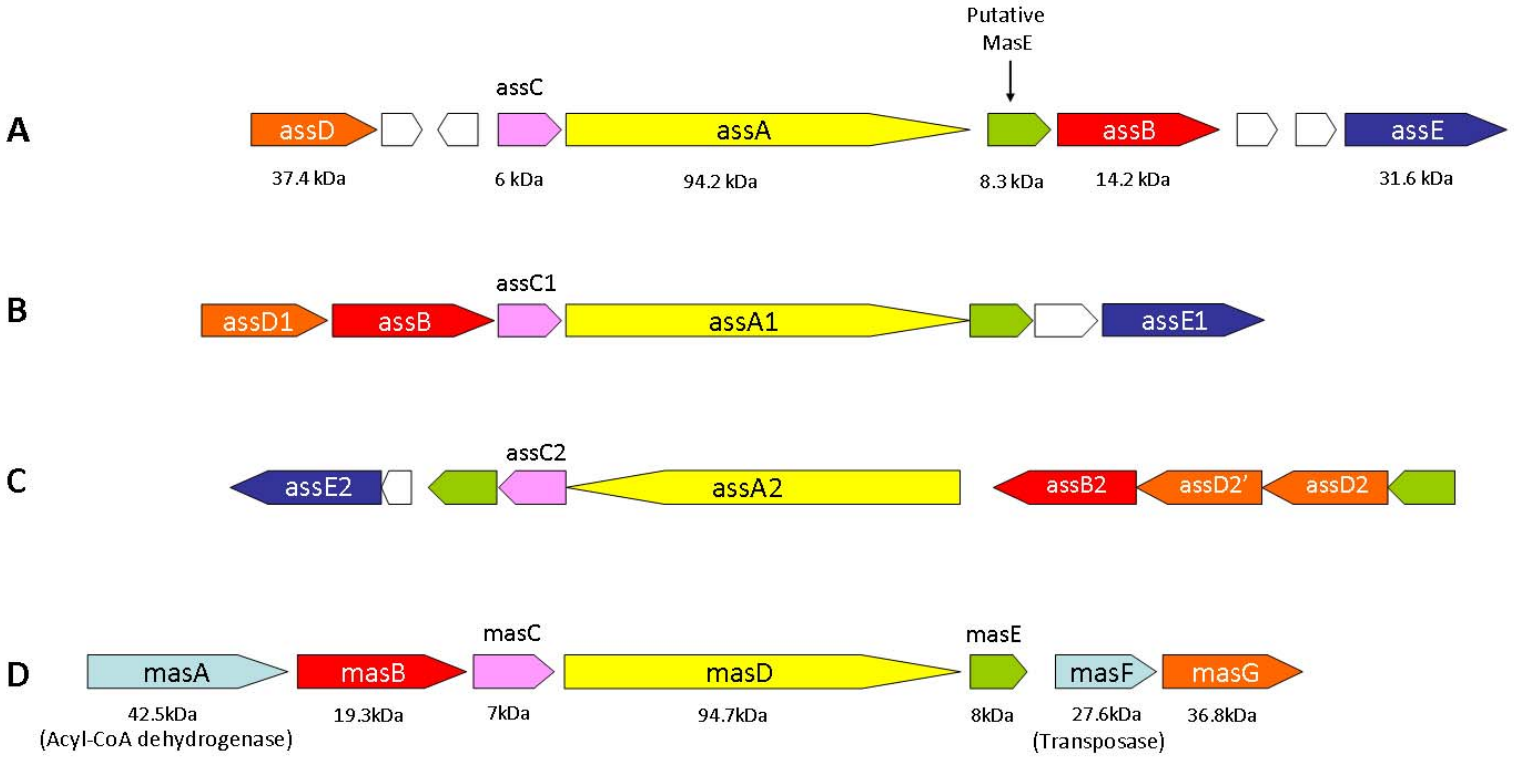

Figure 14. Alkylsuccinate synthase operon present in the MOS metagenome (**A**); strain AK-01 (**B** and **C**) and strain HxN1 (**D**). Gene abbreviations: ***assD*** – alkylsuccinate synthase glycyl radical activating enzyme; ***assC*** – alkylsuccinate synthase, putative γ-subunit; ***assA*** – alkylsuccinate synthase, α-subunit (catalytic); ***masE*** -- putative uncharacterized protein; ***assB*** – alkylsuccinate synthase, putative β-subunit; ***assE1*** – chaperone protein. Colours show homologue genes while white arrows represent hypothetical proteins.

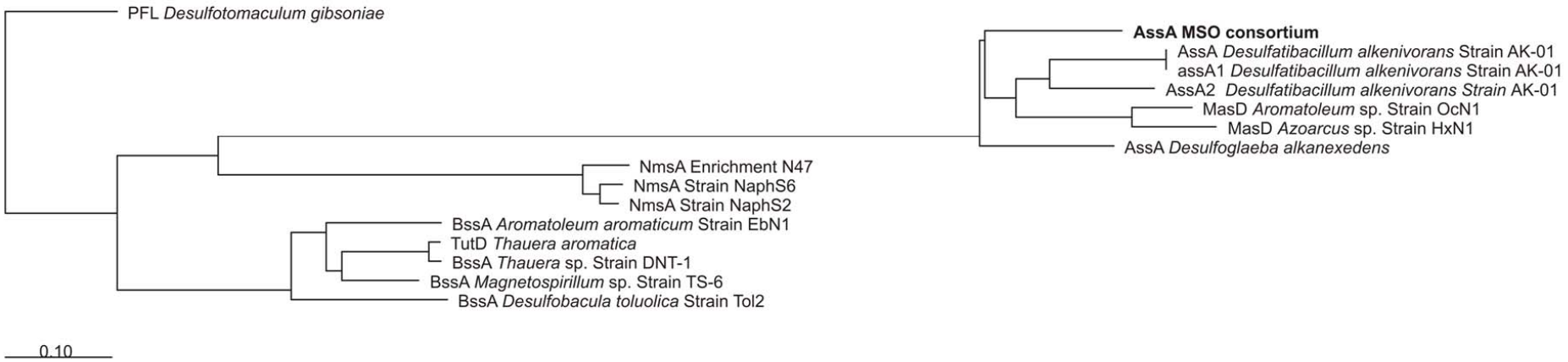

Figure 15. Phylogenetic affiliation of the α-subunit (catalytic) of alkylsuccinate synthase (AssA), the alkylsuccinate synthase retrieved from the MSO consortium metagenome (marked in bold), and radical-bearing subunits of other glycyl radical enzymes. **Bss:** benzylsuccinate synthase; **Tut**: synonym of Bss; **PFL**: pyruvate formate lyase; Accession No. (from top to bottom): ZP_09103333.1, ABH11460.1, YP_002430896.1, YP_002431360.1, CBK27727.1, CAO03074.1, ADJ51097.1, ADB04297.1, CAO72222.1, CAO72219.1, YP_158060.1, AAC38454.1, BAC05501.1, BAD42366.1, CAO72221.1; Amino acidic sequences were aligned with CLUSTAL W and tree reconstruction was performed by Neighbour Joining taking in account 830 homologous positions.

Table 4. Enzyme-coding genes involved in fatty acids β-oxidation and putative hydrocarbon transporters detected in the OIL03 contig.

OIL03	aa	kDa	Encoded protein	% id.	Close relative	Pfam	E.C.
2	385	42.9	acyl-CoA dehydrogenase domain protein	74	*Desulfatibacillum alkenivorans* AK-01	00441	1.3.99…
3	429	45.1	acetyl-CoA acetyltransferase	73.6	*Desulfobacterium autotrophicum*	00108	2.3.1.9
6	263	28.6	enoyl-CoA hydratase/isomerase	68.6	*Desulfatibacillum alkenivorans* AK-01	00378	4.2.1.17
9	537	58.3	3-hydroxyacyl-CoA dehydrogenase	35.5	*Heliangium ochraceum*	02737	4.2.1.17…
10	148	15.6	3-hydroxyacyl-CoA dehydrogenase	39.6	*Sphingobium japonicum (* α*-proteobacteria)*		4.2.1.5.5
11	373	39.9	acetyl-CoA acetyltransferase	45.8	*Geobacter metallireduces*	02803	2.3.1.9
15	515	57.7	long-chain-fatty-acid--CoA ligase	60.7	Strain NaphS2	00501	6.2.1.3
51	398	42.1	propanoyl-CoA C-acyltransferase	66.5	*Desulfarculus barsii*		2.3.1.16
53	265	29.3	enoyl-CoA hydratase/isomerase	53	*Desulfatibacillum alkenivorans* AK-01	00378	4.2.1.17
59	545	60	propionyl-CoA carboxylase, beta subunit	69.5	*Desulfatibacillum alkenivorans* AK-01	01039	6.4.1.3
60	404	44	acyl-CoA transferase	51	*Syntrophobacter fumaroxidans*	02515	5.1.99.4
66	178	19.3	fatty-acid-CoA ligase	58.1	*Desulfatibacillum alkenivorans* AK-01		6.2.1…
69	262	27.8	3-hydroxyacyl-CoA dehydrogenase	65.1	*Desulfobacterium autotrophicum*	00106	1.1.1.35
72	388	42.3	acyl-CoA dehydrogenase domain-containing protein	55.1	*Desulfatibacillum alkenivorans* AK-01	00441	1.3.99…
73	380	42.3	long-chain acyl-CoA dehydrogenase	58.5	*Desulfococcus oleovorans* Hxd3	00441	1.3.99…
75	647	71.1	acyl-CoA dehydrogenase domain-containing protein	58.8	*Desulfatibacillum alkenivorans* AK-01	00441	1.3.99…
19	265	30.6	Hydrocarbon transport protein	44	*Desulfococcus oleovorans* Hxd3	03349	
20	300	31.2	Hydrocarbon transport protein	44.1	*Desulfococcus oleovorans* Hxd3	03349	
61	484	54.1	Hydrocarbon transport protein	29.2	*Pseudomonas mendocina*	03349	

3. References

Annweiler, E., Michaelis, W., and Meckenstock, R.U. (2001) Anaerobic cometabolic conversion of benzothiophene by a sulfate-reducing enrichment culture and in a tar-oil-contaminated aquifer. *Appl. Environ. Microbiol.* **67**: 5077-5083.

Annweiler, E., Michaelis, W., and Meckenstock, R.U. (2002) Identical ring cleavage products during anaerobic degradation of naphthalene, 2-methylnaphthalene, and tetralin indicate a new metabolic pathway. *Appl. Environ. Microbiol.* **68**: 852-858.

Bak, F., and Widdel, F. (1986) Anaerobic degradation of indolic compounds by sulfate-reducing enrichment cultures, and description of *Desulfobacterium indolicum* gen. nov., sp. nov. *Arch. Microbiol.* **146**: 170-176.

Boll, M., and Heider, J. (2010) Anaerobic degradation of hydrocarbons: mechanisms of C-H-bond activation in the absence of oxygen. *In* Handbook of hydrocarbon and lipid microbiology. Timmis, K. N. (ed). Berlin Heidelberg, DE: Springer-Verlag, pp. 1012-1024.

Boll, M., Fuchs, G., Meier, C., Trautwein, A., El Kasmi, A., Ragsdale, S.W. et al. (2001) Redox centers of 4-hydroxybenzoyl-CoA reductase, a member of the xanthine oxidase family of molybdenum-containing enzymes. *J. Biol. Chem.* **276**: 47853-47862.

Callaghan, A.V., Morris, B.E., Pereira, I.A., McInerney, M.J., Austin, R.N., Groves, J.T. et al. (2011) The genome sequence of *Desulfatibacillum alkenivorans* AK-01: a blueprint for anaerobic alkane oxidation. *Environ. Microbiol.* **14**: 101-113.

Finn, R.D., Tate, J., Mistry, J., Coggill, P.C., Sammut, S.J., Hotz, H.R. et al. (2008) The Pfam protein families database. *Nucleic Acids Res.* **36**: D281-288.

Fuchs, G., Boll, M., and Heider, J. (2011) Microbial degradation of aromatic compounds - from one strategy to four. *Nat. Rev. Microbiol.* **9**: 803-816.

Fujita, Y., Matsuoka, H., and Hirooka, K. (2007) Regulation of fatty acid metabolism in bacteria. *Mo.l Microbiol.* **66**: 829-839.

Galushko, A., Minz, D., Schink, B., and Widdel, F. (1999) Anaerobic degradation of naphthalene by a pure culture of a novel type of marine sulphate-reducing bacterium. *Environ. Microbiol.* **1**: 415-420.

Grundmann, O., Behrends, A., Rabus, R., Amann, J., Halder, T., Heider, J., and Widdel, F. (2008) Genes encoding the candidate enzyme for anaerobic activation of n-alkanes in the denitrifying bacterium, strain HxN1. *Environ. Microbiol.* **10**: 376-385.

Higashioka, Y., Kojima, H., Nakagawa, T., Sato, S., and Fukui, M. (2009) A novel *n*-alkane-degrading bacterium as a minor member of *p*-xylene-degrading sulfate-reducing consortium. *Biodegradation.* **20**: 383-390.

Jendrossek, D. (2009) Polyhydroxyalkanoate granules are complex subcellular organelles (carbonosomes). *J. Bacteriol.* **191**: 3195-3202.

Johansen, S.S., Licht, D., Arvin, E., Mosbaek, H., and Hansen, A.B. (1997) Metabolic pathways of quinoline, indole and their methylated analogs by *Desulfobacterium indolicum* (DSM 3383). *Appl. Microbiol. Biotechnol.* **47**: 292-300.

Joint, I., Muhling, M., and Querellou, J. (2010) Culturing marine bacteria - an essential prerequisite for biodiscovery. *Microb. Biotechnol.* **3**: 564-575.

Kniemeyer, O., and Heider, J. (2001) Ethylbenzene dehydrogenase, a novel hydrocarbon-oxidizing molybdenum/iron-sulfur/heme enzyme. *J. Biol. Chem.* **276**: 21381-21386.

Leuthner, B., and Heider, J. (2000) Anaerobic toluene catabolism of *Thauera aromatica*: the bbs operon codes for enzymes of beta oxidation of the intermediate benzylsuccinate. *J. Bacteriol.* **182**: 272-277.

Li, L., Patterson, D.P., Fox, C.C., Lin, B., Coschigano, P.W., and Marsh, E.N. (2009) Subunit structure of benzylsuccinate synthase. *Biochemistry* **48**: 1284-1292.

Lizama, H.M., Wilkins, L.A., and Scott, T.C. (1995) Dibenzothiophene sulfur can serve as the sole electron acceptor during growth of sulfate-reducing bacteria. *Biotechnol. Lett.* **17**: 113-116.

Madsen, E.L., and Bollag, J.-M. (1989) Pathway of indole metabolism by a denitrifying microbial community. *Arch. Microbiol.* **151**: 71-76.

Martin-Cuadrado, A.B., Lopez-Garcia, P., Alba, J.C., Moreira, D., Monticelli, L., Strittmatter, A. et al. (2007) Metagenomics of the deep Mediterranean, a warm bathypelagic habitat. *PLoS One* **2**: e914.

Mbadinga, S.M., Wang, L.-Y., Zhou, L., Liu, J.-F., and Mua, B.-Z. (2011) Microbial communities involved in anaerobic degradation of alkanes. *Int. Biodeter. Biodegr.* **65**: 1-13.

Musat, F., and Widdel, F. (2008) Anaerobic degradation of benzene by a marine sulfate-reducing enrichment culture, and cell hybridization of the dominant phylotype. *Environ. Microbiol.* **10**: 10-19.

Musat, F., Galushko, A., Jacob, J., Widdel, F., Kube, M., Reinhardt, R. et al. (2009) Anaerobic degradation of naphthalene and 2-methylnaphthalene by strains of marine sulfate-reducing bacteria. *Environ. Microbiol.* **11**: 209-219.

Muthusamy, K., Gopalakrishnan, S., Ravi, T.K., and Sivachidambaram, P. (2008) Biosurfactants: properties, commercial production and application. *Curr. Science.* **94**: 736-747.

Neuwald, A.F., Aravind, L., Spouge, J.L., and Koonin, E.V. (1999) AAA+: A class of chaperone-like ATPases associated with the assembly, operation, and disassembly of protein complexes. *Genome Res.* **9**: 27-43.

Rabus, R., Jarling, R., Lahme, S., Kuhner, S., Heider, J., Widdel, F., and Wilkes, H. (2011) Co-metabolic conversion of toluene in anaerobic n-alkane-degrading bacteria. *Environ. Microbiol.* **13**: 2576-2586.

Ragsdale, S.W. (2008) Enzymology of the Wood-Ljungdahl pathway of acetogenesis. *Ann. NY Acad. Sci.* **1125**: 129-136.

Reemstma, T. (2009) Determination of molecular formulas of natural organic matter molecules by (ultra-) high-resolution mass spectrometry. Status and needs. *J. Chromatogr. A* **1216**: 3687–3701.

Safinowski, M., and Meckenstock, R.U. (2006) Methylation is the initial reaction in anaerobic naphthalene degradation by a sulfate-reducing enrichment culture. *Environ. Microbiol.* **8**: 347-352.

Santos, S.R., and Ochman, H. (2004) Identification and phylogenetic sorting of bacterial lineages with universally conserved genes and proteins. *Environ Microbiol* **6**: 754-759.

Selesi, D., Jehmlich, N., von Bergen, M., Schmidt, F., Rattei, T., Tischler, P. et al. (2010) Combined genomic and proteomic approaches identify gene clusters involved in anaerobic 2-methylnaphthalene degradation in the sulfate-reducing enrichment culture N47. *J. Bacteriol.* **192**: 295-306.

Shranker, R., and Bollag, J.-M. (1990) Transformation of indole by methanogenic and sulphate-reducing microorganisms isolated from digested sludge. *Microb. Ecol.* **20**: 171-183.

Skerker, J.M., Prasol, M.S., Perchuk, B.S., Biondi, E.G., and Laub, M.T. (2005) Two-component signal transduction pathways regulating growth and cell cycle progression in a bacterium: a system-level analysis. *PLoS Biol* **3**: e334.

So, C.M., and Young, L.Y. (1999) Initial reactions in anaerobic alkane degradation by a sulfate reducer, strain AK-01. *Appl Environ Microbiol* **65**: 5532-5540.

Strittmatter, A.W., Liesegang, H., Rabus, R., Decker, I., Amann, J., Andres, S. et al. (2009) Genome sequence of *Desulfobacterium autotrophicum* HRM2, a marine sulfate reducer oxidizing organic carbon completely to carbon dioxide. *Environ. Microbiol.* **11**: 1038-1055.

Trautwein, K., Kuhner, S., Wohlbrand, L., Halder, T., Kuchta, K., Steinbuchel, A., and Rabus, R. (2008) Solvent stress response of the denitrifying bacterium "*Aromatoleum aromaticum*" strain EbN1. *Appl. Environ. Microbiol.* **74**: 2267-2274.

Widdel, F., Knittel, K., and Galushko, A. (2010) Anaerobic hydrocarbon-degrading microorganisms: an overview. *In* Handbook of hydrocarbon and lipid microbiology. Timmis, K. N. (ed). Berlin Heidelberg, DE: Springer-Verlag, pp. 1998-2021.

Yarza, P., Richter, M., Peplies, J., Euzeby, J., Amann, R., Schleifer, K.H. et al. (2008) The All-Species Living Tree project: A 16S rRNA-based phylogenetic tree of all sequenced type strains. *Syst. Appl. Microbiol.* **31**: 241-250.

Yilmaz, P., Kottmann, R., Pruesse, E., Quast, C., and Glockner, F.O. (2011) Analysis of 23S rRNA genes in metagenomes - a case study from the Global Ocean Sampling Expedition. *Syst. Appl. Microbiol.* **34**: 462-469.

Zhang, X., Sullivan, E.R., and Young, L.Y. (2000) Evidence for aromatic ring reduction in the biodegradation pathway of carboxylated naphthalene by a sulfate reducing consortium. *Biodegradation* **11**: 117-124.

Concluding remarks

This research provides first insights into the diversity, abundance and physiology of sulphate reducing bacteria inhabiting the permanent anoxic layer of bare carbonated sandy sediment from the Mediterranean Sea. Despite of the oligotrophic character of the environment, the sediment harbored a large microbial biomass with community dynamics primarily driven by a seasonal increase of temperature. The predominance and diversity of *Deltaproteobacteria,* in both bare and vegetated sediments at the Balearic Islands, evidenced the importance of this group in the oxidation of deposited OM. Viable counts revealed a dominance of complete oxidizers and autotrophs and pointed out to acetate and hydrogen as the most relevant electron donors for sulphate respiration.

Considering the essential role of the sediment's biocatalytic filter, and the ecological and economical repercussions that any perturbation at this level might have over the Mediterranean ecosystem, the effect of the crude oil contamination was investigated *in situ*. In field monitorization revealed that the seasonal increase of microbial biomass was attenuated after contamination with crude oil and naphthalene. However, far from the impact observed at the whole community level, the presence of hydrocarbons did not have a negative effect over the deltaproteobacterial population. The crude oil contamination significantly enhanced the *in situ* sulphate reducing activity and the culturability of SRBs. Thus, the Mediterranean sediment contained an autochthonous SRB microbiota that could prosper after a crude oil spill and which activity could be crucial for the transformation and removal of hazardous organic compounds.

A SRB crude oil degrading consortium enriched from the Mediterranean sediment provided the first insights into the phylogeny and physiology of the anaerobic hydrocarbon degraders inhabiting this environment. The MSO consortium was integrated by members of the *Desulfobacteraceae* family related to other alkane- and naphthalene-degrading SRBs (e.g. strains AK-01 and NaphS2), and a filament shaped bacterium which phylogeny remains unknown. The consortium was able to degrade both, aliphatic and alkylated polycyclic aromatic hydrocarbons, while causing a further weathering of polar organic compounds. Metagenomic and metabolomic studies

pointed to hydroxylation and fumarate addition as the possible biochemical reactions ruling the hydrocarbon degradation. However, additional enzymatic reactions might remain undetected due to their novelty or to methodological constrains. Further experiments based in stable isotope probing and transcriptomic and/or proteomic analyses of the MSO consortium might contribute to the understanding of cooperative crude oil degradation.

Annex

Annex 1. Fluorescence in situ *hybridization (FISH)*

Table A.1. NaCl concentration in the washing buffer according to the percentage of formamide used during hybridization. In bold the percentages of formamide used in this study (from www.arb-silva.de, Experimental procedures, Section 5.9)

% formamide	**Washing at 48ºC**	
In the hybridization	**[NaCl] mM**	**µl 5M NaCl in 50 ml**
buffer	**final concentration**	
0	0.900	9000
5	0.636	6300
10	**0.450**	**4500**
15	0.318	3180
20	0.225	2150
25	0.159	1490
30	0.112	1020
35	**0.080**	**700**
40	0.056	460
45	0.040	300
50	0.028	180
55	0.020	100
60	0.014	40
65	-	-
70	-	-

Annex 2. Artificial seawater medium for the cultivation of SRB (Experimental procedures, Section 7.1).

Table A.2. Trace elements solution

Reactive	Final concentration (mM)	Add (mg)
HCl 25%	100	12.5 ml
$FeSO_4.7H_2O$	7.5	2100
$CoCl_2.6H_2O$	0.8	190
$ZnSO_4.7H_2O$	0.5	144
$MnCl_2.4H_2O$	0.5	100
$Na_2MoO_4.2H_2O$	0.15	36
H_3BO_3	0.5	30
$NiCl_2.6H_2O$	0.1	24
$CuCl_2.2H_2O$	0.01	2
MilliQ H_2O		Add up to 1000 ml

Table A.3. Selenite-tungstate solution

Reactive	Final concentration (mM)	Add (mg)
NaOH	10	400
$Na_2SeO_3.5H_2O$	6	0.02
$Na_2WO_4.2H_2O$	8	0.02
MilliQ H_2O	Add 1000 ml	

Table A.4. Vitamin solution

Reactive	mg
Pyridoxyn-hydrochloride	15
Nicotinic acid	10
Ca-D(+)-pantothenat	5
4-Aminobenzoic acid	4
D(+)-Biotin	1
Phosphate buffer (pH 7.1)	Add 100 ml

- Thiamin solution: 10 mg of thiamin chloride-hydrochlorid in 100 ml of phosphate buffer (pH 3.7)

- Riboflavin solution: 0.1 ml of concentrated acetic acid and 2.5 mg of riboflavin in 100 ml of MilliQ water.

- B_{12} solution: 5 mg of cyanocobalamin in 100 ml of MilliQ water.

All vitamin solutions were sterilized by filtration (0.22 μm) in sterile brown-glass bottles and stored at 4° in dark.

Annex 3. Chapter 1, Section 2.2.

Table A.5. Phylogenetic affiliation of the bacterial phylotypes contained in the 16S rDNA clone libraries.

OPUs	OTUs (accession no.)	OTUs (no.)	Clones (no.) CTO/3 mo.	Phylogenetic affiliation	Accession no. Closest relative phylotype	Id (%±SD)	Accession no. Closest cultivated relative	Id (%±SD)
1	**FJ949237**	2	2	*Deltaproteobacteria*	DQ811829 Uncultured bacterium	94.2±1.9	M34407 *Desulfosarcina variabilis*	91.8±0.6
	FJ949236							
2	**FJ949241**	1	1					
3	**FJ949238-FJ949240**	1	3					
4	**FJ949244**	3	3					
	FJ949242, FJ949243							
5	**FJ949245**	3	2					
	FJ949246							
6	**FJ949247**	1	1					
7	**FJ949248**	2	1		AF099063 *Desulfofaba gelida*	87.8±0.7		
8	**FJ949249**	1	1					
9	**FJ949250**	1	1					
10	**FJ949251**	1	1					
11	**FJ949252, FJ949253**	4	4		EU181461 Uncultured bacterium	92.8±2.0	AY493562 *Desulfatibacillum alkenivorans*	88.4±1.4
	FJ949254, FJ949255							
12	**FJ949258**	1	1		AJ237601 *Desulfobacterium anilini*	92.4±1.4		
13	**FJ949256**	2	2					
	FJ949257							
14	**FJ949259**	1	1		DQ811819 Uncultured	97.6	AF002671 *Desulfobacca*	88.1

					bacterium		*acetoxidans*	
15	**FJ949260**	2	1		AB110542 *Desulfopila aestuarii*	91.8		
16	**FJ949261-FJ949263**	1	3		EU617849 Uncultured bacterium	95.9±3.5		
17	**FJ949264**	1	1					
18	**FJ949265**	1	1				DQ303457 *Desulfoglaeba alkanexedens*	
19	**FJ949266**	4	2		AJ241001 Uncultured bacterium	95.3±2.9		86.5±1.0
	FJ949267				DQ463694 Uncultured bacterium	95.4		
20	**FJ949268**	1	1		DQ394946 Uncultured *Geobacteraceae* bacterium	92.4	X79415 *Desulfuromusa succinoxidans*	83.3
21	**FJ949272**	1	1	*Deltaproteobacteria*				
22	**FJ949269**	2	2		EU290707 Uncultured bacterium	87.3±3.0	DQ148944 *Desulfovibrio ferrireducens*	80.9±1.3
	FJ949270							
23	**FJ949273**	1	1					
24	**FJ949271**	1	1					
25	**FJ949274**	3	1		AF084854 *Bacteriovorax marinus*	88.2		
26	**FJ949276**	2	2		DQ331004 Uncultured bacterium	94.5±0.7	AF084859 *Bacteriovorax litoralis*	82.7±4.2
	FJ949275							
27	**FJ949277, FJ949278**	3	2		AB189713 *Ifremeria nautilei* gill symbiont	92.9±2.4		
28	**FJ949279**	1	1		AB278144 Uncultured bacterium	94.5	AJ879933 Candidatus *Thiobios zoothamnicoli*	90.5±2.4
29	**FJ949280**	1	1		DQ351809 Uncultured bacterium	97.0		
30	**FJ949283**	2	3		AM410704 *Acinetobacter junii*	99.4		
	FJ949281, FJ949282			*Gammaproteobacteria*	AY633608 "*Acinetobacter seohaensis*"	98.5±0.2		
31	**FJ949284**	3	1		AY532642 Candidatus	95.9		

					Endobugula glebosa			
32	**FJ949285**	2	2		EF999373 Uncultured bacterium	91.7±1.3	DQ834966 *Methylohalomonas lacus*	89.6±1
	FJ949286							
33	**FJ949287**	1	1					
34	**FJ949288**	1	1					
35	**FJ949289**	1	1					
36	**FJ949290**	2	2					
	FJ949291							
37	**FJ949292, FJ949294**	3	4					
	FJ949293							
	FJ949295							
38	**FJ949297**	1	1		AY74140 *Legionella*-like amoebal pathogen	87.45±0.4	AF383621 *Rickettsiella* sp.	82.75±1.2
39	**FJ949296**	1	1					
40	**FJ949298-FJ949318**	2	22	*Gammaproteobacteria*	AM162659 *Vibrio lentus*	98.1±0.8		
	FJ949319							
41	**FJ949320-FJ949326, FJ949329**	3	10		AY554009 *Photobacterium lipolyticum*	97.8±2.2		
	FJ949327							
	FJ949328							
42	**FJ949330-FJ949347**	1	18		AB304807 *Psychromonas* sp.	98.4±0.3		
43	**FJ949349-FJ949350**	1	2	*Alphaproteobacteria*	D12785 *Brevundimonas bullata*	99.8±0.1		
44	**FJ949348**	2	1		DQ289904 Uncultured bacterium	93.7	AY387398 *Parvibaculum lavamentivorans*	88.3±3.5
45	**FJ949351-FJ949358**	1	8					

46	**FJ949359**	1	1	*Epsilonproteobacteria*	AJ132729 Uncultured bacterium	95.4±1.6	AF513455 *Arcobacter halophilus*	92.2±0.8
47	**FJ949360**	2	2					
	FJ949361, FJ949185							
48	**FJ949362**	1	1					
49	**FJ949363**	1	1		AB252048 *Sulfurimonas paralvinellae*	92.7±0.1		
50	**FJ949364**	1	1					
51	**FJ949365**	1	1	*Nitrospira*	AY592672 Uncultured bacterium	93.9		
52	**FJ949368**	2	2	Uncultured TM6	DQ787724 Uncultured bacterium	89.8		
	FJ949367				AJ704673 Uncultured bacterium	94.4		
53	**FJ949366**	2	1		DQ394961 Uncultured bacterium	92.9		
54	**FJ949369**	3	3	*Acidobacteria*	DQ351805 Uncultured bacterium	91.1±2.9		
	FJ949370							
	FJ949371							
55	**FJ949372, FJ949373**	2	3		EF492943 Uncultured bacterium	83.8±1.4		
	FJ949374							
56	**FJ949375**	1	1					
57	**FJ949376**	1	1					
58	**FJ949377**	2	1					
59	**FJ949378**	1	1					
60	**FJ949379**	1	1	*Chaldithrix*	EF572713 Uncultured bacterium	83.8±0.5		
61	**FJ949388, FJ949389**	2	3		AY588965 Uncultured bacterium	98.4±0.4		

	FJ949390			*Clostridiales*	EU617877 Uncultured bacterium	98.8	X77845 *Clostridium litorale*	85.4±2.7
62	**FJ949391**	1	1		EU236399 Uncultured bacterium	95.3		
63	**FJ949392**	1	1		X77845 *Clostridium litorale*	99.6		
64	**FJ949380, FJ949381**	1	2					
65	**FJ949382-FJ949387**	1	6	*Fusobacteria*	AY579753 Uncultured bacterium	96.6±3.7	AJ307981 *Ilyobacter polytropus*	93.1±1.4
66	**FJ949393**	1	1					
67	**FJ949394**	2	2		DQ289921 Uncultured bacterium	89.8±2.1	X6291 *Planctomyces limnophilus*	80.3±1.3
	FJ949395							
68	**FJ949396**	3	2	*Planctomycetes*	AB300067 Uncultured bacterium	92±3.9	X62911 *Planctomyces limnophilus*	71.8±2.6
	FJ949397				AB300095 Uncultured bacterium	86.7		
69	**FJ949398**	1	1		DQ329816 Uncultured bacterium	85.7		
70	**FJ949399**	1	1		EU652669 Uncultured bacterium	98		
71	**FJ949400**	1	1		AY555803 Uncultured bacterium	87.8	X62911 *Planctomyces limnophilus*	74±3.9
	FJ949401							
72	**FJ949402**	3	3	Uncultured	AB252431 Uncultured bacterium	77.1±2.4		
	FJ949403							
73	**FJ949404**	2	1					
74	**FJ949405**	2	1					
75	**FJ949406, FJ949407**	1	2	*Verrucomicrobia*	EU385802 Uncultured bacterium	85.5	X90515 *Verrucomicrobium spinosum*	78.7±3.7
76	**FJ949408**	1	1					
77	**FJ949409**	1	1	*Lentisphaerae*	AJ431235 *Cytophaga* sp.	87.2±2.5		
78	**FJ949410**	1	1					

79	**FJ949411** **FJ949412**	3	2	*Actinobacteria*	AB099989 Uncultured bacterium	93.1±0.6	AB184655 *Streptomyces flavidofuscus*	81.2±0.3
80	**FJ949428**	2	1	*Chloroflexi*	DQ463707 Uncultured bacterium	95.4		
81	**FJ949427**	1	1		AY356381 Uncultured bacterium	87.9		
82	**FJ949413** **FJ949414** **FJ949415**	5	3					
83	**FJ949416**	2	1	*Chloroflexi* (*Dehalococcoides*)	EF061968 Uncultured bacterium	84.9±2.2	AB067647 *Caldilinea aerophila*	79.4±1.1
84	**FJ949417**	1	1					
85	**FJ949418**	2	1					
86	**FJ949419** **FJ949420**	2	2					
87	**FJ949421**	1	1					
88	**FJ949422**	1	1					
89	**FJ949423** **FJ949424, FJ949425**	2	3					
90	**FJ949426**	1	1					
91	**FJ949429**	1	1	Uncultured	EU181475 Uncultured bacterium	91.9±2.7		
92	**FJ949430**	1	1					
92	**FJ949431**	1	1					
94	**FJ949432**	2	1					
95	**FJ949433**	1	1					
96	**FJ949434**	1	1					
97	**FJ949435**	1	1					
98	**FJ949436**	1	1					
99	**FJ949437**	2	1	*Bacteroidetes*	AF419690 Uncultured bacterium	92.1±4.8	AY918928 *Prolixibacter bellariivorans*	81.5±1.5
100	**FJ949438**	1	1					
101	**FJ949439**	1	1					
102	**FJ949440**	1	1					
103	**FJ949441**	3	1	Uncultured	AM259912 Uncultured	83.9		

					bacterium				
104	**FJ949442**	3	2						
	FJ949443								
105	**FJ949444**	2	1	Uncultured	EU246222 Uncultured bacterium	81.3±2			
106	**FJ949445**	1	1						
107	**FJ949446**	1	1						
108	**FJ949447, FJ949448**	1	2	Uncultured	EU574672 Uncultured bacterium	97.9±1.6			
109	**FJ949449**	1	1		DQ234160 Uncultured bacterium	92.7			

Figure A.1. Phylogenetic affiliation of the partial SRB 16S rRNA gene sequences retrieved from the sediment at the beginning of the experiment (named ad **MS_number of clone)** and from the MPN cultures. Sequences from the MPN cultures are named according to: isolation source (**MS**: Marine Sediment)_growth substrate (**ACE**: Acetate, **LAC**: lactate, **H2**: Hydrogen, **NAP**: Naphthalene, **ANT**: Anthracene, **OIL**: crude oil)_mesocosm (**N:** Naphthalene, **O:** Crude oil, **U:** Untreated). Genbank accession numbers are specified in brackets. Colors correspond to the mesocosm from which the sequences were retrieved, being **green: untreated**, **blue: naphthalene** and **orange: crude oil** mesocosms. In brackets it is represented the number of clones with identity equal to or higher than 97%. The sequences related to previously described anaerobic hydrocarbon degraders are marked in bold (in brackets the accession number and the hydrocarbon that can degrade, based on Widdel *et al.*, 2010).

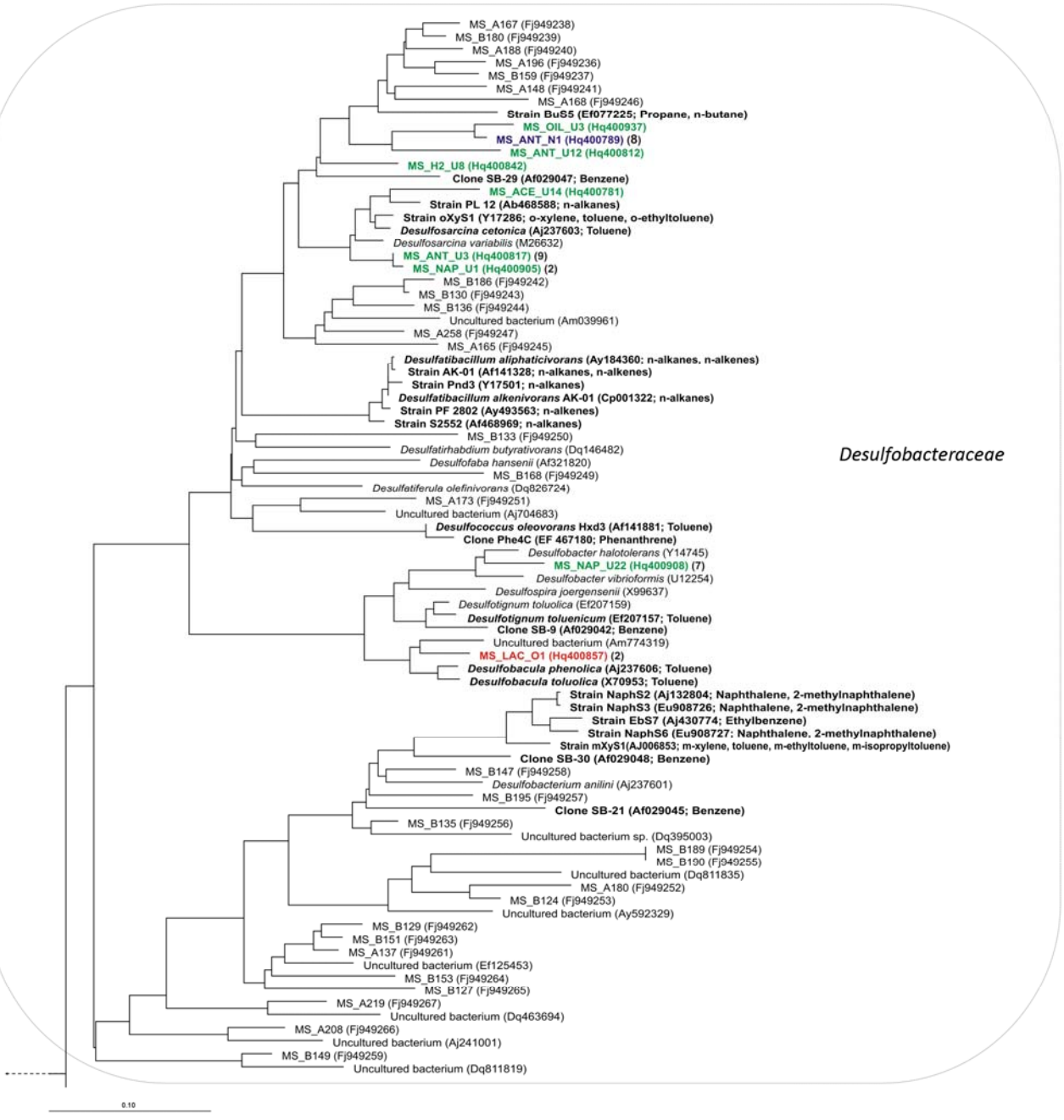

Figure A.1. (Continued)

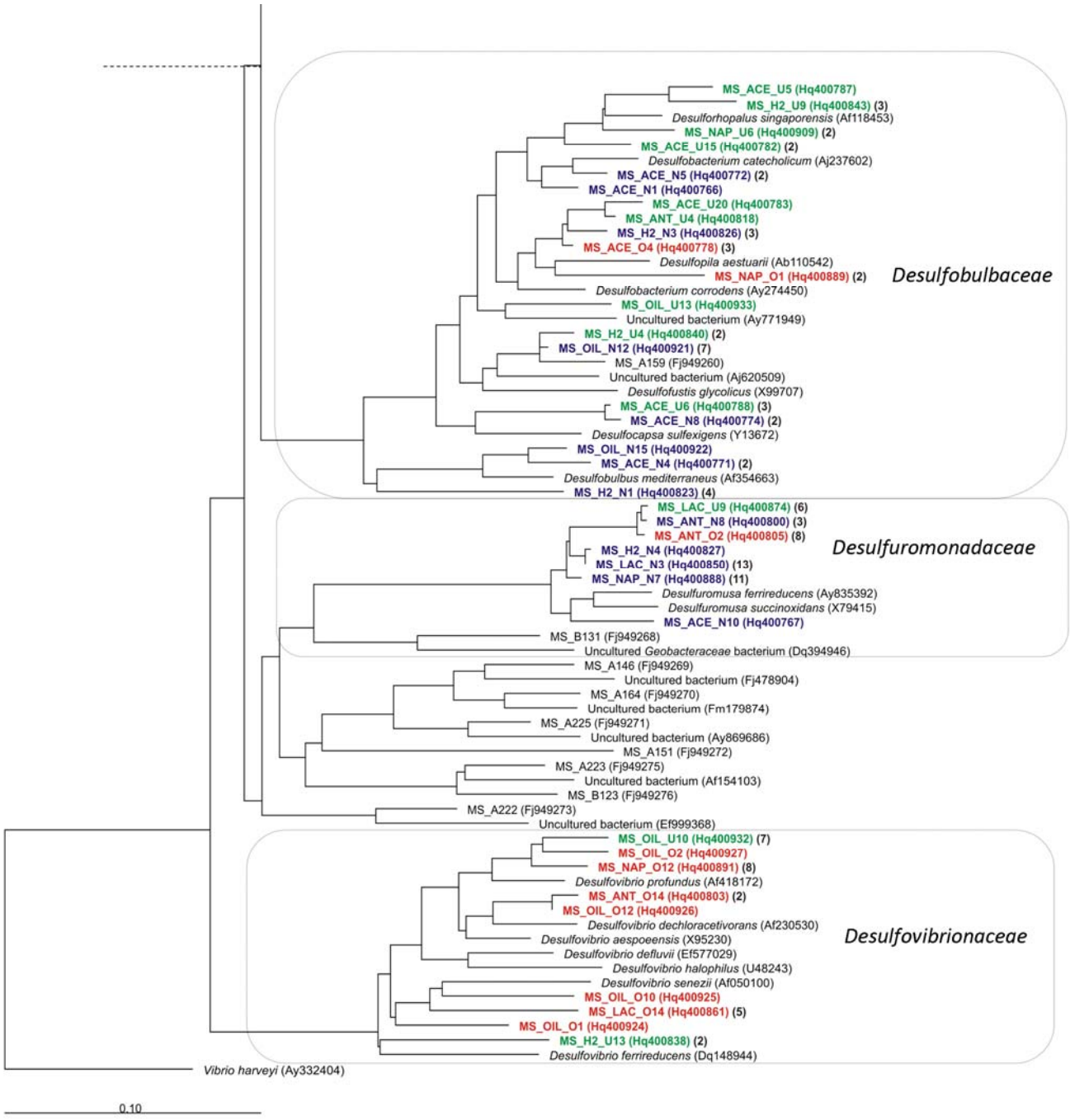

Annex 4. Chapter 3

Table A.6. Phylogenetic affiliation of the most relevant housekeeping genes identified in the MSO metagenome.

Housekeeping gene	AA	kDa	Phylogenetic affiliation	Family	Class	id (%)	e value	Acc
	154	17. 455	*Flavobacterium psychrophilum*	*Flavobacteriaceae*	*Flavobacteria*	63	1.0E-49	YP_001295365
RRF	185	21. 081	Unculture *Desulfobacterium* sp. N47	*Desulfobacteraceae*	*δ-proteobacteria*	80	1.0E-81	CBX26991
(ribosomal recycling factor)	185	21. 570	Strain NaphS2	*Desulfobacteraceae*	*δ-proteobacteria*	74.1	6.0E-77	ZP_07200117
	127	14. 872	*Robiginitalea biformata*	*Flavobacteriaceae*	*Flavobacteria*	50	1.0E-27	YP_003194413
RBFA	113	12. 430	Unculture *Desulfobacterium* sp. N47	*Desulfobacteraceae*	*δ-proteobacteria*	55.7	1.0E-28	CBX29053
(ribosome-binding factor)	122	13. 908	Strain NaphS2	*Desulfobacteraceae*	*δ-proteobacteria*	60	2.0E-34	ZP_07204059
	200	21. 744	Unculture *Desulfobacterium* sp. N47	*Desulfobacteraceae*	*δ-proteobacteria*	61.4	6.0E-72	CBX27496
RecR	196	21. 698	*Bacteroides fluxus*	*Bacteroidaceae*	*Bacteroidia*	64.4	2.0E-72	ZP_08301835
(recombination protein)	203	22. 143	Strain NaphS2	*Desulfobacteraceae*	*δ-proteobacteria*	67.5	6.0E-80	ZP_07199440
	122	14. 022	Strain NaphS2	*Desulfobacteraceae*	*δ-proteobacteria*	63.1	5.0E-37	ZP_07203828
DUF143	137	15. 430	Unculture *Desulfobacterium* sp. N47	*Desulfobacteraceae*	*δ-proteobacteria*	63.6	3.0E-36	CBX30073
(iojap-like protein)	123	13. 936	*Kordia algicida*	*Flavobacteriaceae*	*Flavobacteria*	55.7	2.0E-23	ZP_02162891
	96	10. 769	*Thermoanaerobacter tengcongensis*	*Thermoanaerobacteraceae*	*Clostridia*	40.7	8.0E-10	NP_622272
Glu-tRNAGln	106	12. 079	Strain NaphS2	*Desulfobacteraceae*	*δ-proteobacteria*	60	1.0E-28	ZP_07198247
(Glutamyl-tRNA amidotransferase)	94	10. 223	*Desulfatibacillum alkenivorans* AK-01	*Desulfobacteraceae*	*δ-proteobacteria*	56.4	2.0E-22	YP_002433641
Ribosomal_S3_C	219	25. 111	Strain NaphS2	*Desulfobacteraceae*	*δ-proteobacteria*	80.3	3.0E-96	ZP_07198590
(30S ribosomal protein S3)	216	24. 609	Unculture *Desulfobacterium* sp. N47	*Desulfobacteraceae*	*δ-proteobacteria*	77.5	4.0E-94	CBX29577
Ribosomal_L16	137	15. 413	Unculture *Desulfobacterium* sp. N47	*Desulfobacteraceae*	*δ-proteobacteria*	80	3.0E-61	CBX29576
(50S ribosomal protein L16)	139	15. 838	*Sphingobacterium spiritivorum*	*Sphingobacteriaceae*	*Sphingobacteriia*	86.3	6.0E-63	ZP_03968760
Ribosomal_L20	114	13. 190	Strain NaphS2	*Desulfobacteraceae*	*δ-proteobacteria*	71.8	9.0E-25	ZP_07200109
(50S Ribosomal protein L20)	101	11. 347	Unculture *Desulfobacterium* sp. N47	*Desulfobacteraceae*	*δ-proteobacteria*	78	8.0E-32	CBX29290
Ribosomal_L12	128	13. 407	*Desulfococcus oleovorans* Hxd3	*Desulfobacteraceae*	*δ-proteobacteria*	76.7	2.0E-39	YP_001528588
(50S ribosomal protein L7/L12)	128	13. 448	Strain NaphS2	*Desulfobacteraceae*	*δ-proteobacteria*	76.6	1.0E-29	ZP_07200160
SecE	119	12. 958	*Desulfobacterium autotrophicum*	*Desulfobacteraceae*	*δ-proteobacteria*	53	3.0E-11	YP_002604867
(Preprotein translocase subunit)	125	14. 040	*Desulfobacca acetoxidans*	*Syntrophaceae*	*δ-proteobacteria*	62.1	1.0E-13	YP_004370505
GlutR_dimer	423	47. 331	Strain NaphS2	*Desulfobacteraceae*	*δ-proteobacteria*	64.1	9.0E-149	ZP_07198332
(Glutamyl-tRNA reductase)	424	47. 413	Unculture *Desulfobacterium* sp. N47	*Desulfobacteraceae*	*δ-proteobacteria*	60.4	4.0E-145	CBX28030
Ribosomal_L21p	108	12. 212	Unculture *Desulfobacterium* sp. N47	*Desulfobacteraceae*	*δ-proteobacteria*	62.4	2.0E-17	CBX30079
(50S ribosomal protein L21)	103	11. 590	*Desulfatibacillum alkenivorans* AK-01	*Desulfobacteraceae*	*δ-proteobacteria*	70	3.0E-30	YP_002433267
Ribosomal_S16	78	8. 687	Strain NaphS2	*Desulfobacteraceae*	*δ-proteobacteria*	63.6	7.0E-24	ZP_07203991
(30S ribosomal protein S16)	64	7. 048	*Desulfobacterium autotrophicum*	*Desulfobacteraceae*	*δ-proteobacteria*	55.7	1.0E-15	YP_002604348

Table A.6. (Continued)

Housekeeping gene	AA	kDa	Phylogenetic affiliation	Family	Class	id (%)	e value	Acc
EF_TS	192	21. 329	*Desulfococcus oleovorans* Hxd3	*Desulfobacteraceae*	*δ-proteobacteria*	74.2	2.0E-83	YP_001528362
(Elongation factor Ts)	193	21. 315	Strain NaphS2	*Desulfobacteraceae*	*δ-proteobacteria*	79.9	2.0E-75	ZP_07202754
Ribosomal_L27	84	9. 081	Strain NaphS2	*Desulfobacteraceae*	*δ-proteobacteria*	71.4	1.0E-28	ZP_07203831
(50S ribosomal protein L27)	102	11. 355	*Desulfobacterium autotrophicum*	*Desulfobacteraceae*	*δ-proteobacteria*	77.4	5.0E-32	YP_002604416
RNA_pol_Rpb6	66	7. 349	*Desulfatibacillum alkenivorans* AK-01	*Desulfobacteraceae*	*δ-proteobacteria*	79.4	3.0E-21	YP_002430409
(DNA-directed RNA polymerase, Ω subunit)	118	13. 311	Strain NaphS2	*Desulfobacteraceae*	*δ-proteobacteria*	79.7	3.0E-20	ZP_07203207
Ribosomal_L17	205	22. 023	*Desulfococcus oleovorans* Hxd3	*Desulfobacteraceae*	*δ-proteobacteria*	77.8	1.0E-47	YP_001528621
(50S ribosomal protein L17)	139	15. 884	Strain NaphS2	*Desulfobacteraceae*	*δ-proteobacteria*	82	2.0E-50	ZP_07198584
Ribosomal_L19	113	13. 115	Strain NaphS2	*Desulfobacteraceae*	*δ-proteobacteria*	82.3	5.0E-36	ZP_07204010
(50S ribosomal protein L19)	115	13. 300	*Desulfatibacillum alkenivorans* AK-01	*Desulfobacteraceae*	*δ-proteobacteria*	74.6	1.0E-35	YP_002433790
Ribosomal_S6	144	17. 014	Strain NaphS2	*Desulfobacteraceae*	*δ-proteobacteria*	55.2	1.0E-28	ZP_07203308
(30S ribosomal protein S6)	143	16. 395	Unculture *Desulfobacterium* sp. N47	*Desulfobacteraceae*	*δ-proteobacteria*	62.6	7.0E-34	CBX29661
Ribosomal_L9_N	122	14. 011	Strain NaphS2	*Desulfobacteraceae*	*δ-proteobacteria*	66.1	4.0E-32	ZP_07203299
(50S ribosomal protein L9)	149	16. 618	Unculture *Desulfobacterium* sp. N47	*Desulfobacteraceae*	*δ-proteobacteria*	64.6	2.0E-47	CBX29659
Ribosomal_L15	146	15. 741	*Desulfatibacillum alkenivorans* AK-01	*Desulfobacteraceae*	*δ-proteobacteria*	62.8	3.0E-44	YP_002431061
(50S ribosomal protein L15)	150	16. 632	*Clostridium methylpentosum*	*Clostridiaceae*	*Clostridia*	58	5.0E-25	ZP_03705458
SmpB	153	18. 075	Desulfococcus multivorans	*Desulfobacteraceae*	*δ-proteobacteria*	70	1.0E-50	CAJ13763
(SsrA-binding protein)	149	17. 530	Strain NaphS2	*Desulfobacteraceae*	*δ-proteobacteria*	71.2	2.0E-52	ZP_07203979
tRNA_m1G_MT	243	27. 368	Strain NaphS2	*Desulfobacteraceae*	*δ-proteobacteria*	62.3	2.0E-78	ZP_07204003
(tRNA [guanine-N(1)-]-methyltransferase)	248	27. 750	*Desulfococcus oleovorans* Hxd3	*Desulfobacteraceae*	*δ-proteobacteria*	58.3	2.0E-79	YP_001530187
RimM	177	20. 093	Strain NaphS2	*Desulfobacteraceae*	*δ-proteobacteria*	45.1	3.0E-44	ZP_07204029
(16S rRNA processing protein)	177	18. 809	*Desulfococcus oleovorans* Hxd3	*Desulfobacteraceae*	*δ-proteobacteria*	45.6	4.0E-33	YP_001530188
RuvC	162	17. 290	Unculture *Desulfobacterium* sp. N47	*Desulfobacteraceae*	*δ-proteobacteria*	64	3.0E-51	CBX28465
(Crossover junction endodeoxyribonuclease)	164	18. 116	Strain NaphS2	*Desulfobacteraceae*	*δ-proteobacteria*	61.2	8.0E-50	ZP_07201032
tRNA_synt_2f	693	74. 641	Unculture *Desulfobacterium* sp. N47	*Desulfobacteraceae*	*δ-proteobacteria*	53.3	0	CBX28008
(Glycyl-tRNA synthetase β subunit)	445	50. 422	Strain NaphS2	*Desulfobacteraceae*	*δ-proteobacteria*	57.7	5.0E-150	ZP_07201795
YgbB	164	17. 407	*Desulfatibacillum alkenivorans* AK-01	*Desulfobacteraceae*	*δ-proteobacteria*	60	6.0E-50	YP_002429941
(methylerythritol cyclodiphosphate synthase)	184	19. 973	Strain NaphS2	*Desulfobacteraceae*	*δ-proteobacteria*	63.5	2.0E-53	ZP_07199968

Table A.6. (Continued)

Housekeeping gene	AA	kDa	Phylogenetic affiliation	Family	Class	id (%)	e value	Acc
RecO	269	29. 973	Unculture *Desulfobacterium* sp. N47	*Desulfobacteraceae*	*δ-proteobacteria*	51.6	5.0E-63	CBX28005
(DNA repair protein)	247	27. 557	Strain NaphS2	*Desulfobacteraceae*	*δ-proteobacteria*	55.14	4.0E-70	ZP_07204581
DUF150	134	15. 162	Unculture *Desulfobacterium* sp. N47	*Desulfobacteraceae*	*δ-proteobacteria*	52.6	5.0E-36	CBX29058
(Ribosome maturation factor rimP)	173	19. 935	Strain NaphS2	*Desulfobacteraceae*	*δ-proteobacteria*	51.3	7.0E-42	ZP_07204050
Tyr_ Deacylase	146	15. 560	*Desulfococcus oleovorans* Hxd3	*Desulfobacteraceae*	*δ-proteobacteria*	62.3	4.0E-38	YP_001530108
(D-tyrosyl-tRNA(Tyr) deacylase)	149	16. 748	Strain NaphS2	*Desulfobacteraceae*	*δ-proteobacteria*	71.1	1.0E-53	ZP_07200341
Phe_tRNA_synt_N	347	39. 679	Strain NaphS2	*Desulfobacteraceae*	*δ-proteobacteria*	75.4	2.0E-153	ZP_07200122
(Phenylalanine--tRNA ligase, α subunit)	335	37. 742	Unculture *Desulfobacterium* sp. N47	*Desulfobacteraceae*	*δ-proteobacteria*	69.5	7.0E-143	CBX29289
SRP_SPB	441	48. 574	Strain NaphS2	*Desulfobacteraceae*	*δ-proteobacteria*	75.5	5.0E-160	ZP_07204041
(Signal recognition particle protein)	443	48. 723	Unculture *Desulfobacterium* sp. N47	*Desulfobacteraceae*	*δ-proteobacteria*	77.1	0	CBX31294
B3_4	789	87. 482	Strain NaphS2	*Desulfobacteraceae*	*δ-proteobacteria*	57.5	0	ZP_07200114
(Phenylalanine--tRNA ligase, β subunit)	804	87. 126	Unculture *Desulfobacterium* sp. N47	*Desulfobacteraceae*	*δ-proteobacteria*	54.5	0	CBX29288
PNPase	699	75. 496	Unculture *Desulfobacterium* sp. N47	*Desulfobacteraceae*	*δ-proteobacteria*	75.7	0	CBX29049
(Polyribonucleotide nucleotidyltransferase)	583	63. 242	Strain NaphS2	*Desulfobacteraceae*	*δ-proteobacteria*	73.8	0	ZP_07203971
SecG	96	9. 535	Strain NaphS2	*Desulfobacteraceae*	*δ-proteobacteria*	76.1	9.0E-12	ZP_07203024
(Preprotein translocase subunit)	108	10. 843	*Desulfobacterium autotrophicum*	*Desulfobacteraceae*	*δ-proteobacteria*	64	2.0E-24	YP_002604048
RuvB_N	334	36. 705	Unculture *Desulfobacterium* sp. N47	*Desulfobacteraceae*	*δ-proteobacteria*	75	9.0E-142	CBX28463
(Holliday junction ATP-dependent DNA helicase)	271	29. 824	Strain NaphS2	*Desulfobacteraceae*	*δ-proteobacteria*	81	9.0E-109	ZP_07201008
Trigger_C	443	50. 612	Strain NaphS2	*Desulfobacteraceae*	*δ-proteobacteria*	52.7	5.0E-121	ZP_07201371
(Trigger factor)	438	49. 660	Unculture *Desulfobacterium* sp. N47	*Desulfobacteraceae*	*δ-proteobacteria*	53.7	4.0E-140	CBX28506
IGPD (Imidazoleglycerol-phosphate dehydratase)	195	21. 416	*Desulfococcus oleovorans* Hxd3	*Desulfobacteraceae*	*δ-proteobacteria*	58.5	2.0E-59	YP_001530036
Ribonuclease_P	101	11.628	*Desulfatibacillum alkenivorans* AK-01	*Desulfobacteraceae*	*δ-proteobacteria*	49.4	7.0E-15	YP_002433287
Ribosomal_S20p (30S ribosomal protein S20)	80	8. 841	Unculture *Desulfobacterium* sp. N47	*Desulfobacteraceae*	*δ-proteobacteria*	53.7	4.0E-14	CBX30191
Uncharacterised family **UPF0054**	119	12. 961	*Desulfotignum balticum*	*Desulfobacteraceae*	*δ-proteobacteria*	59.3	2.0E-27	BAH60902
Exonuc_VII_S (Exodeoxyribonuclease VII, small subunit)	78	8. 695	*Desulfococcus oleovorans* Hxd3	*Desulfobacteraceae*	*δ-proteobacteria*	55	7.0E-14	YP_001529545
DUF177 (Hypothetical protein Pcar_1433	186	20. 117	*Pelobacter carbinolicus*	*Pelobacteraceae*	*δ-proteobacteria*	36	1.0E-30	YP_356849
IF2_N(Translation initiation factor)	920	99. 942	Unculture *Desulfobacterium* sp. N47	*Desulfobacteraceae*	*δ-proteobacteria*	74	0	CBX29056
Ribosomal_L29	67	7. 746	*Megasphaera* genomosp.	*Veillonellaceae*	*Negativicutes*	67.9	3.0E-13	ZP_06559779